LONG-TERM ADAPTATION SCENARIOS FLAGSHIP RESEARCH PROGRAMME (LTAS)

Analysis of downscaled climate model results for the areas of Mopani and Namakwa, South Africa, at the district municipality scale

African Climate & Development Initiative (ACDI)
University of Cape Town (UCT)

Technical Report
30 July 2014

Christopher Brodrick*, Muhammad Rahiz and Mark New
*Christopher.Brodrick@uct.ac.za

Contents

List of Figures

List of Abbreviations

ACDI	African Climate & Development Initiative
ANN	Annual
CCAM	Conformal-Cubic Atmospheric Model
CGCM	Coupled Global Circulation Model
CSAG	Climate System Analysis Group
DJF	December, January, February (Summer)
ensmed	Median of the model ensemble
ens10	10th percentile of the model ensemble
ens90	90th percentile of the model ensemble
ENSO	El Niño Southern Oscillation
IOD	Indian Ocean Dipole
JJA	June, July, August (Winter)
LTAS	Long-Term Adaptation Scenarios Flagship Research Programme
MAM	March, April, May (Autumn)
RCP4.5	Representative Concentration Pathway, radiative forcing of 4.5W/m^2
RCP8.5	Representative Concentration Pathway, radiative forcing of 8.5W/m^2
rnd24	Total precipitation in a 24 hour period
SAHP	South Atlantic High Pressure
SAM	Southern Annual Mode
SON	September, October, November (Spring)
SST	Sea surface temperatures
TC	Tropical cyclone
tmax	Maximum temperature
tmin	Minimum temperature
TTT	Tropical-temperate trough
UCT	University of Cape Town

2020s	2015-2035 (short-term future)
2050s	2040-2060 (medium-term future)
2080s	2075-2095 (long-term future)

Acknowledgements

The African Climate & Development Initiative (ACDI) wish to thank the Council for Scientific and Industrial Research (CSIR) for the provision of the Conformal-Cubic Atmospheric Model (CCAM) data, and the Climate System Analysis Group (CSAG) for the provision of the statistically downscaled CSAG data. Thank you to the South African National Biodiversity Institute (SANBI) for providing GIS data.

1. Introduction

This technical report presents an analysis of downscaled climate model results for the areas of Mopani and Namakwa, South Africa, at the district municipality scale. Future climates are presented for the regions for the short (2020s), medium (2050s) and long (2080s) term futures, as well as for the two emission scenarios, RCP4.5 and RCP8.5.

The climate projection data is visualised by means of graphs and maps. Both regions are summarised – for maximum temperature, minimum temperature, and precipitation – for each time period.

2. Executive summary

The CSAG and CCAM projection results, for both the emission scenarios, and all three of the time periods, can be summarised as follows:

For both regions, it is clear that there is less uncertainty in the temperature projections than the precipitation projections. All approaches show a distinct warming trend, growing stronger towards the end of the 21st Century. In general, there is a tendency for stronger increases in maximum temperatures than for minimum temperatures. The RCP4.5 emission pathway (mitigation) results indicate that extreme warming trends and significant precipitation changes can largely be avoided, especially towards the end of the century.

Many of the projected changes fall within the range of historical natural variability, and – especially in the long-term – the inherent uncertainty is high.

2.1 Mopani

As mentioned above, appreciable warming over the area is projected, in line with the recent historical climatology. In the short-term future, temperature rises will be in the range of 1-2°C, with greater warming in Summer than in the other seasons. The north, and to a lesser extent the west, is projected to warm more than the south, and east. Mid-term sees warming between 1 and 3°C, again more in the west than the east, and particularly in Spring. For the long-term future, warming in the region of between 2 and 5°C is projected, particularly in the south and in Winter, with less warming in the central regions in Autumn. The RCP8.5 emission pathway (no mitigation) results indicate very significant warming in the long-term future – up to 6°C.

Precipitation projections are less clear. In the short-term, a weak annual wetting trend is shown, especially in the east, with more robust evidence of wetting in Autumn. In the Summer and Winter months, however, weak drying is projected, mostly in the north-east and west respectively. In the

Autumn of mid-term, the south-east is set to receive slightly more precipitation, whereas in Summer, the north and east are projected to become drier. With the exception of Winter, the long-term future is projected to dry more in the north than the south.

Please refer to Appendices A and B for a full suite of the visualised data for the Mopani region.

2.2 Namakwa

As with the Mopani region, temperature rises in the short-term future will be in the range of 1-2°C, with greater warming in Spring than in the other seasons. For all the seasons, there is a fairly strong warming bias to the north-east. Mid-term sees warming between 1 and 3°C, with greater warming in the east, particularly in Summer. Long-term sees warming between 2 and 5°C – particularly in Winter – with greater warming projected for the east than the west, across the seasons. Warming is generally less pronounced over the coastal areas of the region. That said, however, Namakwa appears to be more at risk of warming – particularly under RCP8.5 – relative to Mopani. The need for mitigation – and following as closely to the RCP4.5 pathway as possible – needs to be stressed.

For short-term precipitation, there is high variability within and between datasets. As with the Mopani region, weak annual wetting is projected, particularly to the east in Autumn, with a drying Summer. The north-east is set to dry in Autumn, while the south-west is set to wet slightly. Mid-term shows weak wetting in Autumn, particularly in the south-west. In Spring and Summer, however, it is set to dry weakly and moderately respectively, especially in the south-west. In Autumn and Winter of the long-term, weak wetting is projected in the south-west, while weak drying is projected for the south-west in Spring and Summer.

Please refer to Appendices A and B for a full suite of the visualised data for the Mopani region.

3. Regional climate

Both regions will be affected by water balance changes. Increasing temperature results in higher rates of evaporation, leading to changes in atmospheric water vapour concentrations and water vapour transport (Solomon et al. 2009). This effectively alters the hydrological cycle. Although the effects of this may not necessarily relate to large-scale changes in rainfall amounts and variability, higher evaporation rates will most likely result in decreased surface water – both spatially and temporally – which will impact agriculture in particular. Accordingly, hydrological risks are set to increase, especially under the RCP8.5 pathway, where much greater warming is expected.

3.1 Mopani

3.1.1 Current climate

The Mopani District Municipality falls into the Summer rainfall zone of South Africa. Summers are warm – mean maximum and minimum temperatures in the range of 28-38°C (mean of ~30°C), and 16-22°C (mean of ~19°C) respectively – and wet, with the majority of precipitation falling in mid-Summer. Winters are mild – mean maximum and minimum temperatures are in the region of 19-26°C (mean of ~23°C) and 5-11°C (mean of ~8°C) respectively – and dry.

Annual rainfall in the Mopani district varies between 400 and 900mm, largely as a result of the complex topography. To highlight this, Tzaneen – surrounded by large hills – receives mean annual precipitation of 881mm (SA Explorer – Tzaneen climate, 2014), while Giyani only 421mm (SA Explorer – Giyani climate, 2014). There is large interannual variability, with monthly maximum rainfall sometimes reaching 340mm, in comparison to the usual 50-100 monthly totals (FAO, n.d.) for the Summer months. Causes of this variability are described in Sect. 3.1.2 below.

3.1.2 Regional factors that may affect variations in climate

Southern African mean annual precipitation shows an interannual and quasi-decadal (circa 18-year) time-scale of variability (oscillation). Summer rainfall zones that are governed largely by mesoscale convective activity – such as Mopani – are particularly affected. The oscillation manifests itself by means of nine years of above average rainfall followed by nine years of below average rainfall (Tyson & Preston-Whyte, 2000:113).

Dry spells are characterised by greater spatial variability in precipitation, increased thunderstorm activity, and thus increased hail-fall frequencies. Wet spells are characterised by more even precipitation (Tyson & Preston-Whyte, 2000:113), both in nature and in spatial extent.

Tropical temperate troughs (TTTs) are responsible for much of the Summer rainfall in the region. TTTs usually form when a surface easterly low occurs in conjunction with an upper atmosphere westerly wave (van den Heever et al., 1997). Pohl et al. (2009) found that TTTs are modulated by the El Niño Southern Oscillation (ENSO). During an El Niño phase, atmospheric circulation in the Summer rainfall zone of South Africa is influenced sufficiently to shift rain-inducing processes away from the sub-continent (Pohl et al., 2009). Generally speaking, drought conditions are associated with El Niño. Conversely, during the La Nina phase, rain-inducing processes are enhanced, thus producing wetter than normal conditions, increasing the likelihood of heavy rainfall and flood events. ENSO is therefore responsible for appreciable interannual variability in the Summer rainfall zone of South Africa.

Summer rainfall is also linked to the Indian Ocean sea surface temperatures (SSTs). When the SSTs are anomalously high, dry Summer conditions follow (Rocha & Simmonds, 1997). Conversely, anomalously low SSTs precede wetter conditions. Goddard & Graham (1999) intimate that SST variability in the Pacific Ocean may be positively correlated to SST variability in the Indian Ocean. Hence, it is possible that the ENSO phase is linked to Indian Ocean SSTs.

The Indian Ocean Dipole (IOD) is a mode of interannual variability that also manifests itself through changes in tropical ocean SST (Christensen et al., 2013). Anomalously warmer water in the east of the Indian Ocean results in cooler and drier conditions in the west (and thus, *inter alia*, the Limpopo Province), with the converse producing warmer and wetter conditions.

Climate change will increasingly affect ENSO, which in turn will influence the formation of TTTs, and Indian Ocean SSTs. Accordingly, it is possible that interannual variability in rainfall will increase further in this region. That said, the changes in the variation and spatial pattern of ENSO projected by climate models are very large, which means that there is low confidence in any particular projected change in variability (Christensen et al.,2013).

Related to SST are tropical cyclones (TCs). In recorded history, few TCs have penetrated South Africa. With the mean global increase of SSTs due to climate change, the 26°C isotherm (integral to the formation of TCs) is moving further south (Fitchett & Grab, 2014). Along with increased energy in the global atmospheric system, it is possible that these TCs may contribute towards heavy rainfall and flooding in the eastern parts of the Limpopo province, further exacerbating rainfall variability.

3.2 Namakwa

3.2.1 Current climate

The Namakwa District Municipality is very large – thus a single climate is difficult to characterise. The vast majority of the District falls into the Winter rainfall zone of South Africa, mostly receiving its rainfall from mid-latitude cyclones (cold fronts). It is not uncommon, however, for the extreme east of the District to experience thunderstorm-associated rainfall in the Summer months. Summers are hot – mean maximum and minimum temperatures in the range of 26-45°C (mean of ~30°C) and 12-20°C (mean of 17°C) respectively – and dry. Winters are cool – mean maximum and minimum temperatures are in the region of 10-25°C (mean of 17°C) and -8-12 (mean of 1°C) – and wet in places.

Namakwaland is classified as semi-desert, due to its low precipitation amounts. The mean annual rainfall in the Namakwa district varies between less than 100mm along the coastal belt to between 100 and 250mm inland. Much of Namakwaland is succulent Karoo, which receives low – but more importantly – largely predictable winter rainfall (Desmet & Cowling, 1999). Spatially, the largest factor affecting rainfall is the escarpment. On the coast, Port Nolloth only receives 50mm mean annual precipitation (SA Explorer – Port Nolloth climate, 2014), while just over the escarpment, Nieuwoudtville receives 245mm precipitation (SA Explorer – Nieuwoudtville climate, 2014).

3.2.2 Regional factors that may affect variations in climate

One of the principal modes of atmospheric circulation variability in the Southern Hemisphere (Marshall, 2003) is the Southern Annual Mode (SAM). The SAM describes the latitudinal movement of the westerly wind belt. Changes in this movement drive the intensity and position of mid-latitude cyclones (cold fronts), particularly affecting rainfall variability in the winter rainfall zone of South Africa (and thus, *inter alia*, Namakwaland).

The western interior of South Africa – which incorporates the Namakwa region – receives in excess of 80% of possible sunshine, in both Summer and Winter (Tyson & Preston-Whyte, 2000:82). This pre-disposition to solar radiation makes the region particularly sensitive to increasing temperatures, particularly maximum temperature. As mentioned above, the extreme eastern parts of the District can receive Summer rainfall linked to thunderstorm activity. Because total radiation directly affects cloud-producing weather systems (Tyson & Preston-Whyte, 2000:82), this region may receive increased rainfall from such systems in the Summer months.

In the future, Namakwaland is projected to experience changes in rainfall amounts, as well as increased variability in rainfall (Midgley & Thuiller, 2007). The South Atlantic High Pressure (SAHP) largely drives the Benguela current (Tyson & Preston-Whyte, 2000:178), which has an enormous influence on the climate of Namakwaland. Also linked to the SAHP is the West Coast Trough, which produces widespread rain over the western parts of South Africa, from early Summer to Autumn (Tyson & Preston-Whyte, 2000:201). Under current climate changes, increases in energy to the system may affect the SAHP, thus having a direct effect on the area's climate and particularly rain-producing systems.

As a result of a possibly strengthening SAHP, the frontal systems that provide the majority of Namakwaland with its Winter rainfall are projected to move further south, but also increase in intensity. This may result in fewer rainfall events, but with heavier rainfall during such events. This will further increase the variability of rainfall in the region.

It is important to note that climate models are not always able to accurately capture complex ocean-atmosphere interactions, and how these might change in the future. Many of the drivers of variability mentioned above are complex and there is much uncertainty as to how exactly they will respond to climate change in the future. Downscaling rainfall in particular is still limited by our understanding of these large-scale drivers of variability.

4. Data

4.1 Statistically downscaled projections – CSAG

A statistical downscaling technique, downscaled to 0.5° by 0.5° resolution, has been applied for temperature and precipitation fields over the regions. This was done for both the RCP emission scenarios, for each one of a suite of ten different CGCMs.

4.2 Dynamically downscaled projections – CCAM

A dynamical downscaling technique, downscaled to 0.5° by 0.5° resolution, has been applied for temperature and precipitation fields over the regions. A three-model suite was used for RCP4.5, whilst a two-model suite was used for RCP8.5. Further CCAM model information, as well as its strengths and weaknesses, can be found in the previous LTAS report: *Climate Trends and Scenarios for South Africa, LTAS Phase 1, Technical Report (no. 1 of 6).*

The complex topography over small distance scales in the regions – particularly Mopani – must be taken into account when interpreting the model results. The downscaled regional models are unable to accurately resolve large changes in topography over small distance scales.

By way of example: In theory, Tzaneen (mean annual rainfall 881mm) and Giyani (mean annual rainfall 421mm) may fall into the same grid cell at the resolution used in this project (2.5 x 2.5°). Therefore, both sub-regions would share the same grid cell characteristics, whereas in the reality, their rainfall is rather different, due to the topography. This must be borne in mind when assessing the spatial results.

5. Results

5.1 Mopani

5.1.1 2020s

5.1.1.1 Temperature

Annually, maximum temperature is projected to increase by between 1 and 2°C, and minimum temperature by 1°C. For maximum temperature, Summer is projected to warm more significantly than the other seasons, especially in the north and west. The west is projected to experience greater maximum temperatures than the east.

5.1.1.2 Precipitation

Annually, a weak wetting trend is projected, much more so in the east. This is particularly evident in Autumn, which shows a strong trend of wetting, but is also accompanied by high variability within and between datasets. Summer and Winter, however, display weak drying trends, particularly in the north-east and west respectively.

5.1.2 2050s

5.1.2.1 Temperature

On an annual basis, maximum temperature is projected to increase by between 1 and 3°C, and minimum temperature by 2°C. For maximum temperature, Summer is projected to warm more significantly than the other seasons, particularly in the west, while for minimum temperature, Winter is projected to warm less significantly. Furthermore, both annually and in Spring, minimum temperature is set to rise more in the west than in the east. It is worth noting that for maximum temperature, CCAM RCP 8.5 dataset displays a large anomaly range, as well as greater absolute magnitude of anomaly.

5.1.2.2 Precipitation

There is no appreciable annual trend for precipitation. In Autumn, a moderate wetting trend is projected, particularly in the south-east, whereas in Spring and Summer there exists a weak drying trend, in the case of the latter, to the north and east. Winter shows very high variability between the datasets, some showing wetting and others drying.

5.1.3 2080s

5.1.3.1 Temperature

Annually, maximum temperature is projected to increase by between 2 and 5°C and minimum temperature by between 2 and 4°C. For the 2080s, the datasets begin to diverge appreciably from one another, with large anomaly ranges. In Winter, minimum temperature is projected to rise more significantly than the other seasons, particularly in the south. The central part of the region is projected to experience reduced warming in Autumn.

5.1.3.2 Precipitation

A weak drying trend is projected, on an annual basis. Summer, Spring and Autumn are projected to see more drying in the north than the south. Winter is set to dry moderately, with low variability between the datasets.

5.2 Namakwa

5.2.1 2020s

5.2.1.1 Temperature

Annually, maximum temperature is projected to increase by between 1 and 2°C, and minimum temperature by 1°C. For maximum temperature, Summer, Winter and Spring show a warming bias to the north-east; for minimum temperature, this holds true for all the seasons. In Autumn, maximum temperature is projected to rise less significantly than the other seasons, while in Spring, minimum temperature is projected to rise more significantly.

5.2.1.2 Precipitation

A weak wetting trend is projected on an annual basis, and particularly in the east in Autumn, where there is a fairly strong trend. Furthermore, the north east is set to dry in Autumn, while the south-west is projected to wet slightly.

In Summer, rainfall is projected to decrease slightly in some projections, while in others, increase slightly. It must be noted, however, that there is high variability within and between these datasets.

5.2.2 2050s

5.2.2.1 Temperature

On an annual basis, maximum temperature is projected to increase by between 1 and 3°C, and minimum temperature by 2°C. For both maximum and minimum temperature, Summer is projected to warm more significantly than the other seasons. There is a fairly strong trend of increased warming in the east, and to a lesser extent north-east, in all the seasons.

5.2.2.2 Precipitation

Annually, a very weak wetting trend is projected, particularly in Autumn and Winter, and in the south-west. In Spring and Summer, however, it is set to dry weakly and moderately respectively, especially in the south-west. Furthermore, there is low variability between the datasets, indicating higher confidence.

5.2.3 2080s

5.2.3.1 Temperature

An increase of between 2 and 5°C in maximum temperature, and between 2 and 4°C in minimum temperature, is projected on an annual basis, with a fairly strong bias towards the east. For both maximum and minimum temperature, the RCP 8.5 datasets both display a large anomaly range, as well as greater absolute magnitudes of anomaly. For maximum temperature, Winter is projected to warm more significantly than the other seasons. For both Winter and Summer, minimum temperatures are set to rise more significantly than the other seasons.

5.2.3.2 Precipitation

There is no appreciable trend in annual precipitation. In Autumn and Winter, however, weak wetting is projected in the south-west, while weak drying is projected for the south-west in Spring and Summer.

References

Christensen, J.H., K. Krishna Kumar, E. Aldrian, S.-I. An, I.F.A. Cavalcanti, M. de Castro, W. Dong, P. Goswami, A. Hall, J.K. Kanyanga, A. Kitoh, J. Kossin, N.-C. Lau, J. Renwick, D.B. Stephenson, S.-P. Xie and T. Zhou, 2013: Climate Phenomena and their Relevance for Future Regional Climate Change. In: *Climate Change 2013: The Physical Science Basis. Contribution of Working Group I to the Fifth Assessment Report of the Intergovernmental Panel on Climate Change* [Stocker, T.F., D. Qin, G.-K. Plattner, M. Tignor, S.K. Allen, J. Boschung, A. Nauels, Y. Xia, V. Bex and P.M. Midgley (eds.)]. Cambridge University Press, Cambridge, United Kingdom and New York, NY, USA.

Desmet, P.G., & Cowling, R.M. 1999. Biodiversity, habitat and range-size aspects of a flora from a winter-rainfall desert in north-western Namaqualand, South Africa. *Plant Ecology,* 142: 23-33.

FAO. n.d. Drought impact mitigation and prevention in the Limpopo River Basin - Chapter 2: Biophysical characteristics. *FAO Natural Resources Management and Environment Department*. [Online]. Available: http://www.fao.org/docrep/008/y5744e/y5744e05.htm#TopOfPage [17 July 2014].

Fitchett, J.M., & Grab, S.W. 2014. A 66-year tropical cyclone record for south-east Africa: temporal trends in a global context. *Int. J. of Climatol.* (2014). Published online in Wiley Online Library.

Goddard, L., & Graham, N.E. 1999. Importance of the Indian Ocean for simulating rainfall anomalies over eastern and southern Africa. *Journal of Geophysical Research,* 104(D16): 19,099-19,116.

Marshall, G.J. 2003. Trends in the Southern Annular Mode from Observations and Reanalyses. *Journal of Climate*, 16: 4134-4143.

Midgley, G.F., & Thuiller, W. 2007. Potential vulnerability of Namaqualand plant diversity to anthropogenic climate change. *Journal of Arid Environments,* 70: 615-628.

Pohl, B., Fauchereau, N., Richard, Y., Rouault, M., & Reason, C.J.C. 2009. Interactions between synoptic, intraseasonal and interannual convective variability over Southern Africa. *Climate Dynamics,* 33: 1033-1050.

Rocha, A., & Simmonds, I. 1997. Interannual variability of south-eastern African summer rainfall rainfall. Part 1: Relationships with air-sea interaction processes. International Journal of Climatology, 17: 235-265.

Solomon, S., Plattner, G.-K., Knutti, R., & Friedlingstein, P. 2009. Irreversible climate change due to carbon dioxide emissions. *Proceedings of the National Academy of Sciences*, 106(6): 1704-1709.

South Africa Explorer. 2014. *Giyani climate*. [Online]. Available: http://www.saexplorer.co.za/south-africa/climate/giyani_climate.asp [16 July 2014].

South Africa Explorer. 2014. *Nieuwoudtville climate*. [Online]. Available: http://www.saexplorer.co.za/south-africa/climate/nieuwoudtville_climate.asp [16 July 2014].

South Africa Explorer. 2014. *Port Nolloth climate*. [Online]. Available: http://www.saexplorer.co.za/south-africa/climate/port_nolloth_climate.asp [16 July 2014].

South Africa Explorer. 2014. *Tzaneen climate*. [Online]. Available: http://www.saexplorer.co.za/south-africa/climate/tzaneen_climate.asp [16 July 2014].

Tyson, P.D., & Preston-Whyte, R.A. 2000. *The Weather and Climate of Southern Africa*. Cape Town: Oxford University Press.

Van den Heever, S.C., D'Abreton, P.C., & Tyson, P.D. 1997. Numerical simulation of tropical-temperate troughs over southern Africa using CSU RAMS model. *South African Journal of Science,* 93: 359-365.

Appendix A: Time-series and boxplots

A1 Interpretation

Bar graphs

For a given scenario and dataset:

The first column represents the historical period.

The second to forth columns represent the 2020s, 2050s and 2080s, respectively. The bars display the greatest anomaly within the dataset. The anomaly represents the range between the ensemble maximum minus the historical mean, and the ensemble minimum minus the historical mean. Therefore, this gives an indication of the inherent uncertainty in each case.

Time-series (line graphs)

For a given scenario and dataset:

The area making up each 'line' displays the range of the anomaly within the dataset. The anomaly represents the range between the ensemble maximum minus the historical mean, and the ensemble minimum minus the historical mean. Therefore, this gives an indication of the inherent uncertainty in each case.

The two dashed lines in the first column (historical period) indicate two standard deviations above- and below the models' mean, respectively.

Temperature anomaly in °C and precipitation anomaly is % change.

Note: For the Winter months (core JJA), the CCAM raw data was populated almost exclusively with zeroes. It appears as if there is a fault of sorts in the raw data. Please interpret the CCAM spatial plots for this period accordingly.

A1.1 Mopani

A1.1.1 ANN

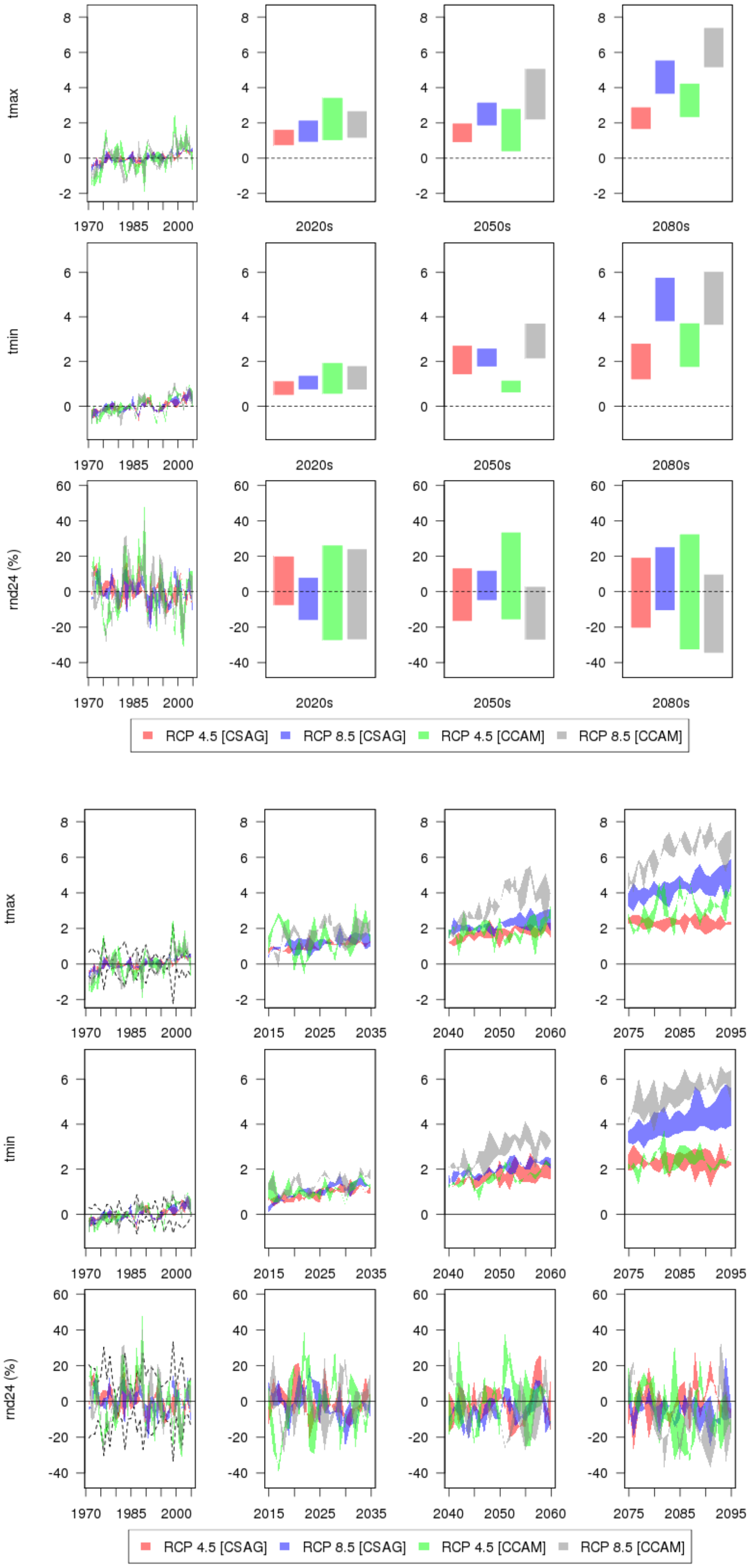

Figure A1.1.1: The annual anomaly with respect to the model historical period – Mopani

A1.1.2 DJF

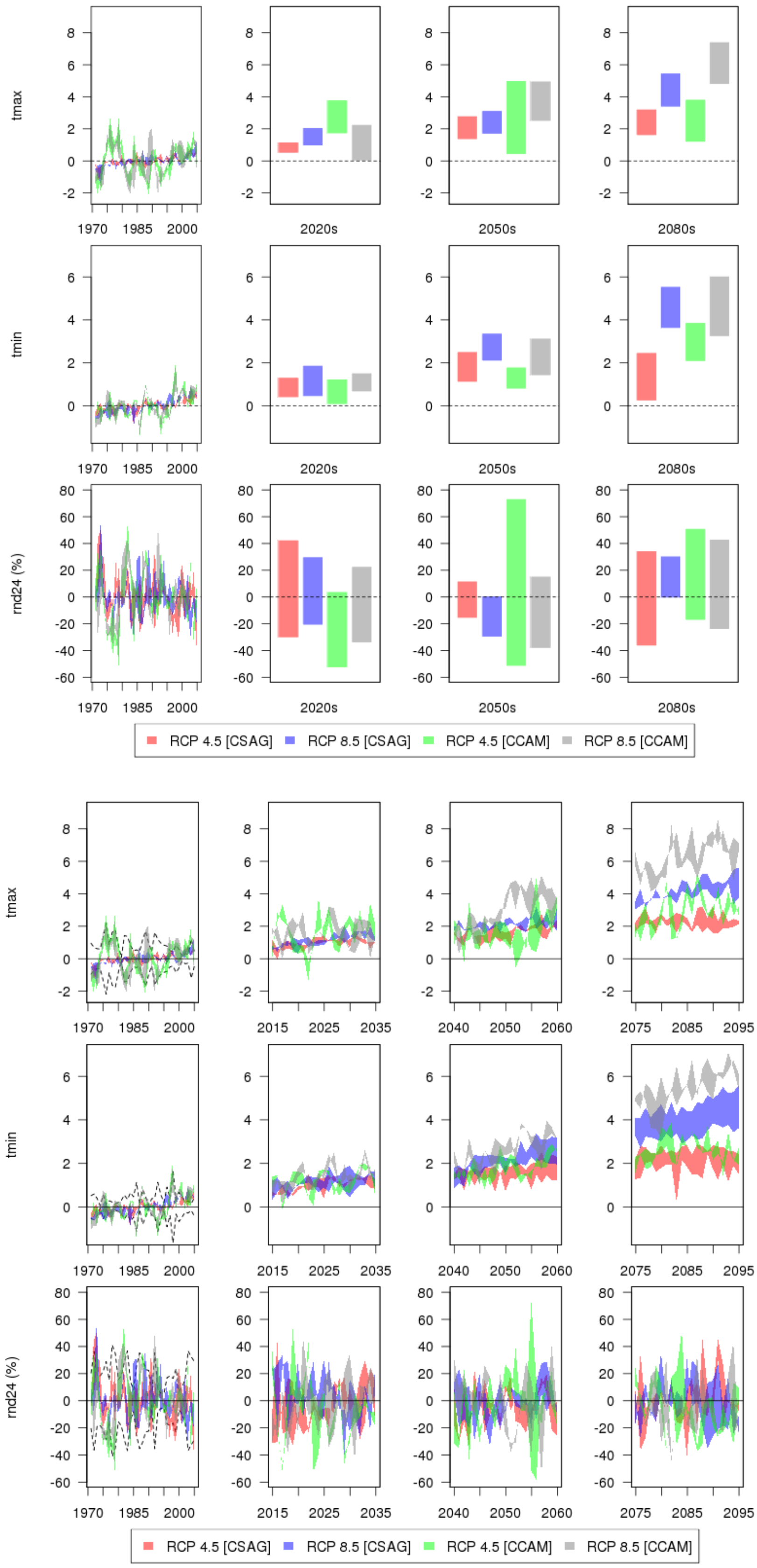

Figure A1.1.2: The DJF anomaly with respect to the model historical period – Mopani

A1.1.3 MAM

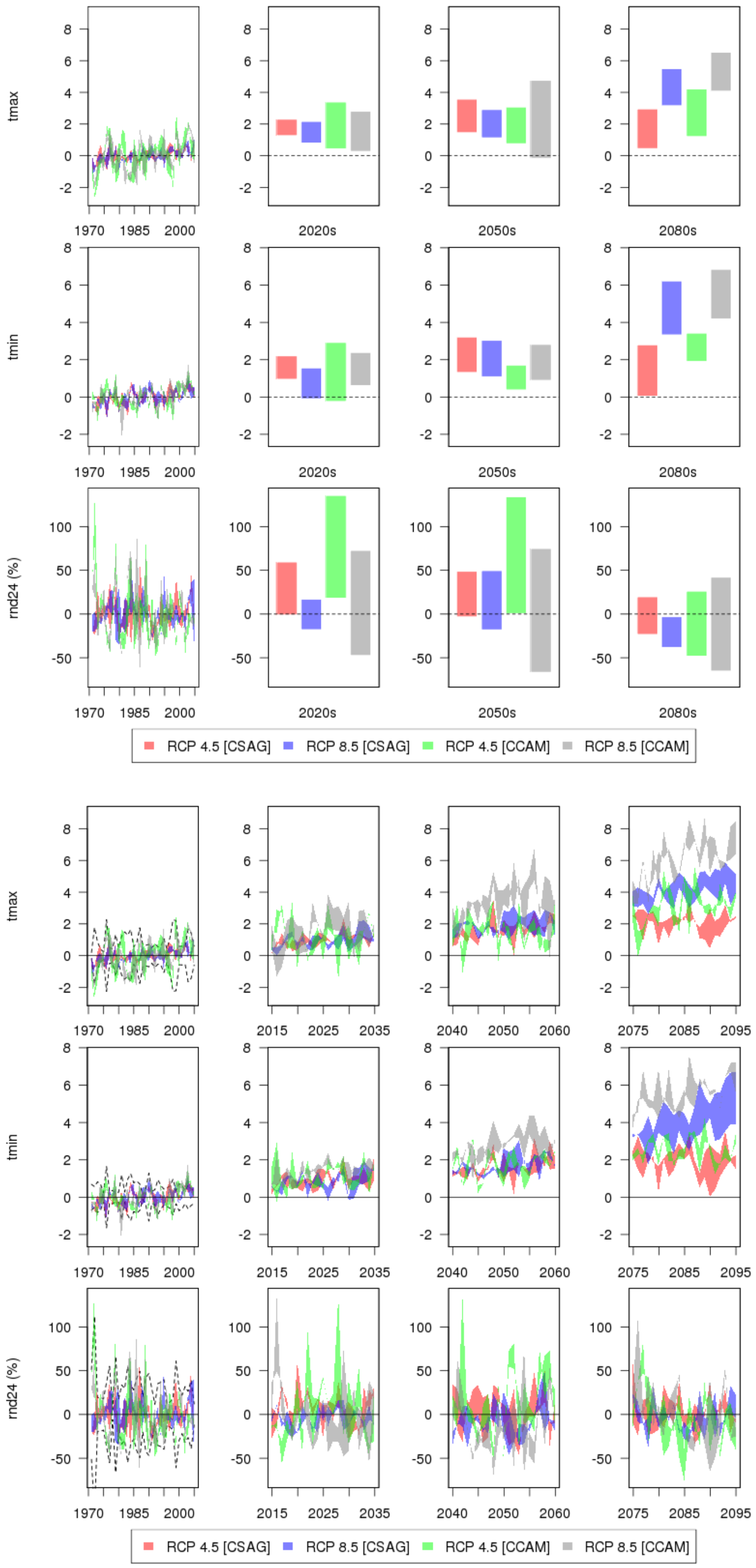

Figure A1.1.3: The MAM anomaly with respect to the model historical period – Mopani

A1.1.4 JJA

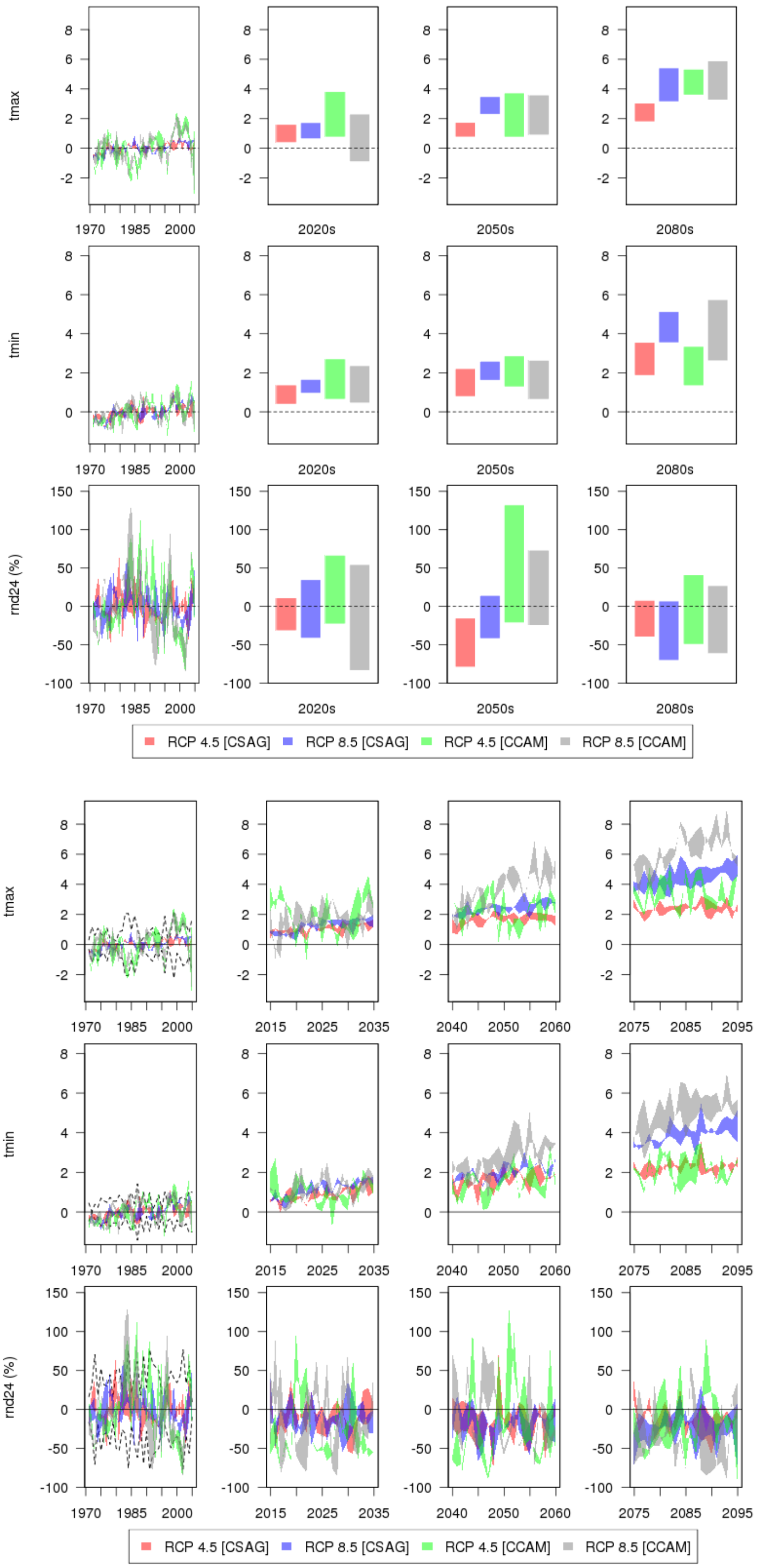

Figure A1.1.4: The JJA anomaly with respect to the model historical period – Mopani

A1.1.5 SON

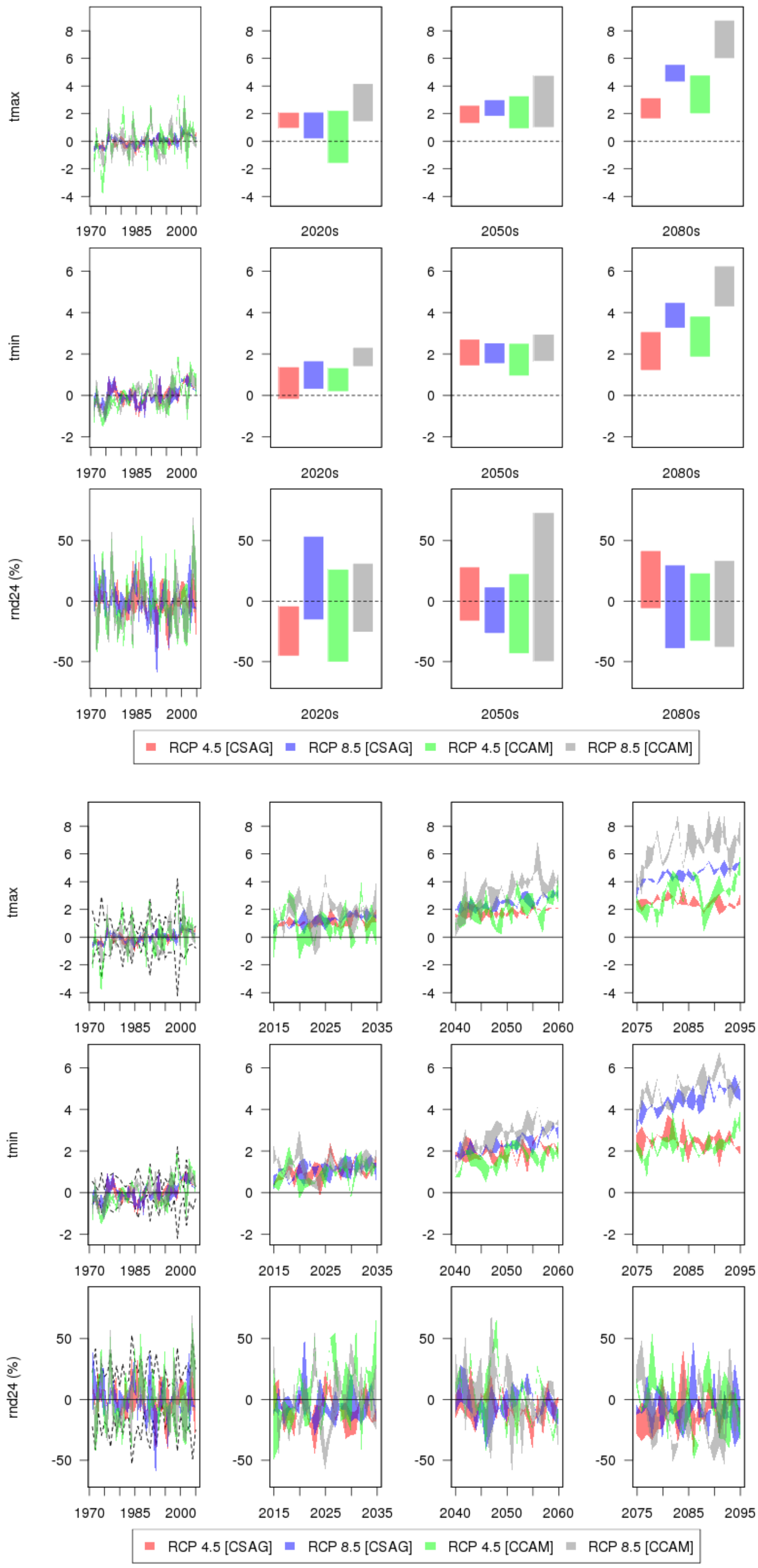

Figure A1.1.5: The SON anomaly with respect to the model historical period – Mopani

A1.2 Namakwa

A1.2.1 ANN

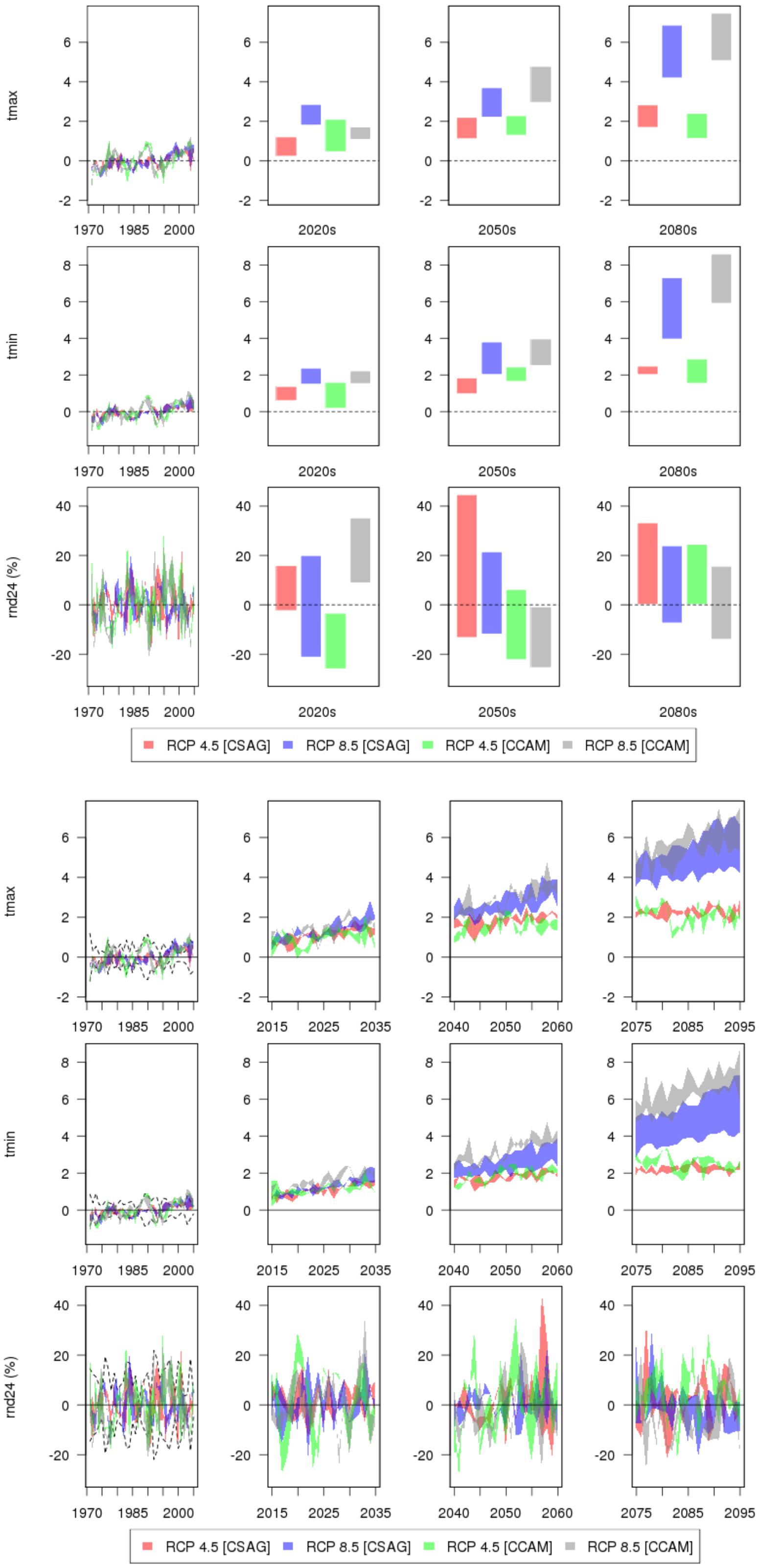

Figure A1.2.6: The ANN anomaly with respect to the model historical period – Namakwa

A1.2.2 DJF

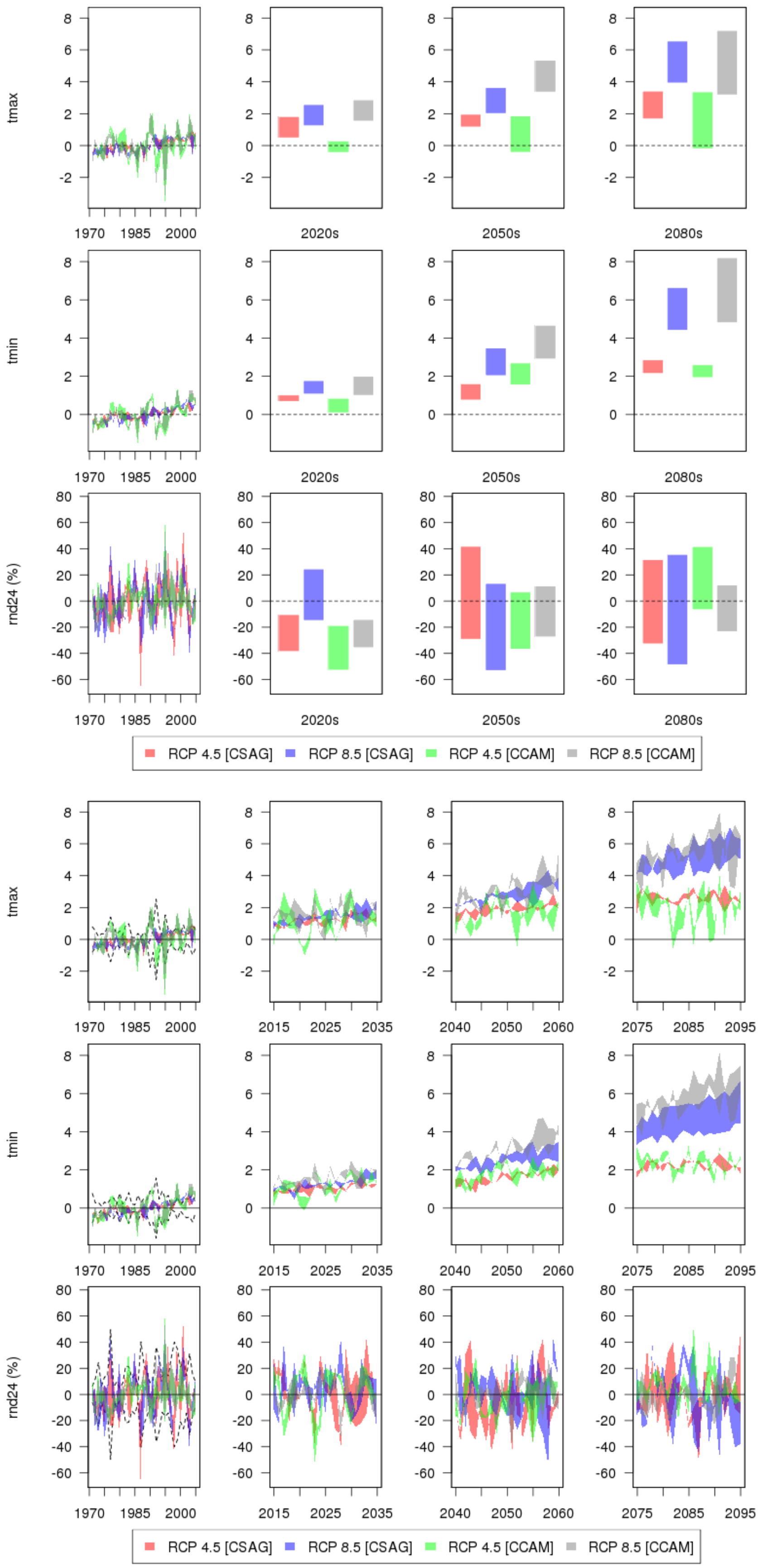

Figure A1.2.7: The DJF anomaly with respect to the model historical period – Namakwa

A1.2.3 MAM

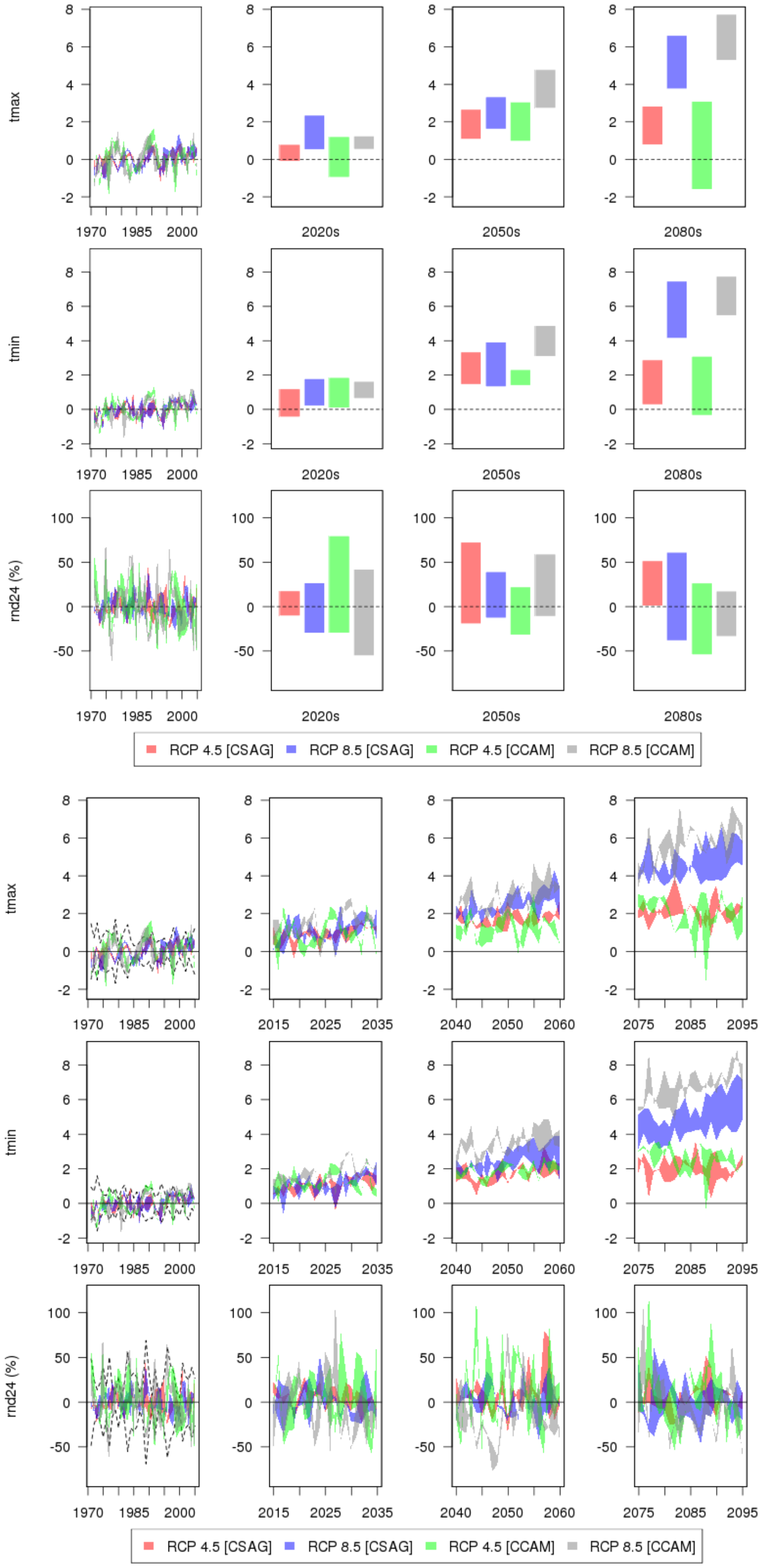

Figure A1.2.8: The MAM anomaly with respect to the model historical period – Namakwa

A1.2.4 JJA

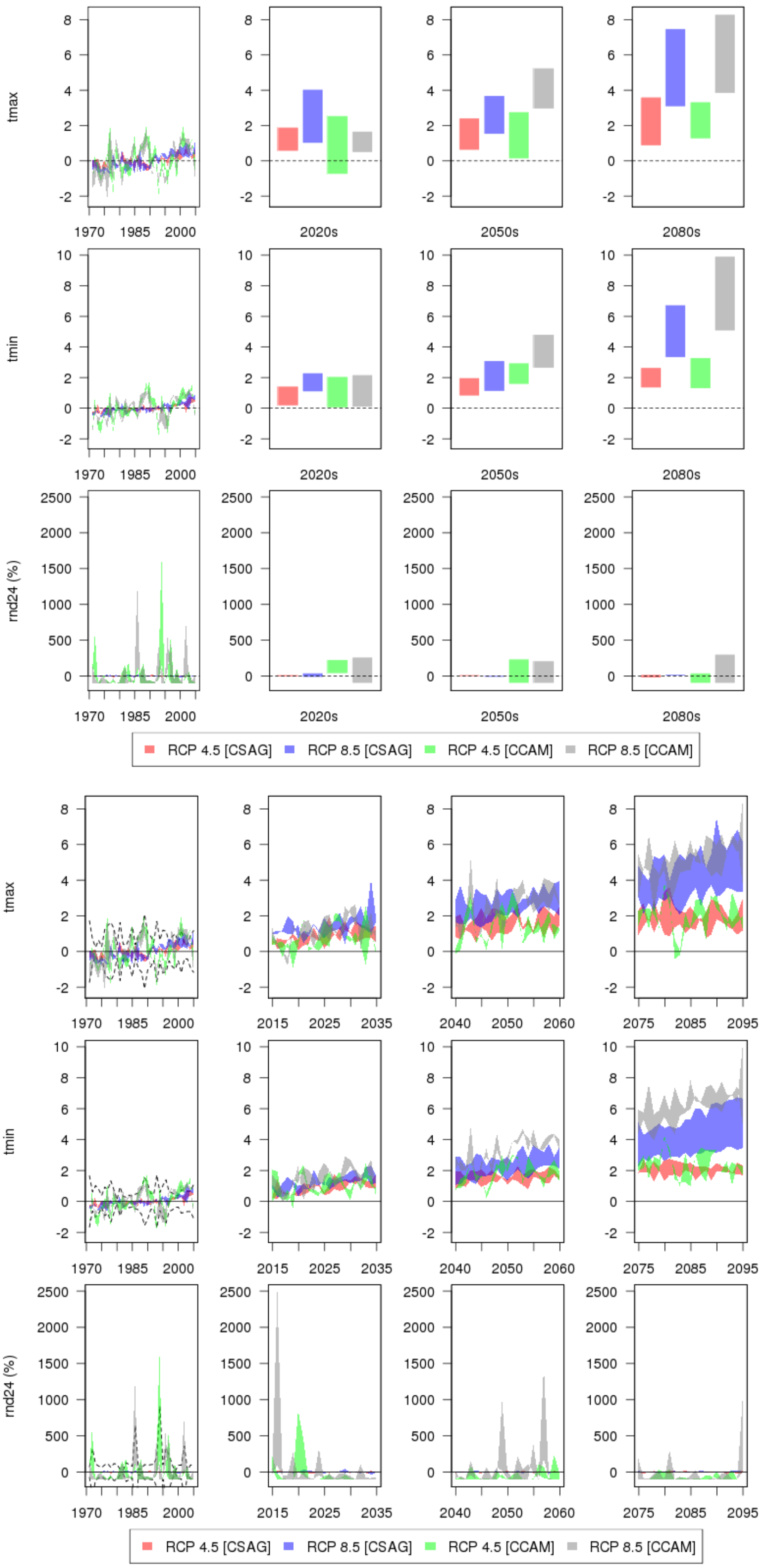

Figure A1.2.9: The JJA anomaly with respect to the model historical period – Namakwa

A1.2.5 SON

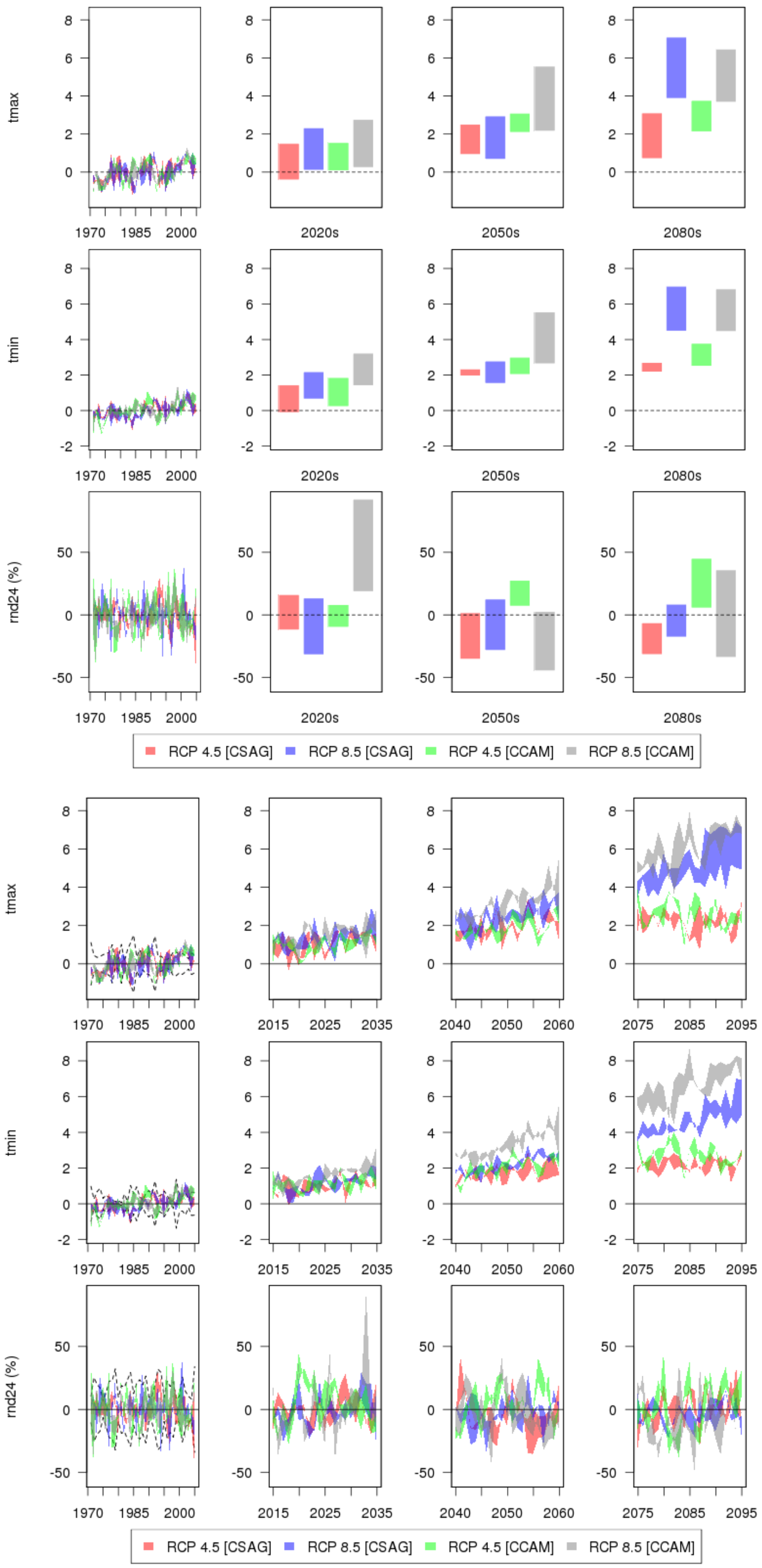

Figure A1.2.10: The SON anomaly with respect to the model historical period – Namakwa

Appendix B: Spatial plots

B1 Interpretation

For a given time-period, scenario and dataset:

The first to third rows represent the anomaly of the: 90th percentile of the model ensemble, the ensemble median, and the 10th percentile of the ensemble, respectively. The first to fifth column display the seasons: ANN, DJF, MAM, JJA, and SON, respectively.

Temperature anomaly in °C and precipitation anomaly in mm.

Note: For the Winter months (core JJA), the CCAM raw data was populated almost exclusively with zeroes. It appears as if there is a fault of sorts in the raw data. Please interpret the CCAM spatial plots for this period accordingly.

B1.1 Mopani

B1.1.1 CSAG

B1.1.1.1 2020s

B1.1.1.1a RCP4.5

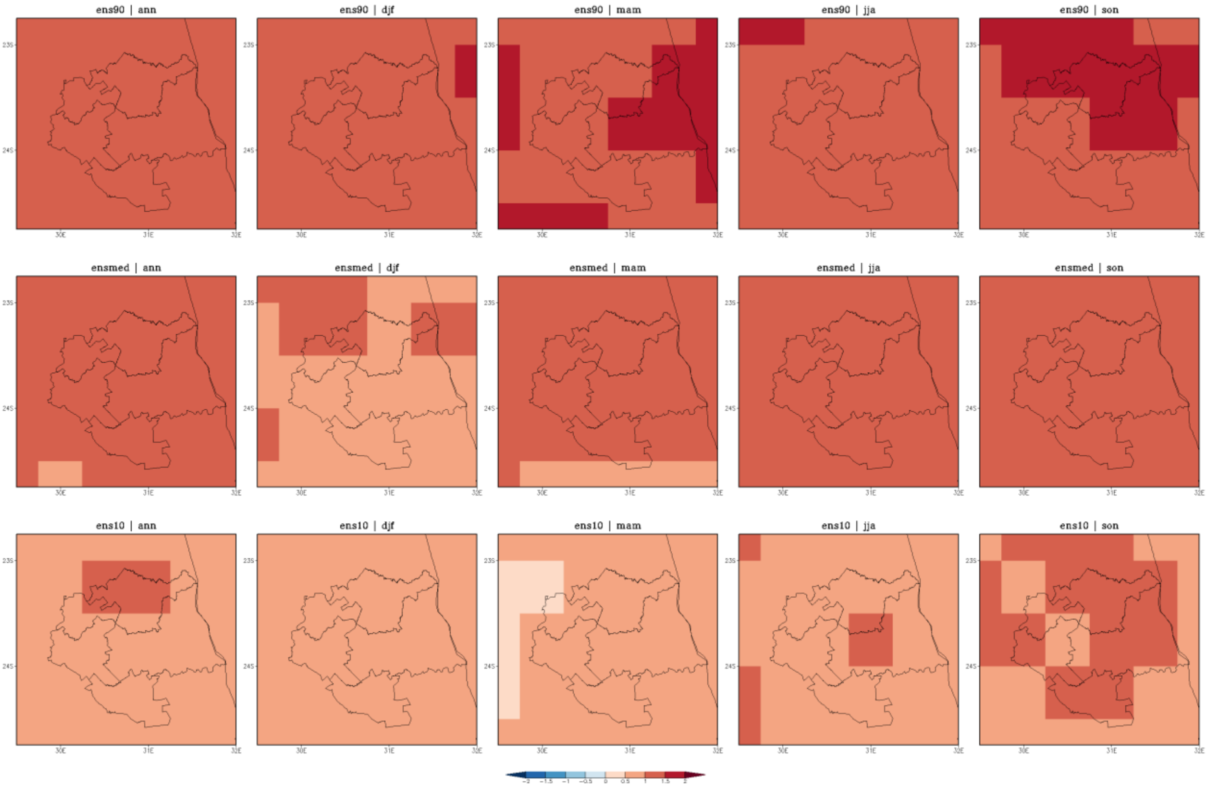

Figure B1.1.1.1a1: The **maximum temperature** anomaly with respect to the model historical period – Mopani

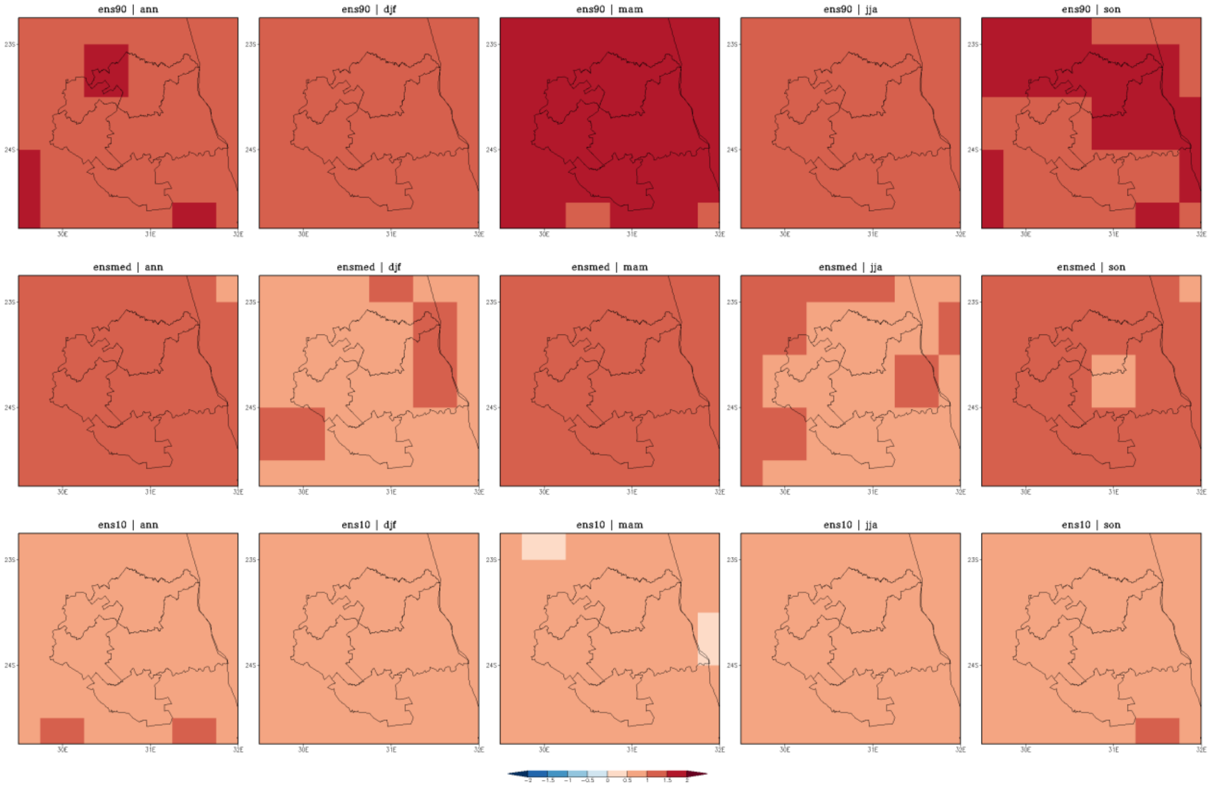

Figure B1.1.1.11a2: The **minimum temperature** anomaly with respect to the model historical period – Mopani

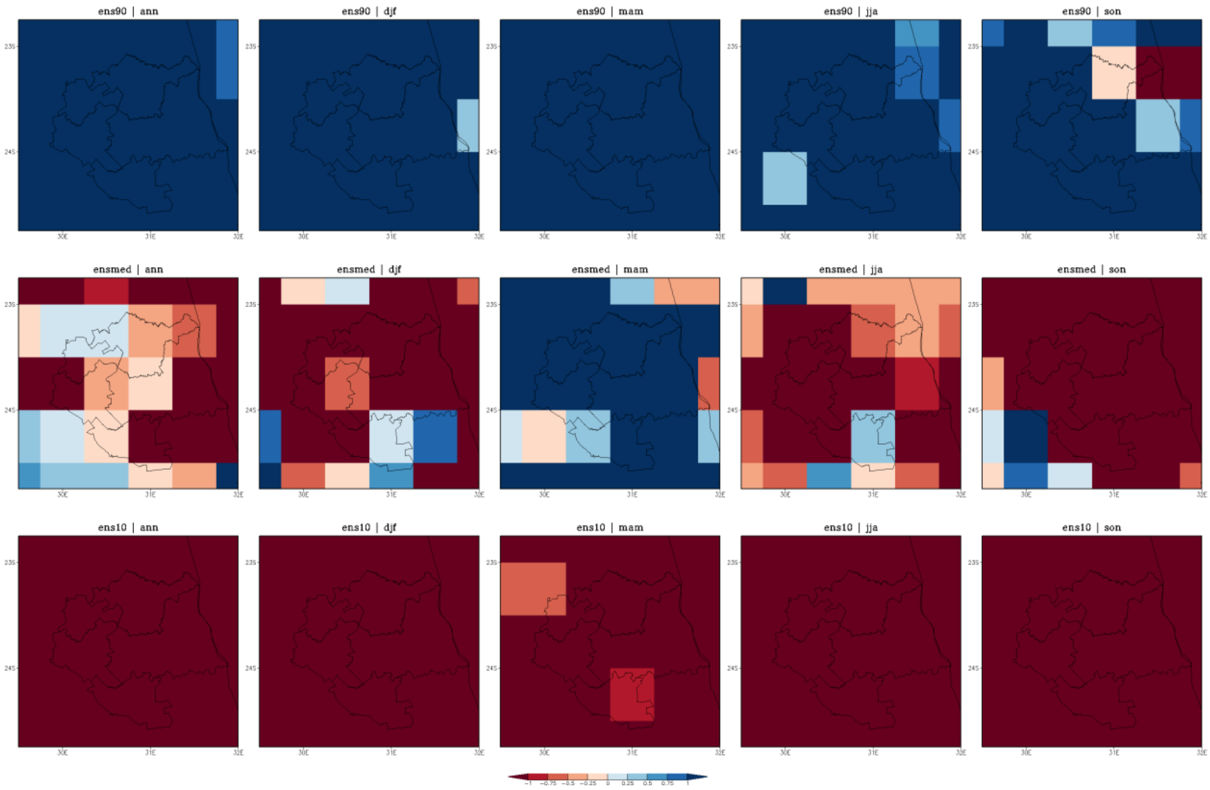

Figure B1.1.1.3a3: The **precipitation** anomaly with respect to the model historical period – Mopani

B1.1.1.1b RCP8.5

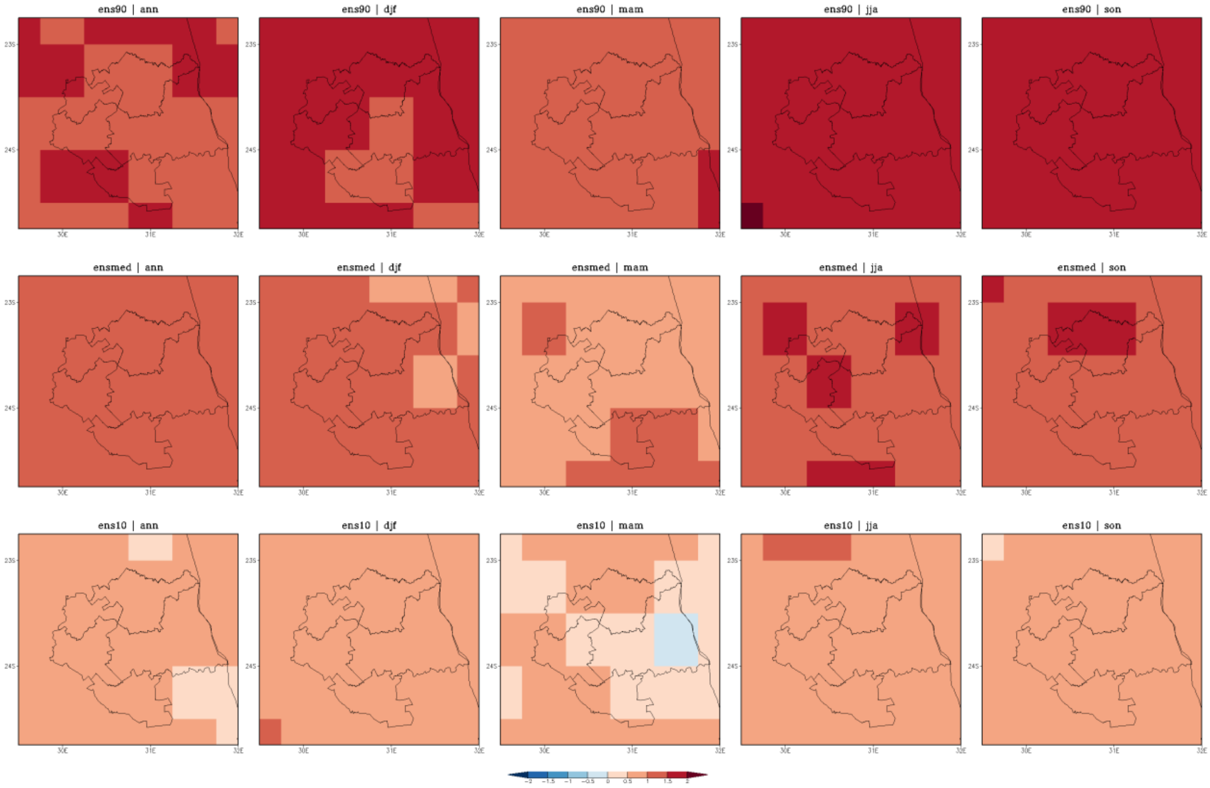

Figure B1.1.1.1b1: The **maximum temperature** anomaly with respect to the model historical period – Mopani

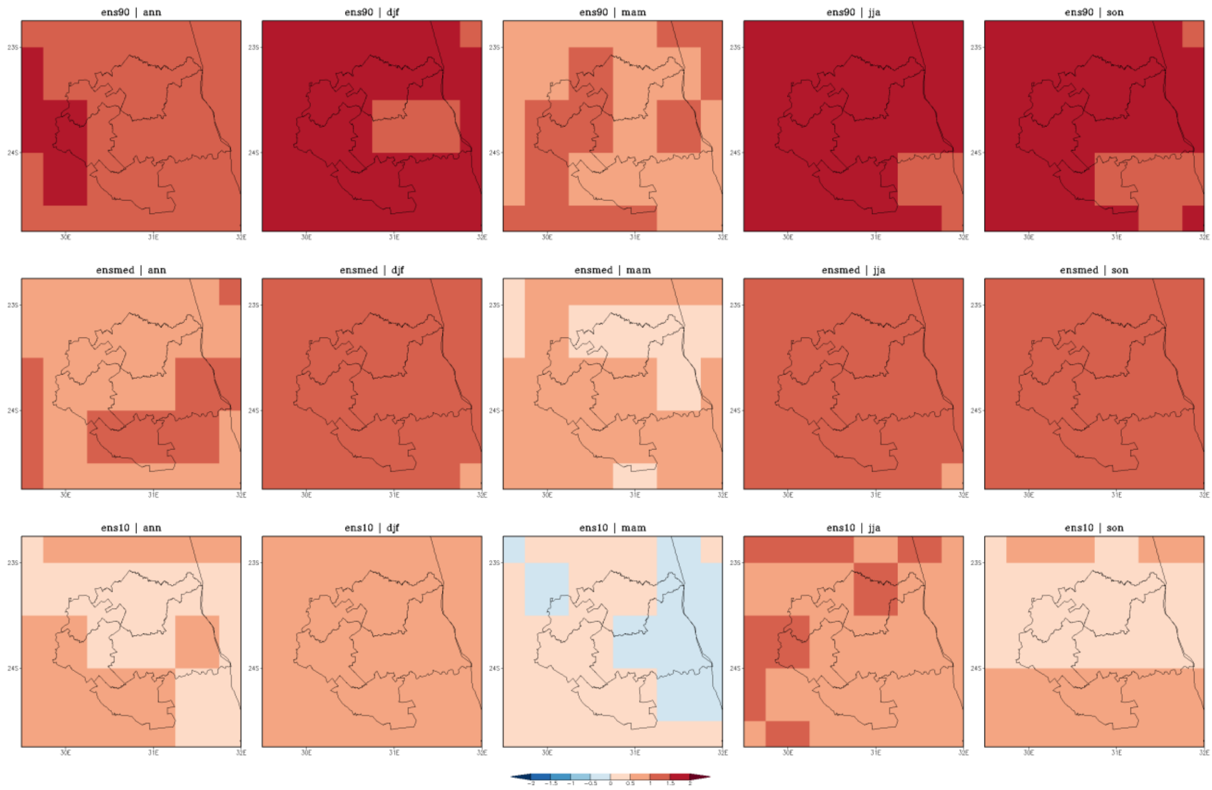

Figure B1.1.1.212b2: The **minimum temperature** anomaly with respect to the model historical period – Mopani

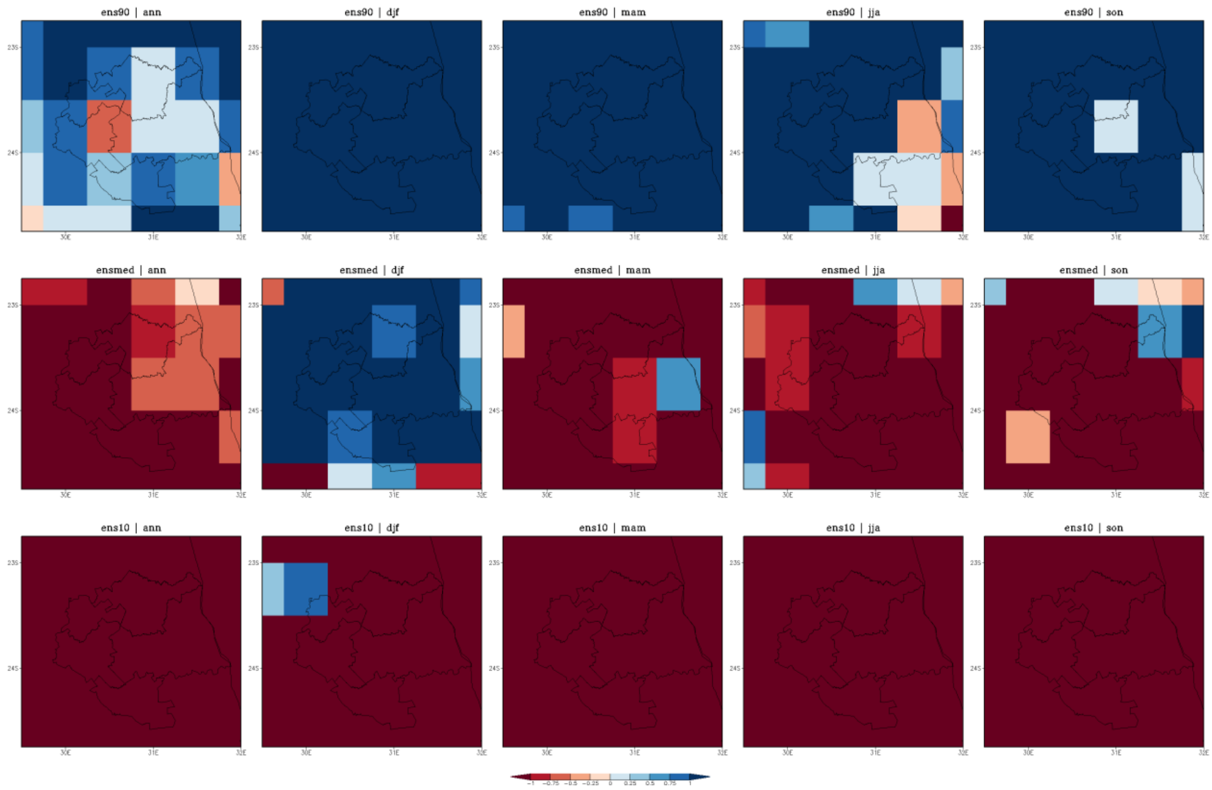

Figure B1.1.1.3b3: The **precipitation** anomaly with respect to the model historical period – Mopani

B1.1.1.2 2050s

B1.1.1.2a RCP4.5

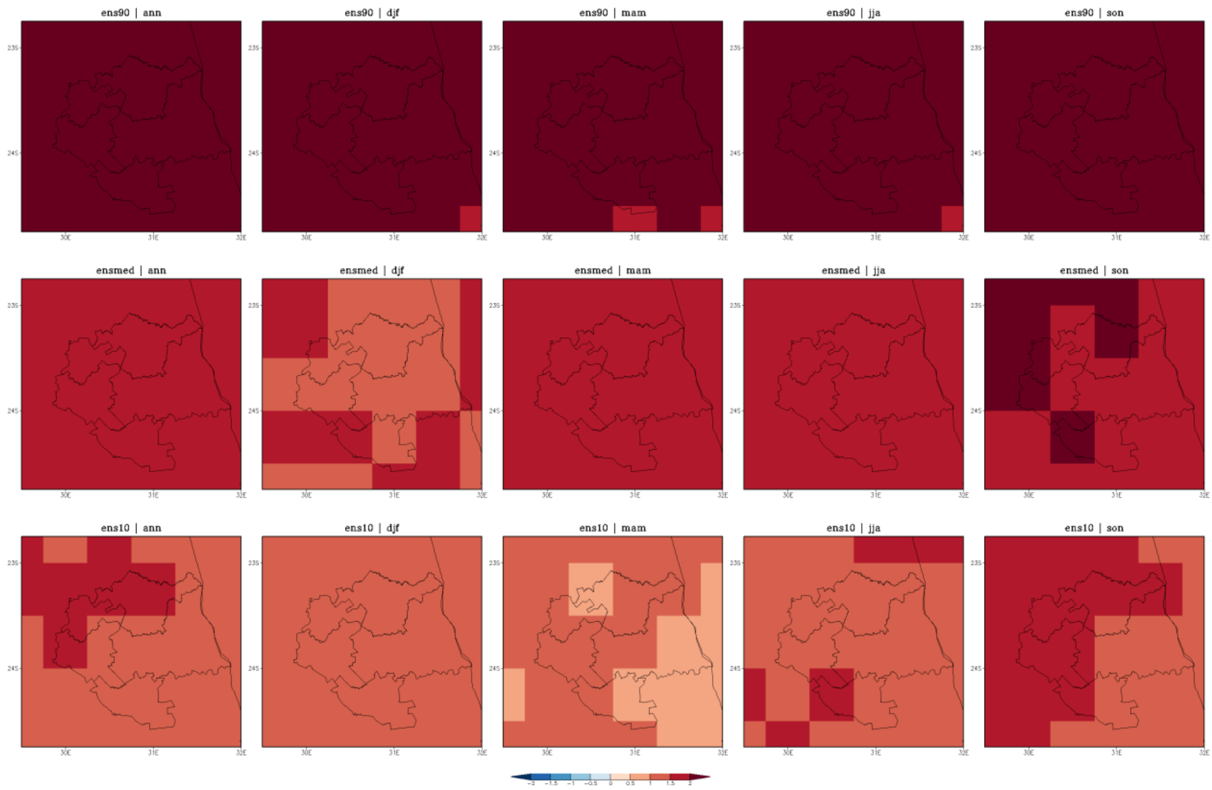

Figure B1.1.1.113a1: The **maximum temperature** anomaly with respect to the model historical period – Mopani

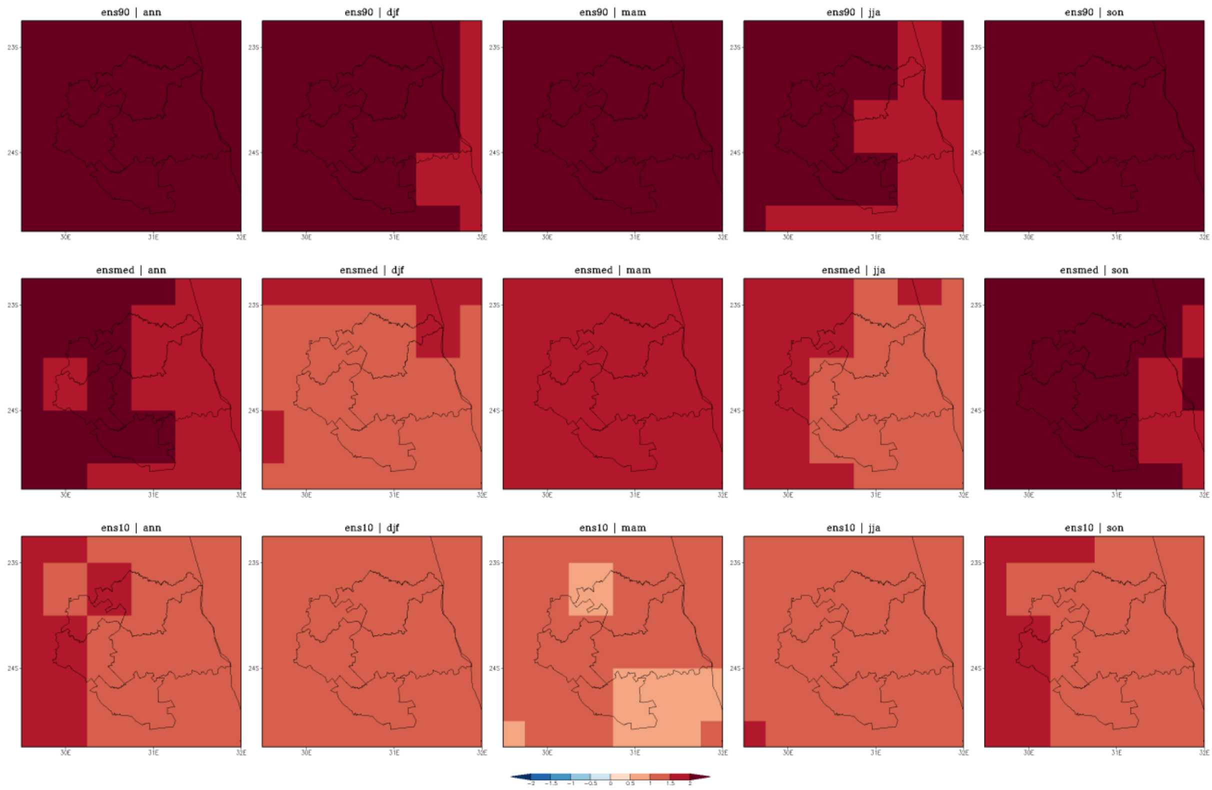

Figure B1.1.1.2a2: The **minimum temperature** anomaly with respect to the model historical period – Mopani

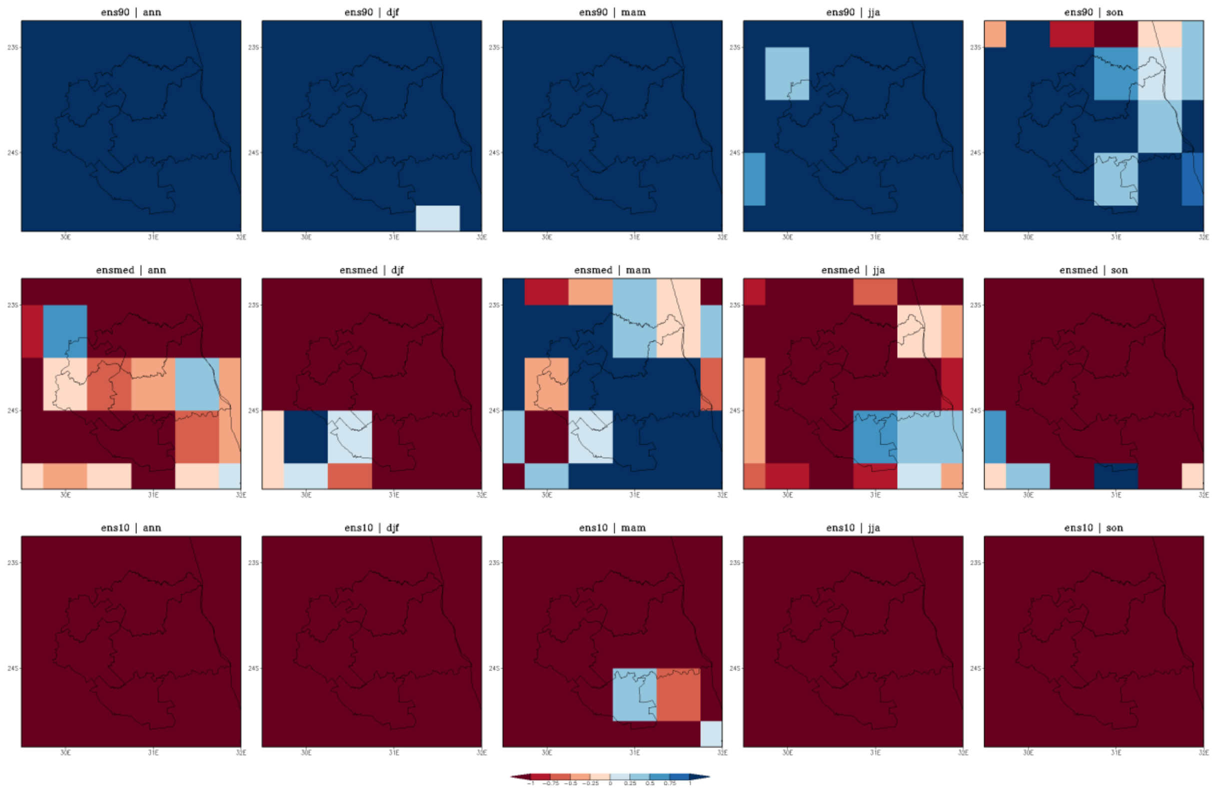

Figure B1.1.1.3a3: The **precipitation** anomaly with respect to the model historical period – Mopani

B1.1.1.2b RCP8.5

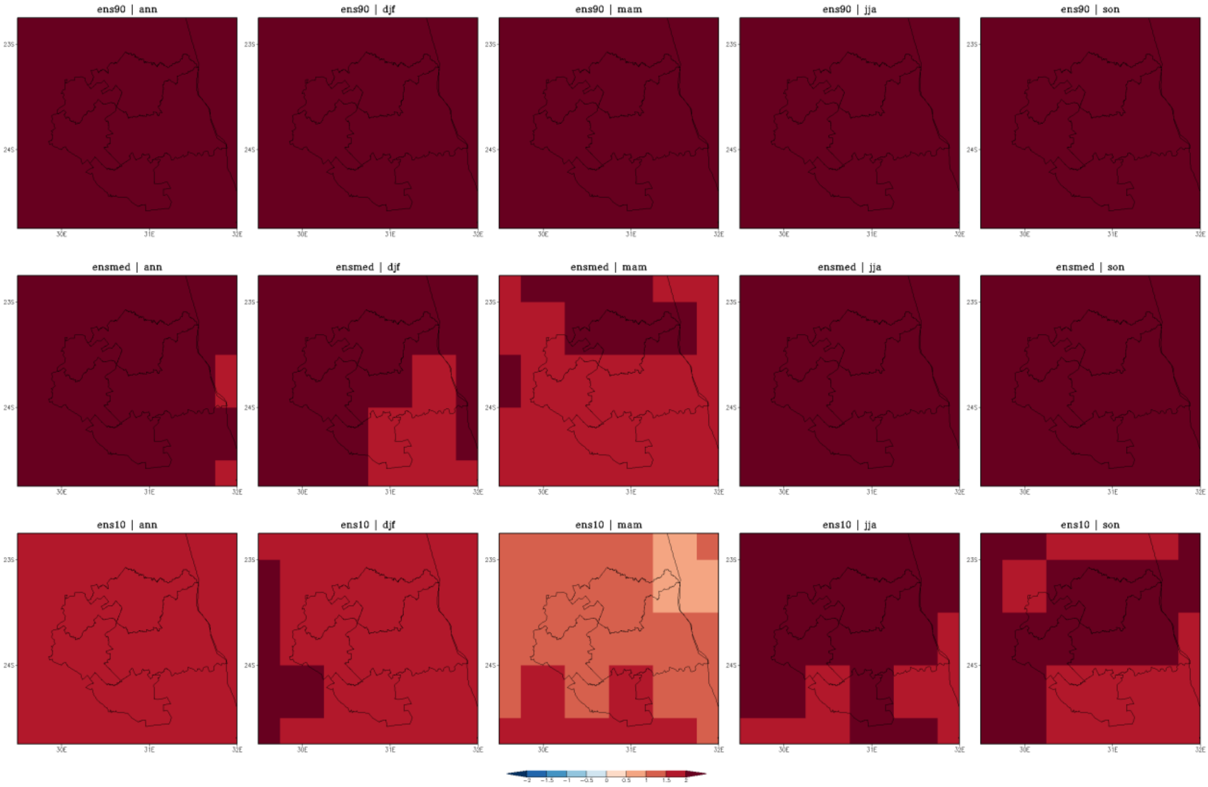

FigureB1.1.1.1b1: The **maximum temperature** anomaly with respect to the model historical period – Mopani

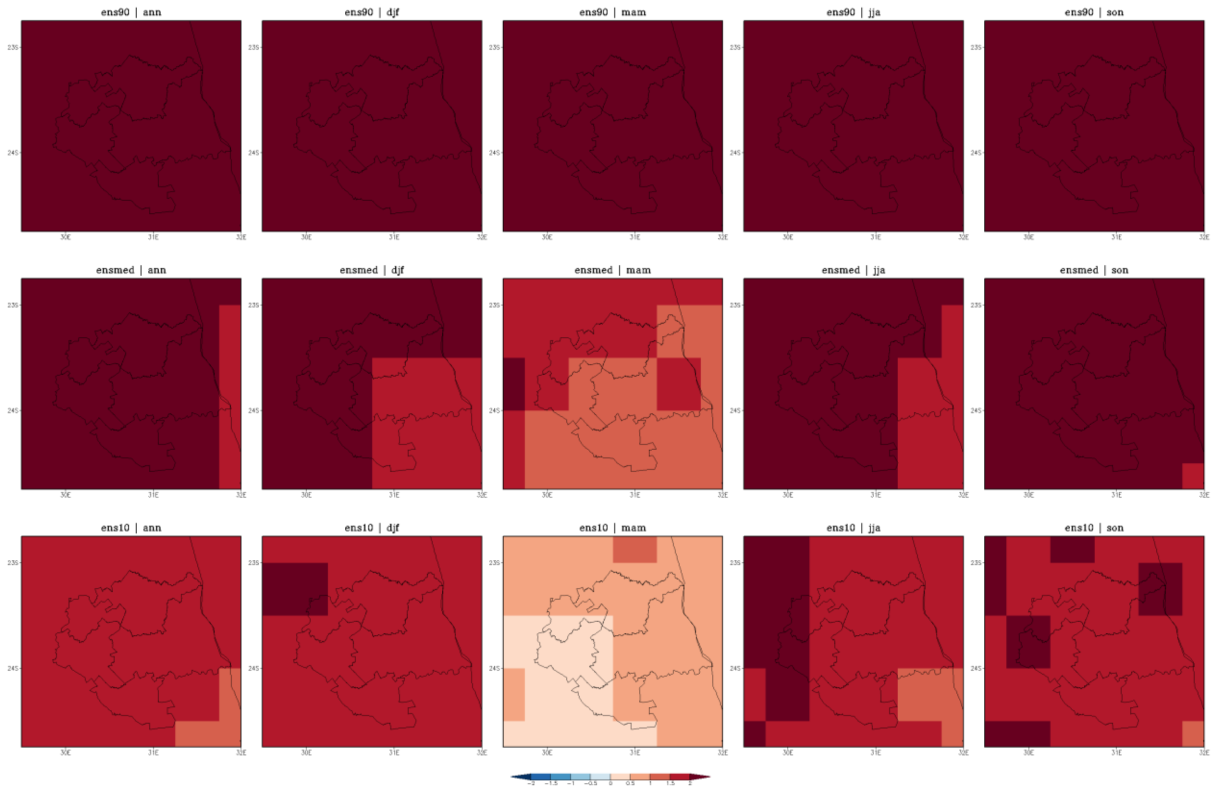

Figure B1.1.1.14b2: The **minimum temperature** anomaly with respect to the model historical period – Mopani

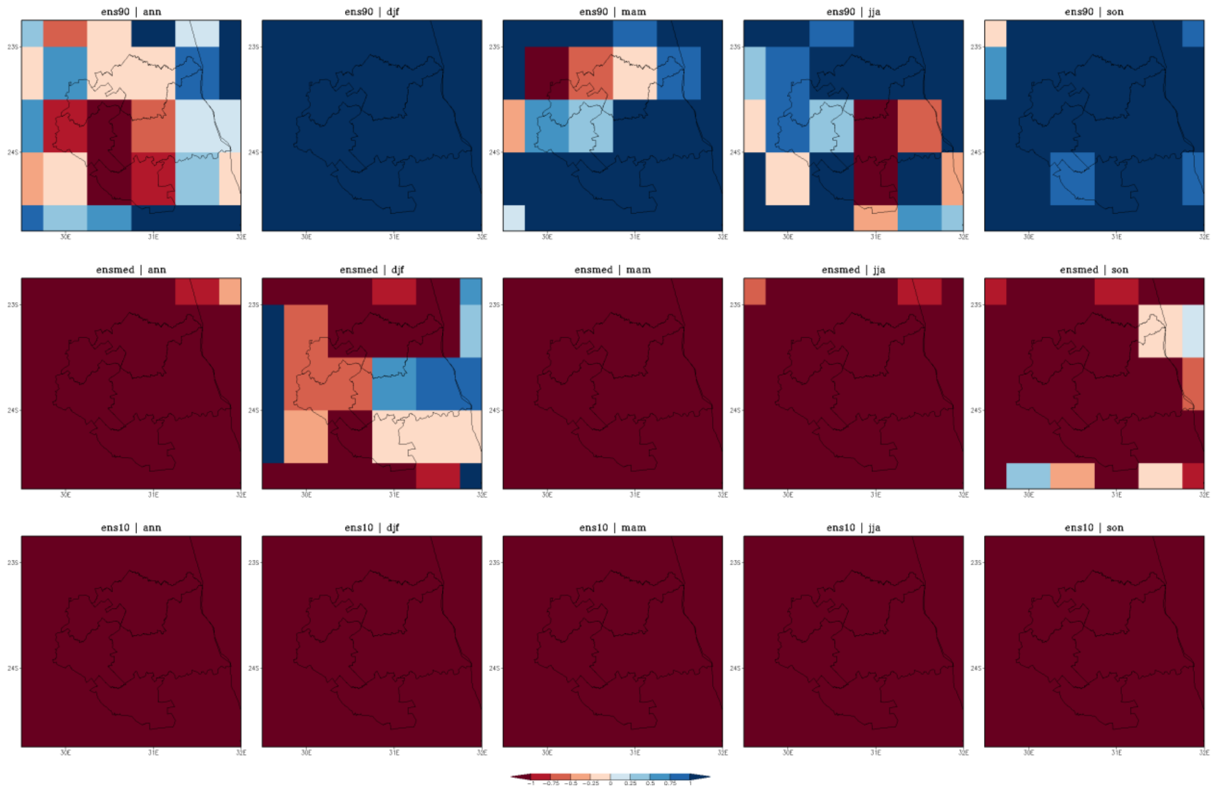

Figure B1.1.1.3b3: The **precipitation** anomaly with respect to the model historical period – Mopani

B1.1.1.3 2080s

B1.1.1.3a RCP4.5

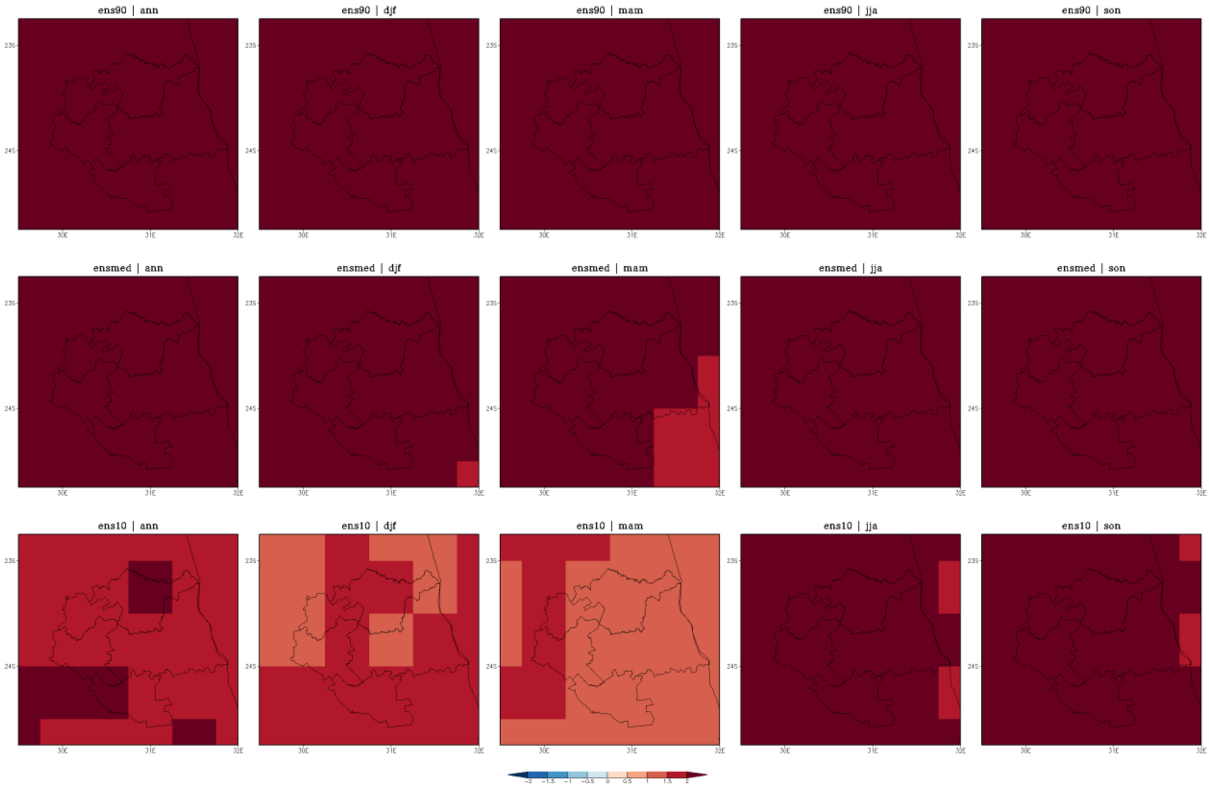

Figure B1.1.1.1a1: The **maximum temperature** anomaly with respect to the model historical period – Mopani

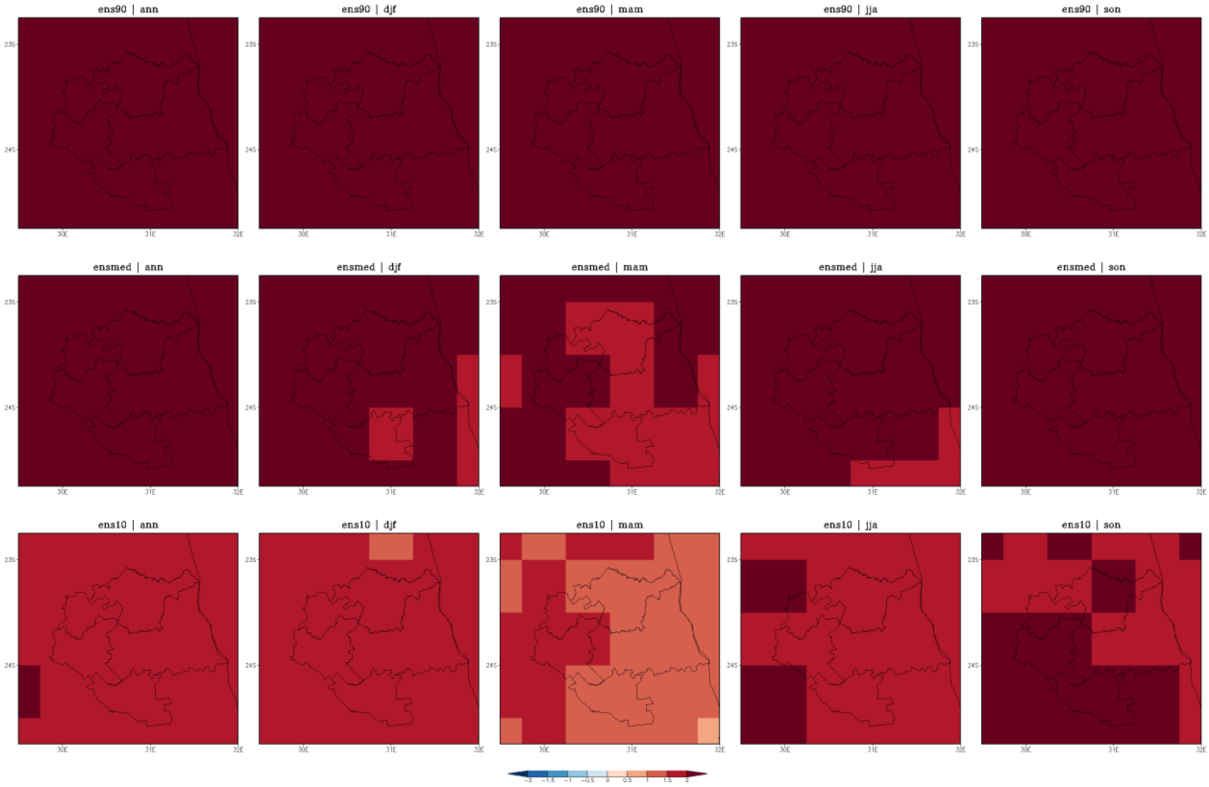

Figure B1.1.1.2a2: The **minimum temperature** anomaly with respect to the model historical period – Mopani

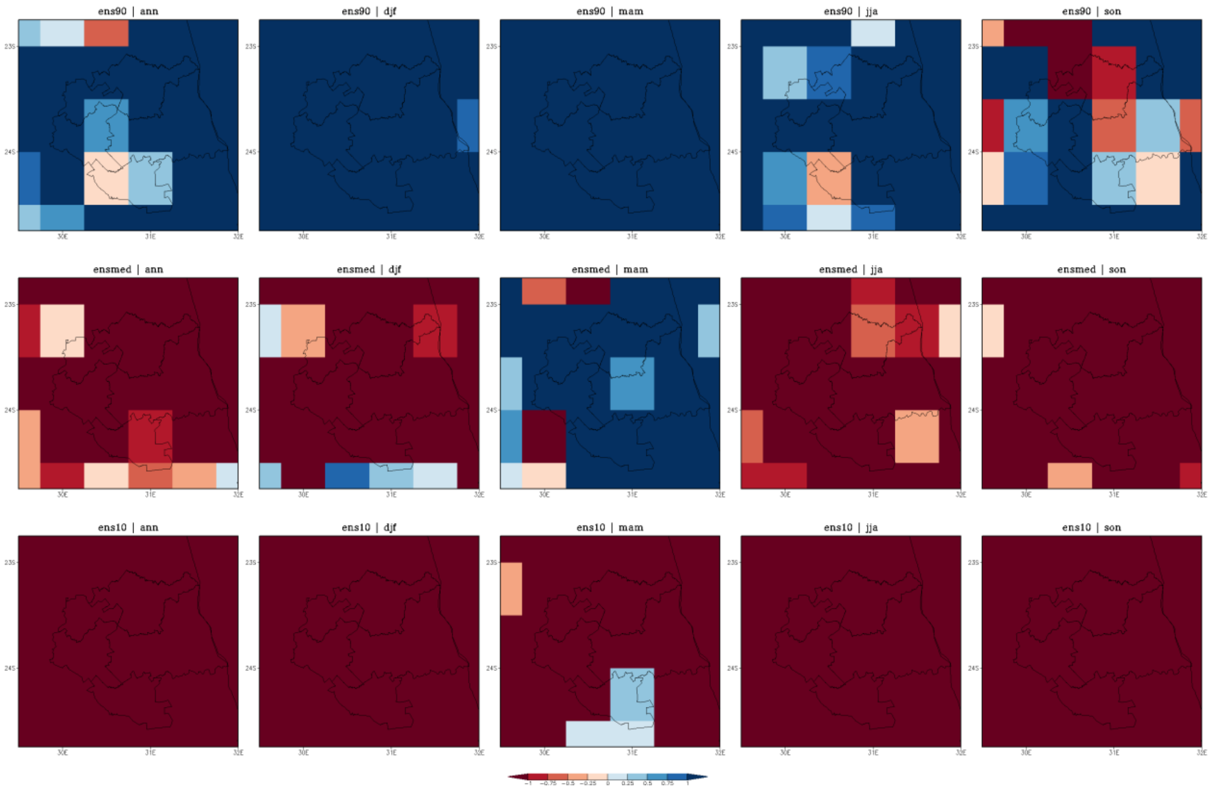

Figure B1.1.1.3a3: The **precipitation** anomaly with respect to the model historical period – Mopani

B1.1.1.3b RCP8.5

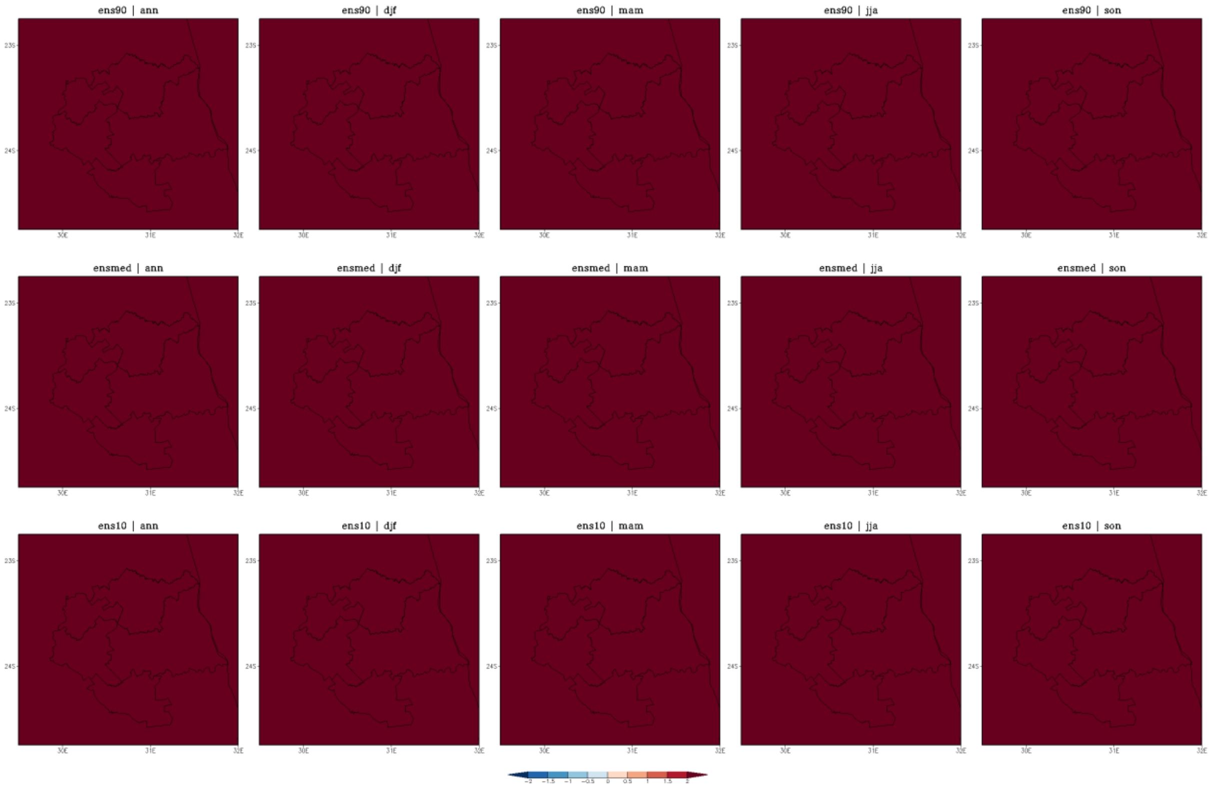

Figure B1.1.1.1b1: The **maximum temperature** anomaly with respect to the model historical period – Mopani

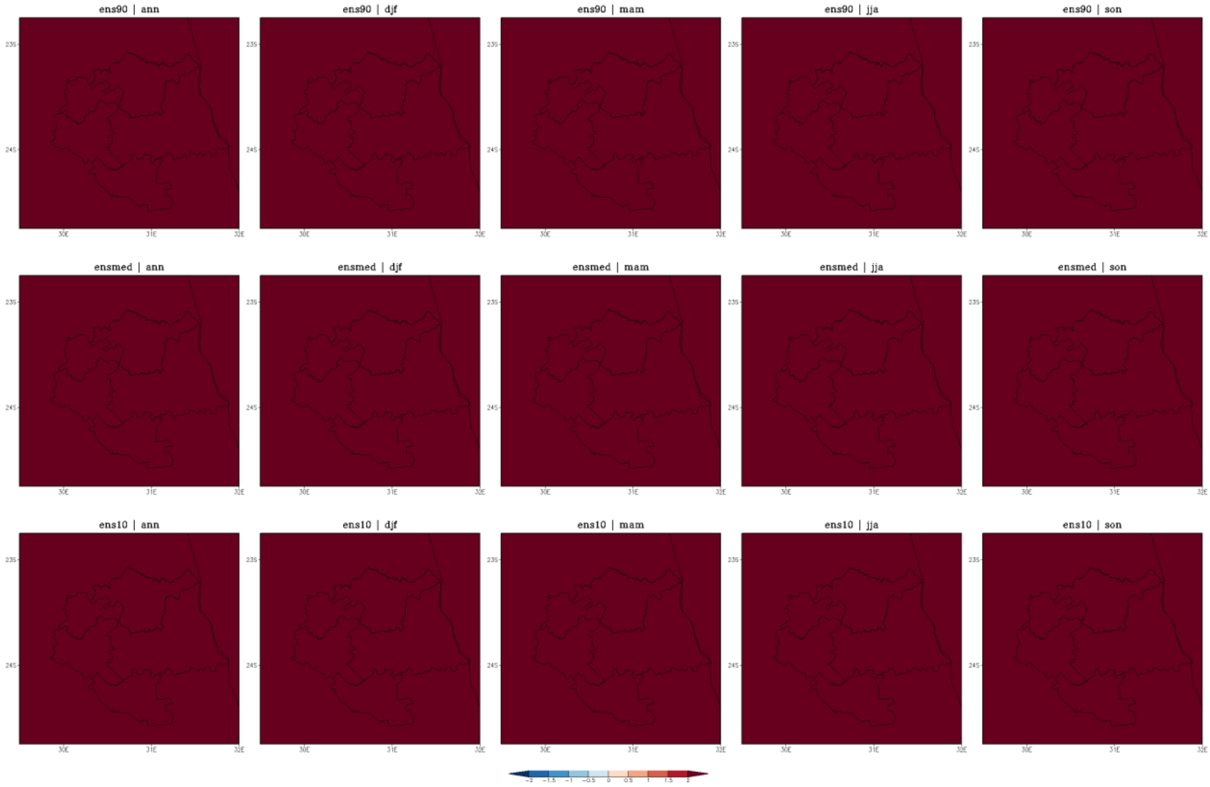

Figure B1.1.1.2b2: The **minimum temperature** anomaly with respect to the model historical period – Mopani

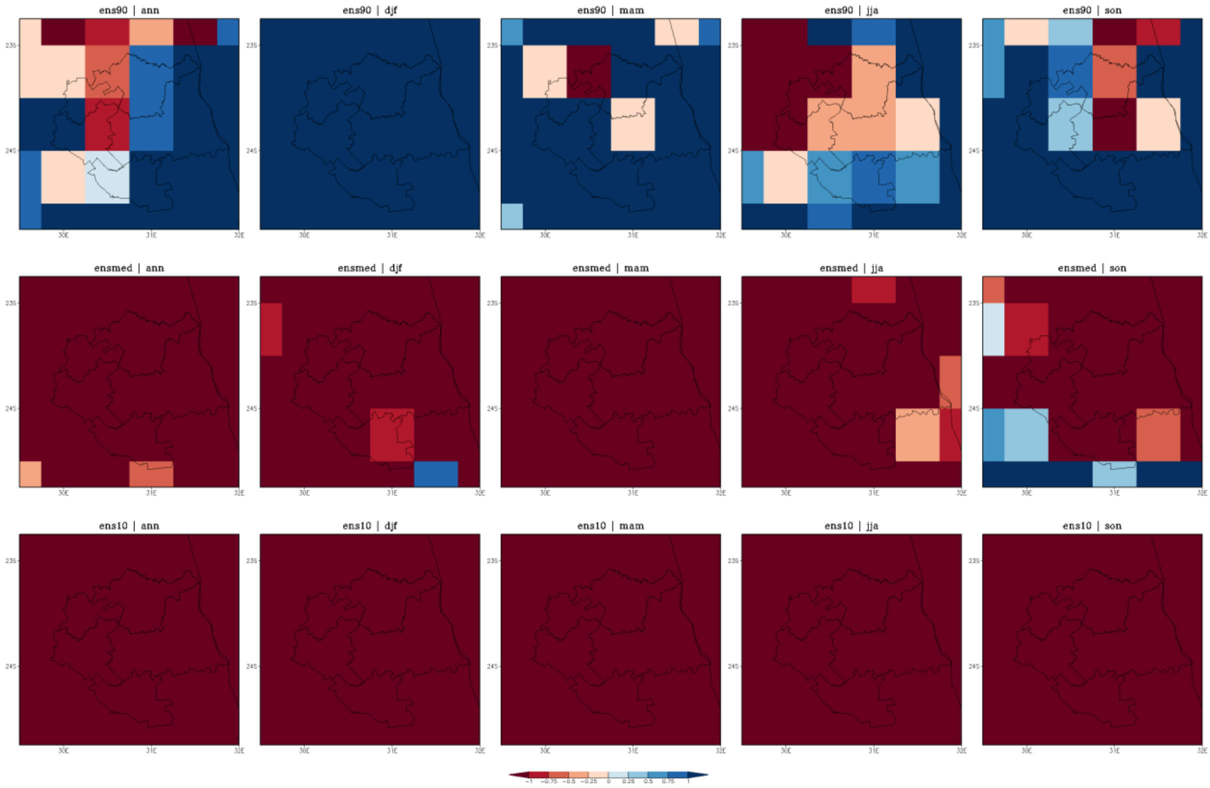

Figure B1.1.1.3b3: The **precipitation** anomaly with respect to the model historical period – Mopani

B1.1.2 CCAM

B1.1.2.1 2020s

B1.1.2.1a RCP4.5

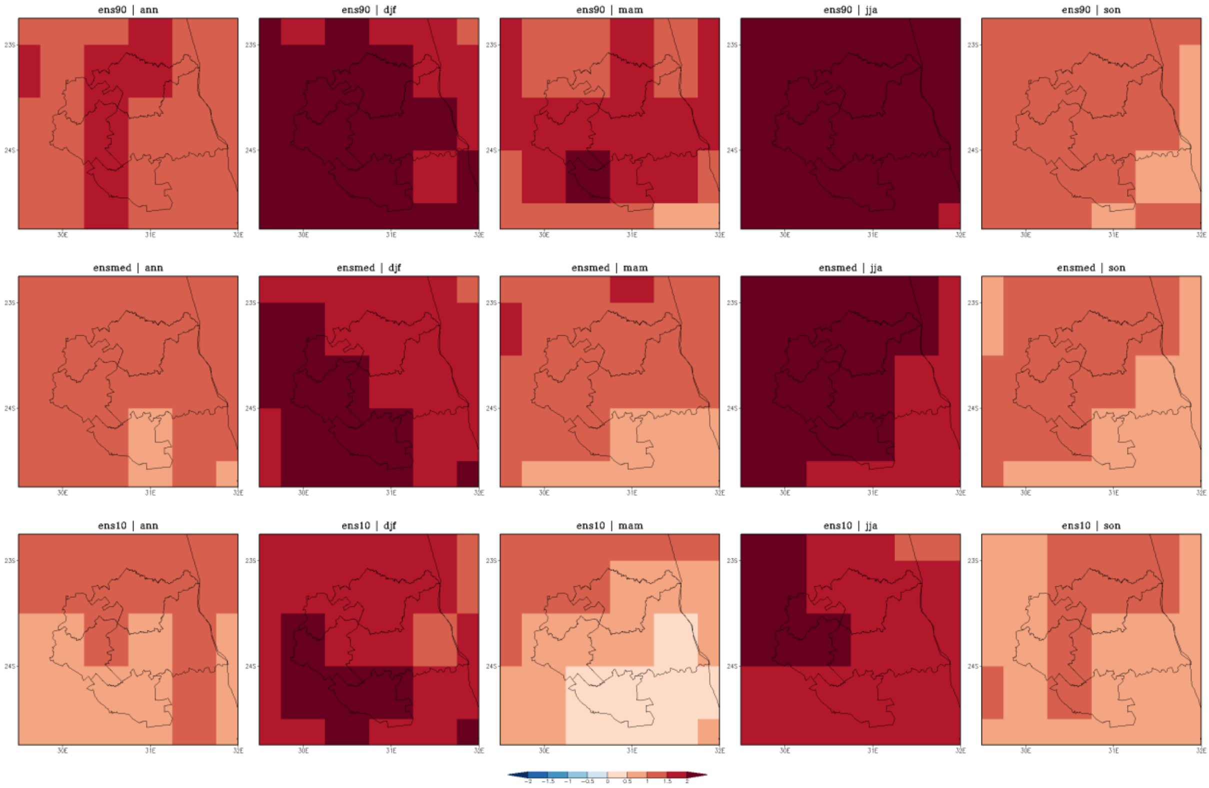

Figure B1.1.2.1a1: The **maximum temperature** anomaly with respect to the model historical period – Mopani

Figure B1.1.2.2a2: The **minimum temperature** anomaly with respect to the model historical period – Mopani

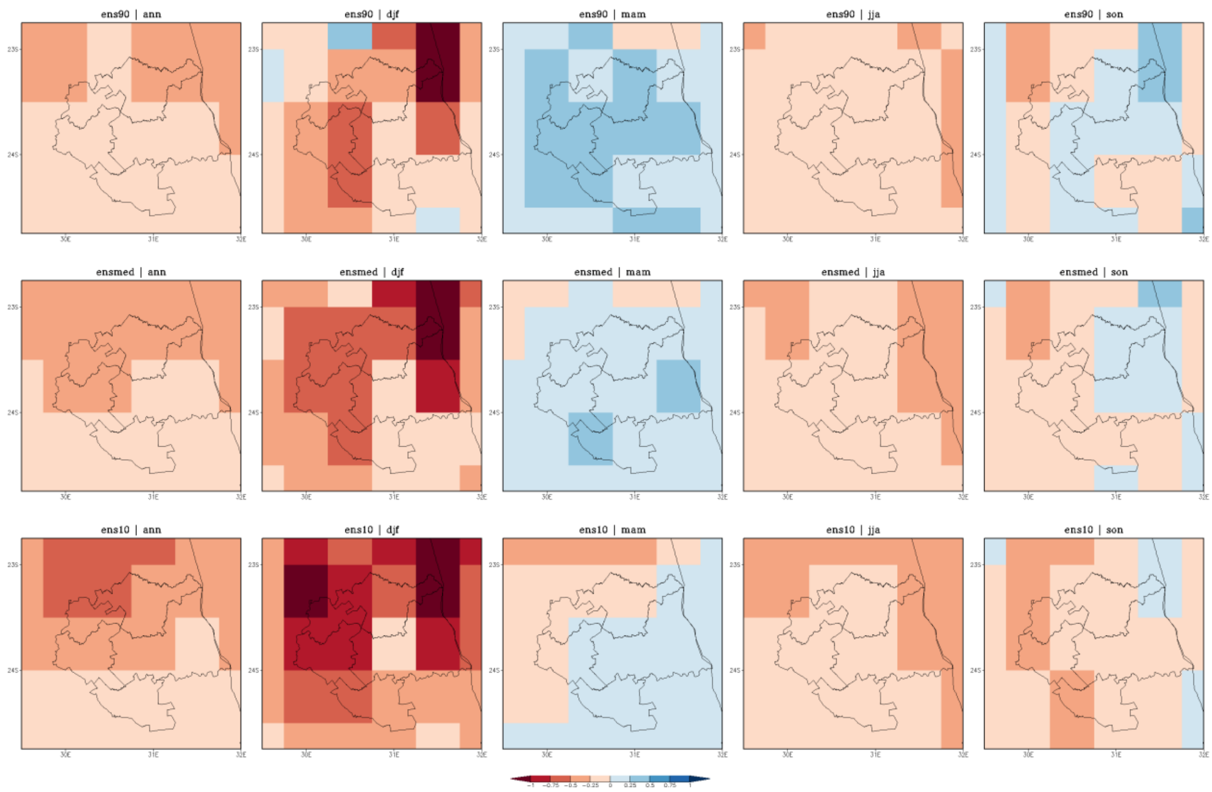

Figure B1.1.2.3a3: The **precipitation** anomaly with respect to the model historical period – Mopani

B1.1.2.1b RCP8.5

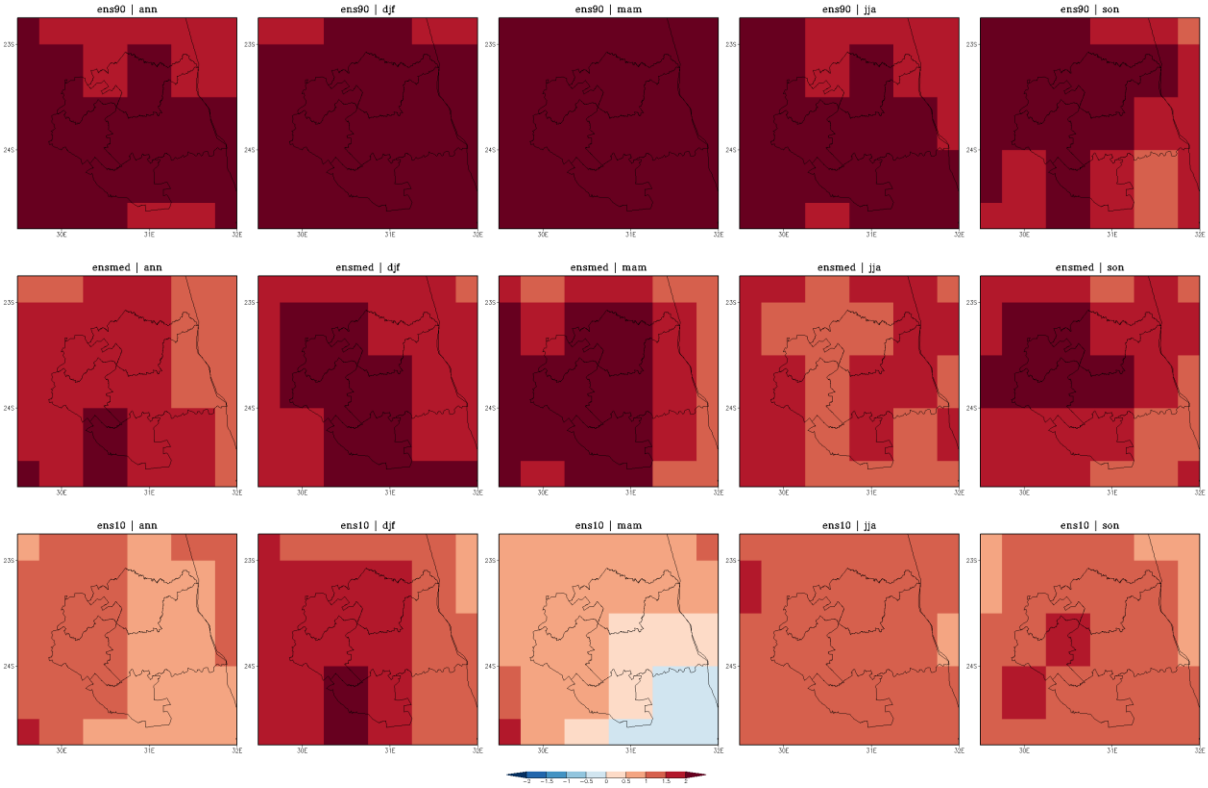

Figure B1.1.2.1b1: The **maximum temperature** anomaly with respect to the model historical period – Mopani

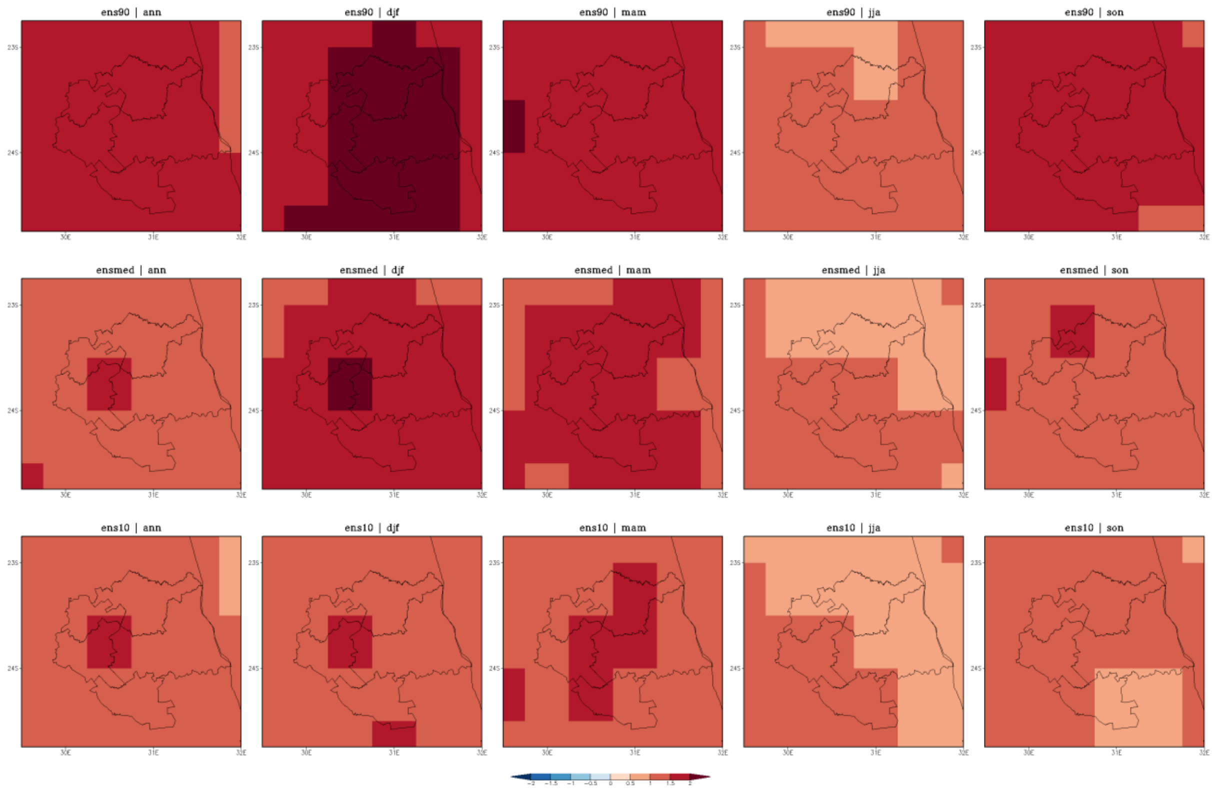

Figure B1.1.2.2b2: The **minimum temperature** anomaly with respect to the model historical period – Mopani

Figure B1.1.2.3b3: The **precipitation** anomaly with respect to the model historical period – Mopani

B1.1.2.2 2050s

B1.1.2.2a RCP4.5

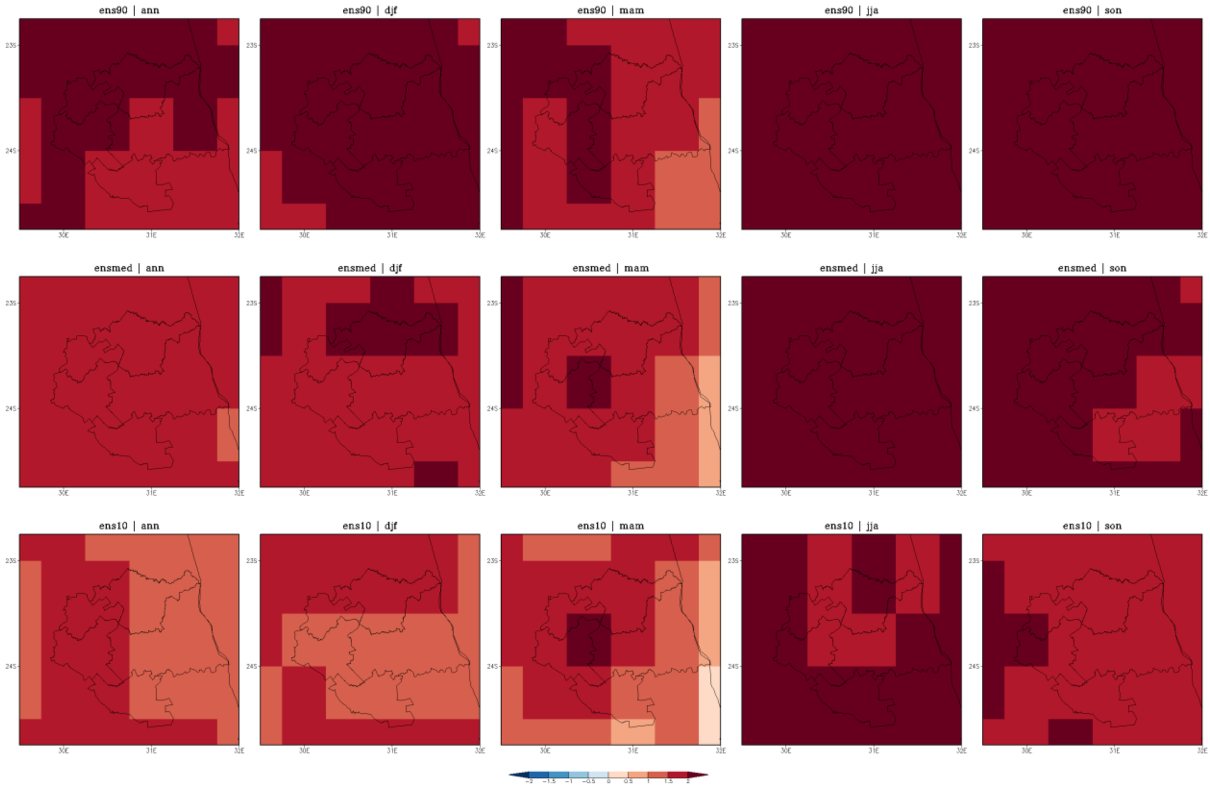

Figure B1.1.2.1a1: The **maximum temperature** anomaly with respect to the model historical period – Mopani

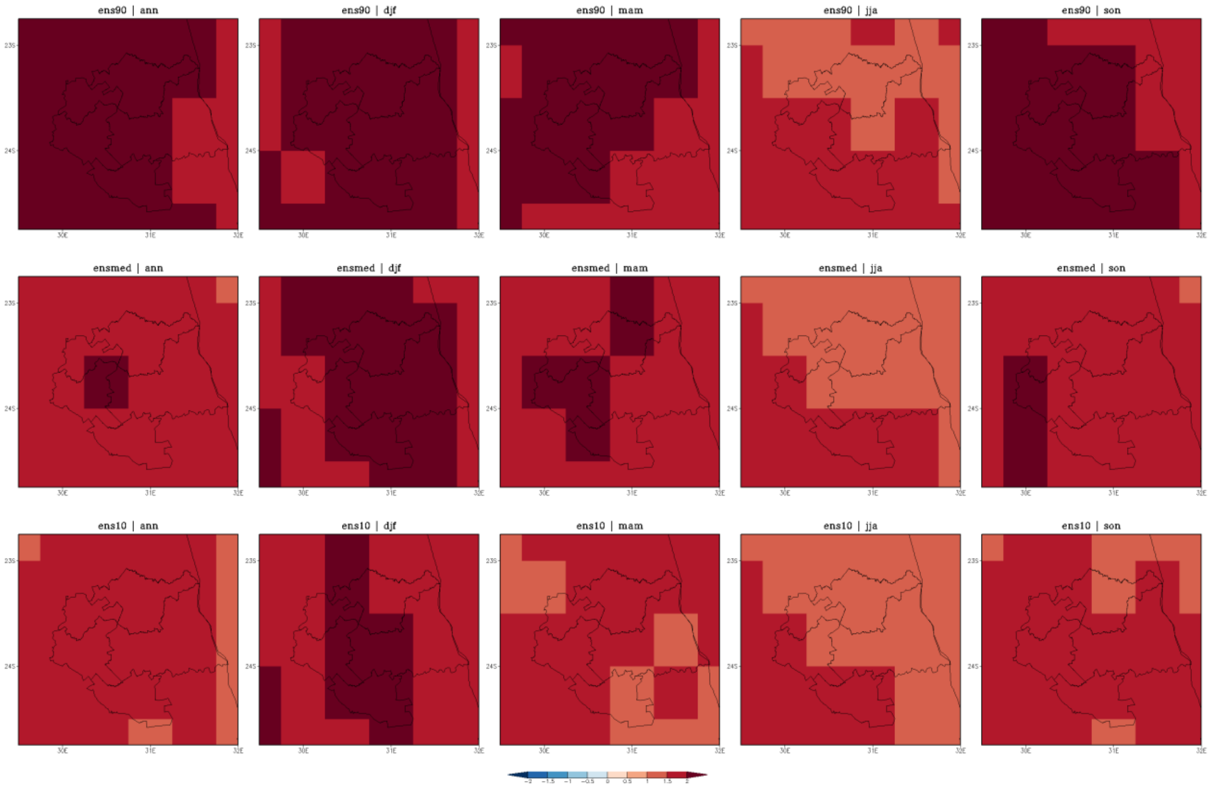

Figure B1.1.2.2a2: The **minimum temperature** anomaly with respect to the model historical period – Mopani

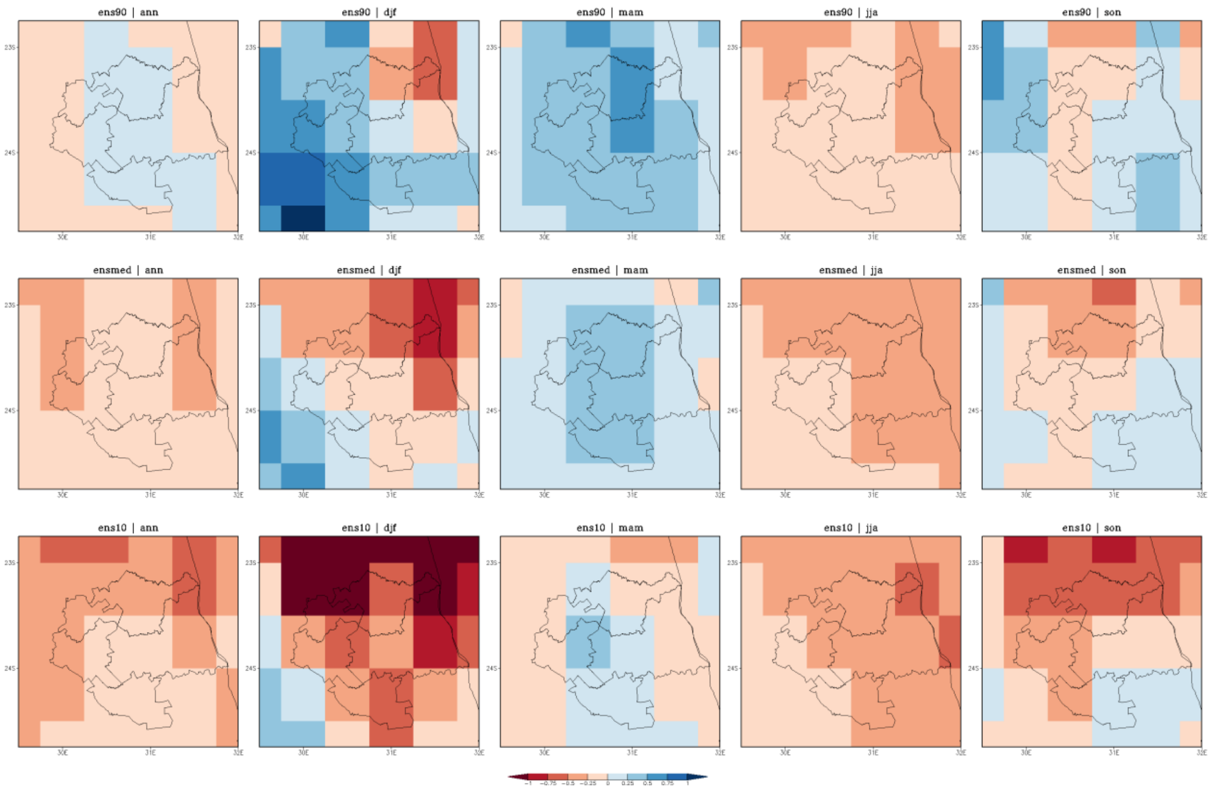

Figure B1.1.2.3a3: The **precipitation** anomaly with respect to the model historical period – Mopani

B1.1.2.2b RCP8.5

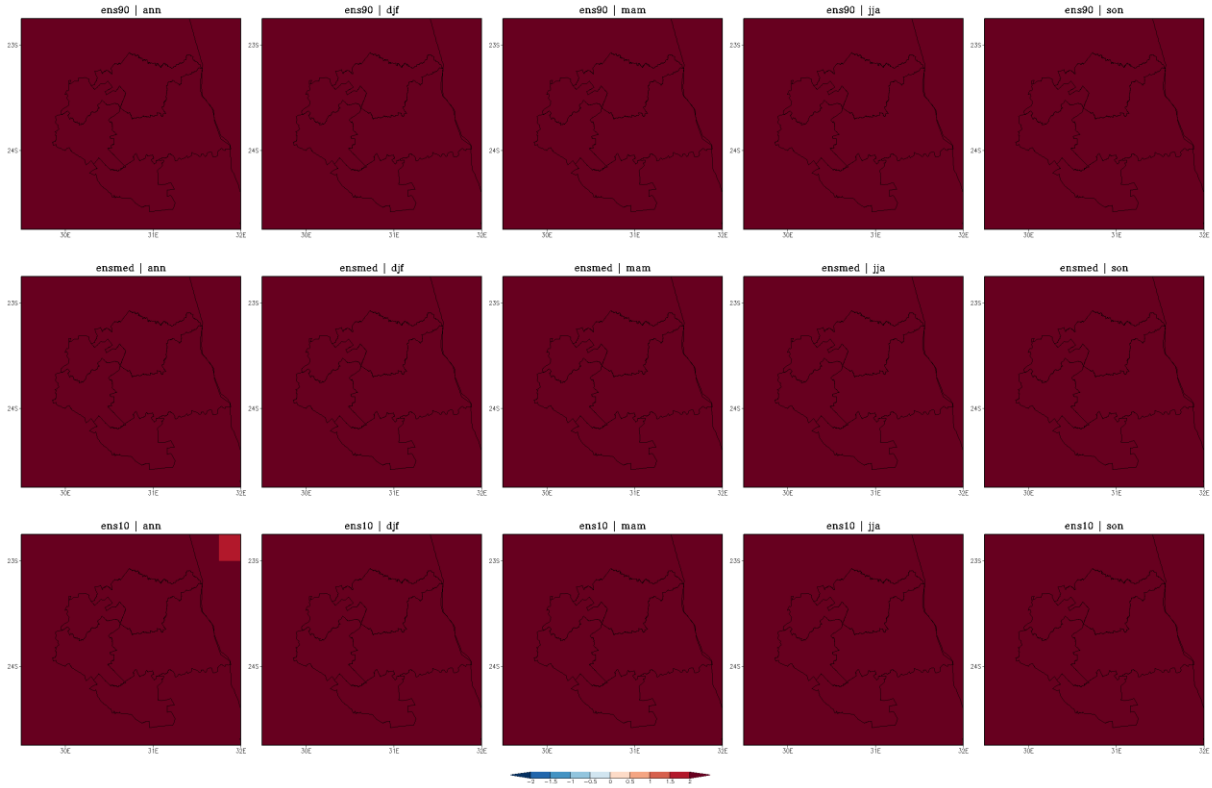

Figure B1.1.2.1b1: The **maximum temperature** anomaly with respect to the model historical period – Mopani

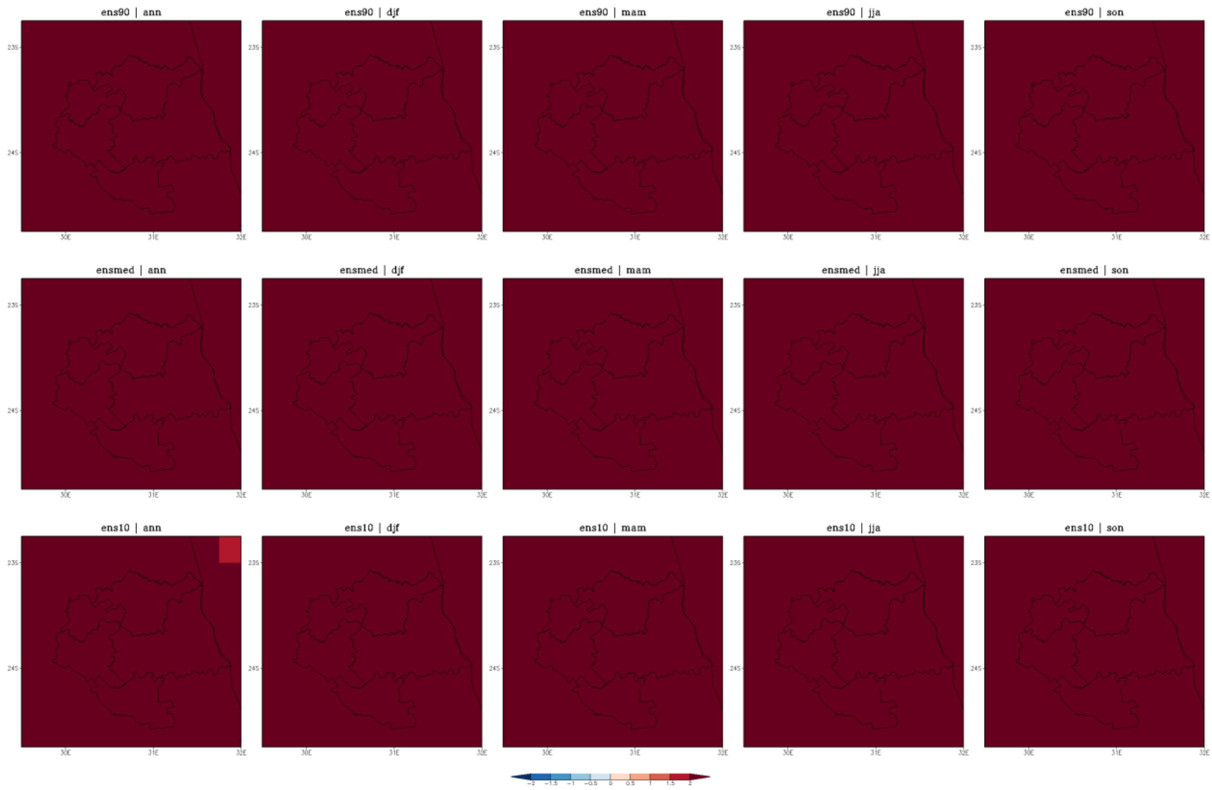

Figure B1.1.2.2b2: The **minimum temperature** anomaly with respect to the model historical period – Mopani

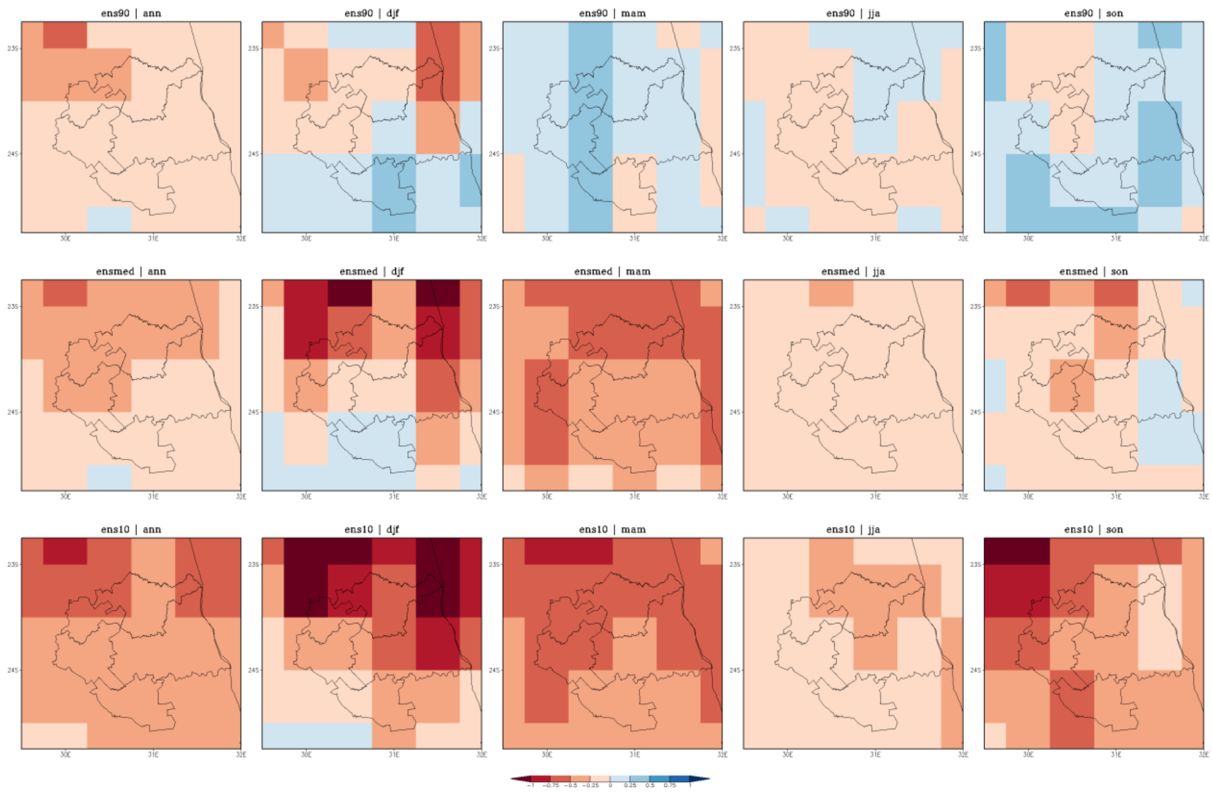

Figure B1.1.2.3b3: The **precipitation** anomaly with respect to the model historical period – Mopani

B1.1.2.3 2080s

B1.1.2.3a RCP4.5

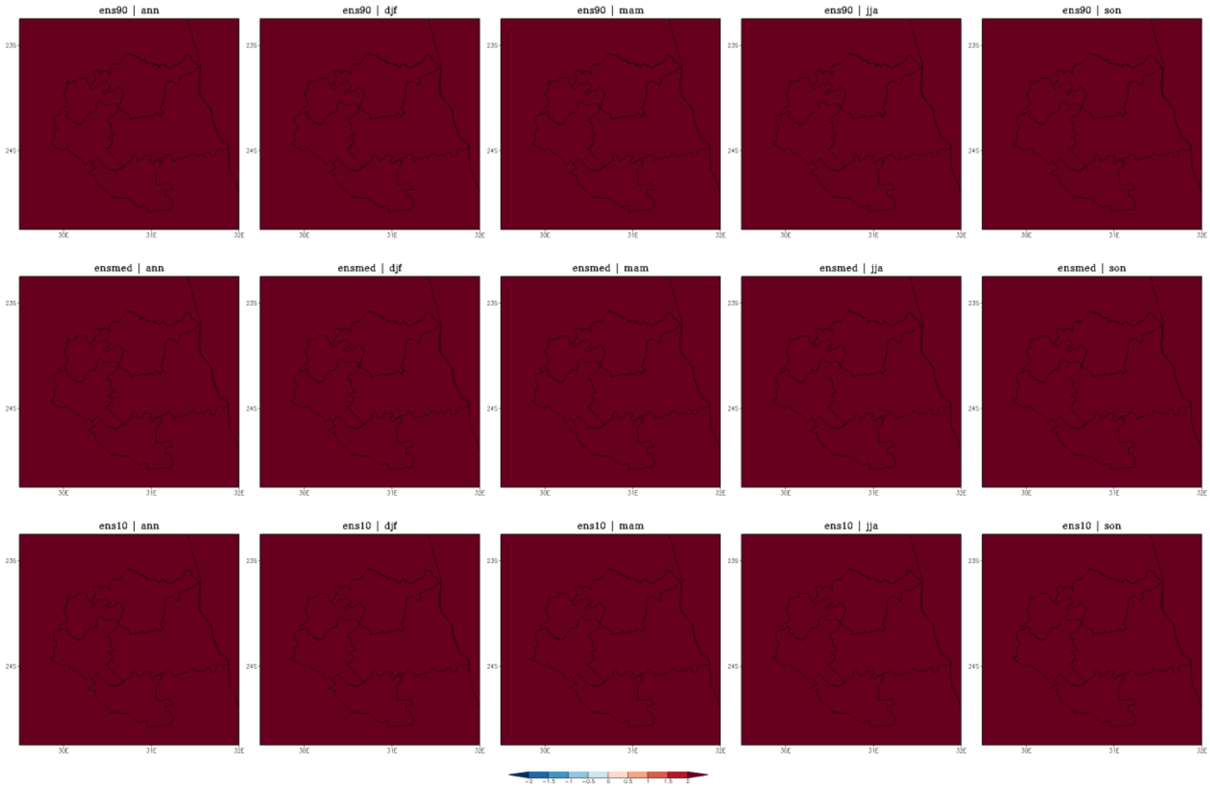

Figure B1.1.2.1a1: The **maximum temperature** anomaly with respect to the model historical period – Mopani

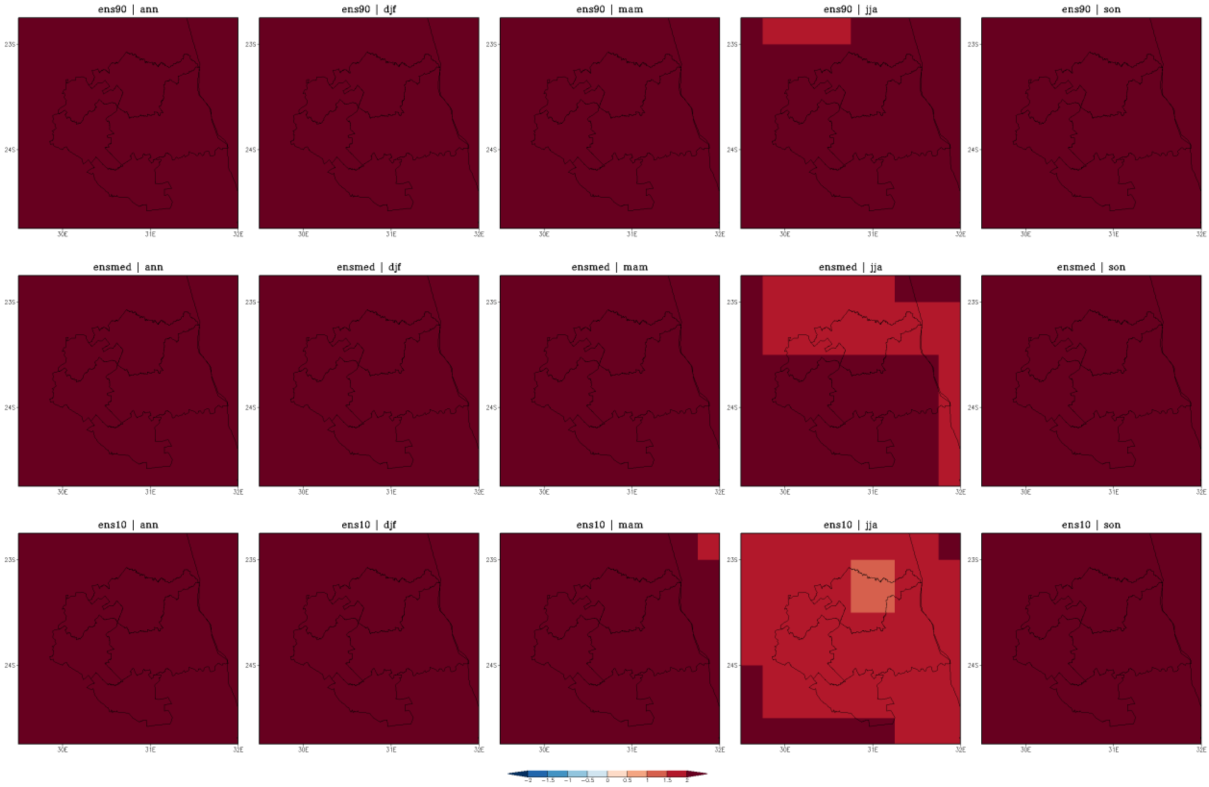

Figure B1.1.2.2a2: The **minimum temperature** anomaly with respect to the model historical period – Mopani

Figure B1.1.2.3a3: The **precipitation** anomaly with respect to the model historical period – Mopani

B1.1.2.3b RCP8.5

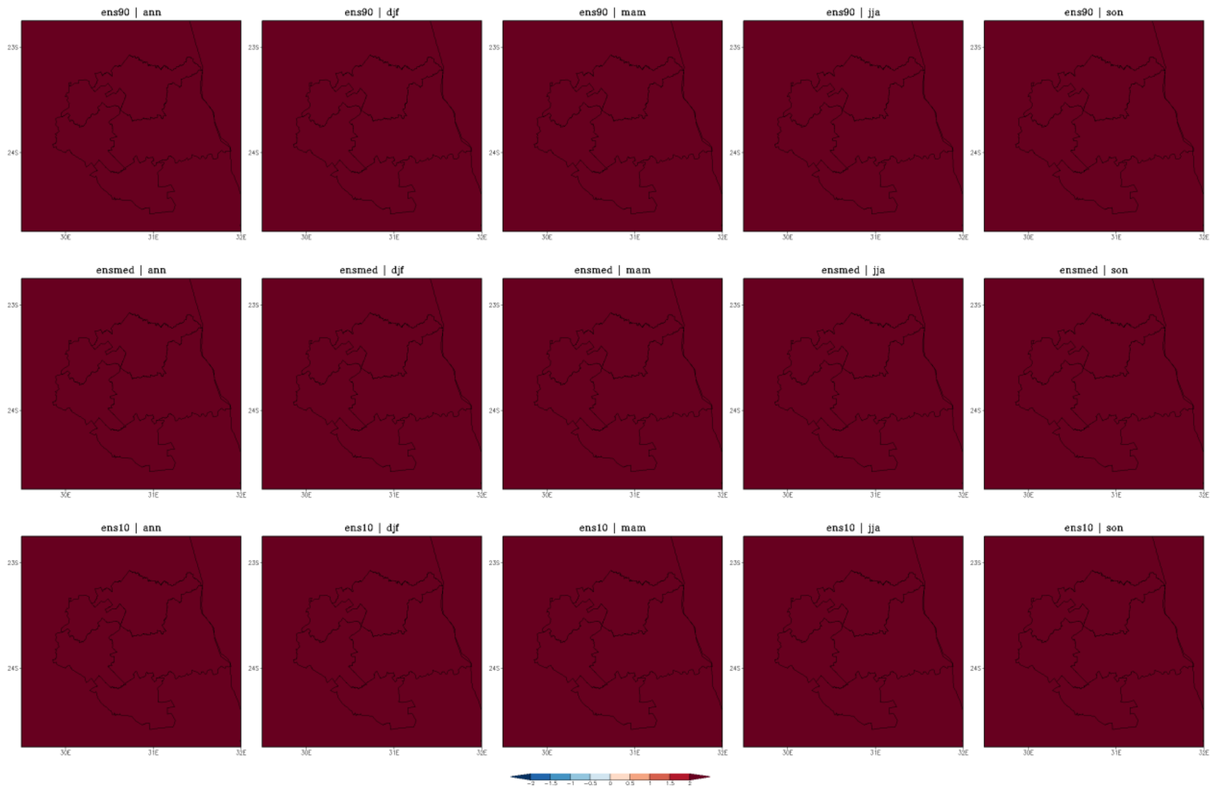

Figure B1.1.2.1b1: The **maximum temperature** anomaly with respect to the model historical period – Mopani

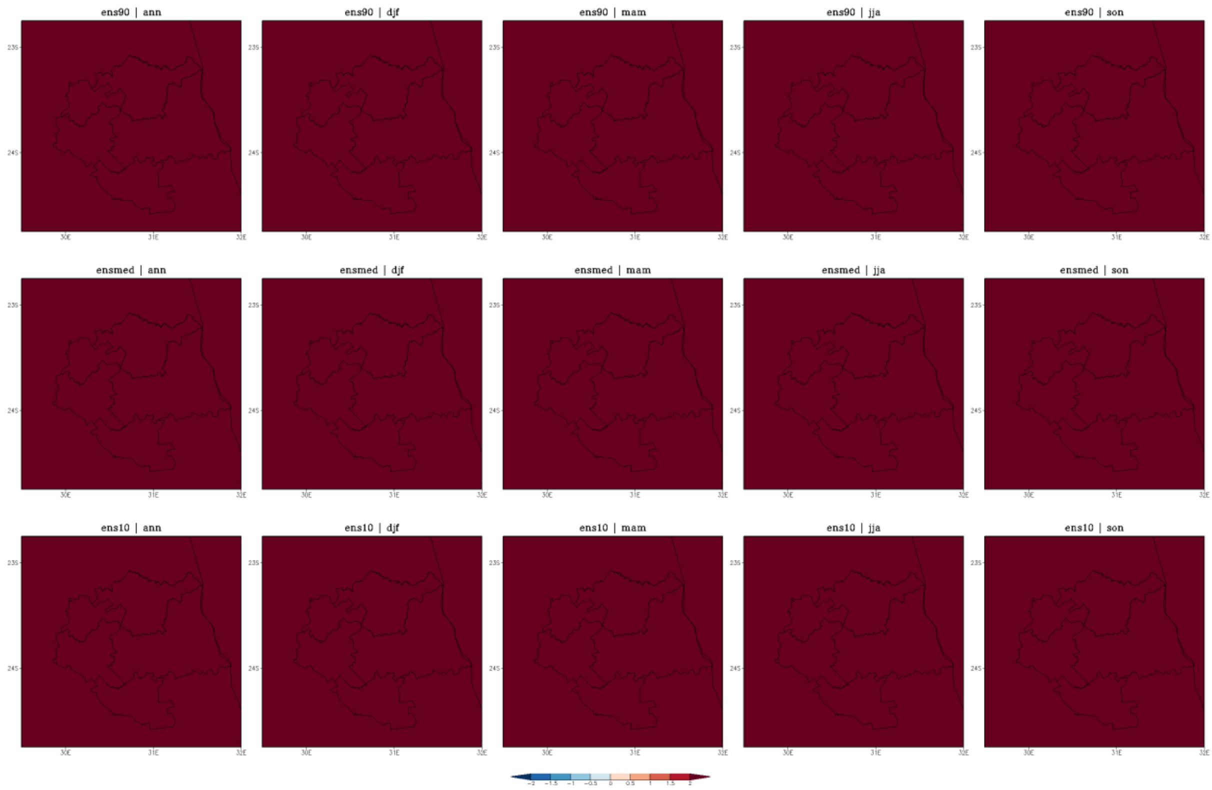

Figure B1.1.2.2b2: The **minimum temperature** anomaly with respect to the model historical period – Mopani

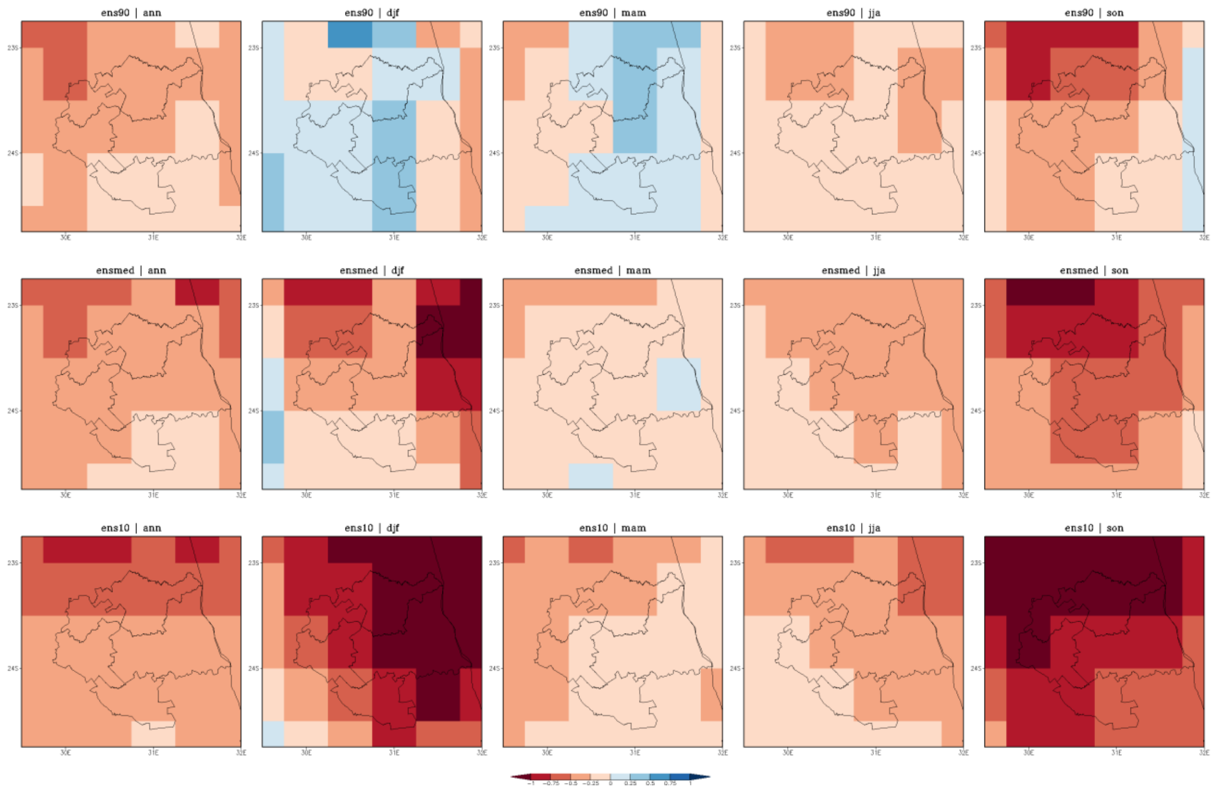

Figure B1.1.2.3b3: The **precipitation** anomaly with respect to the model historical period – Mopani

B1.2 Namakwa

B1.2.1 CSAG

B1.2.1.1 2020s

B1.2.1.1a RCP4.5

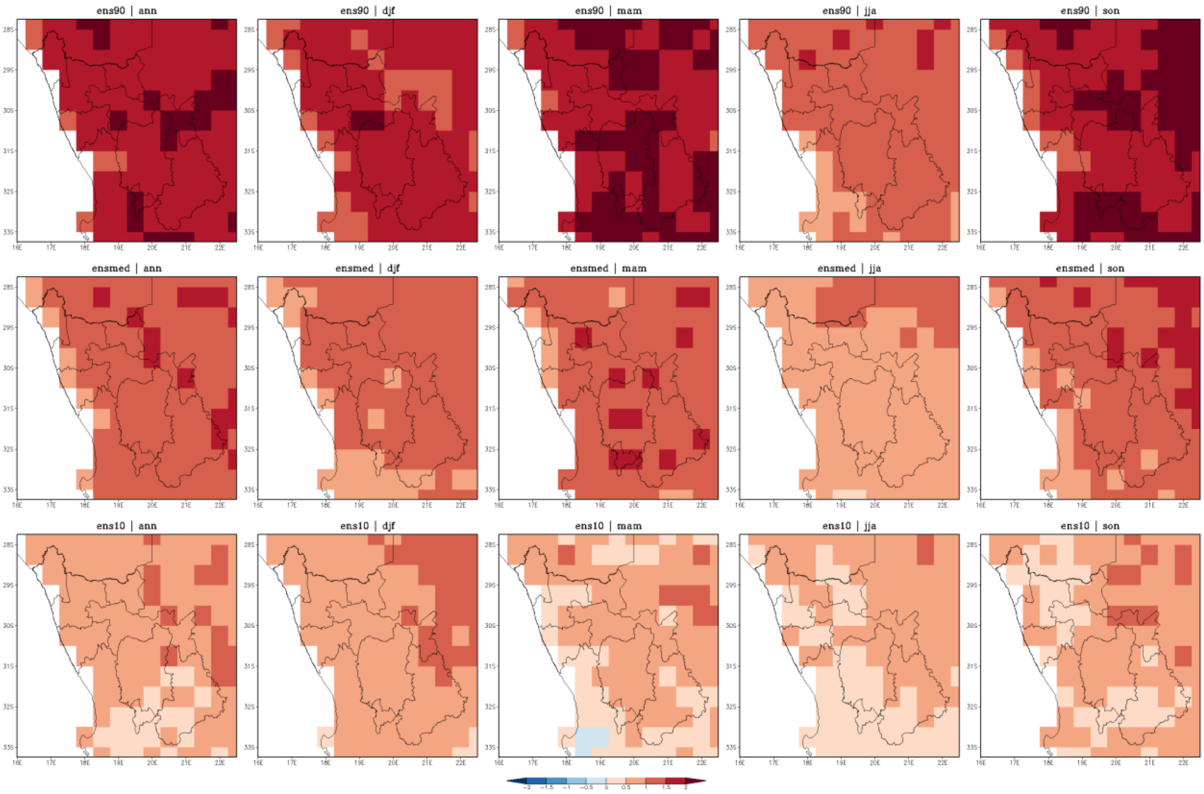

Figure B1.2.1.1a1: The **maximum temperature** anomaly with respect to the model historical period – Namakwa

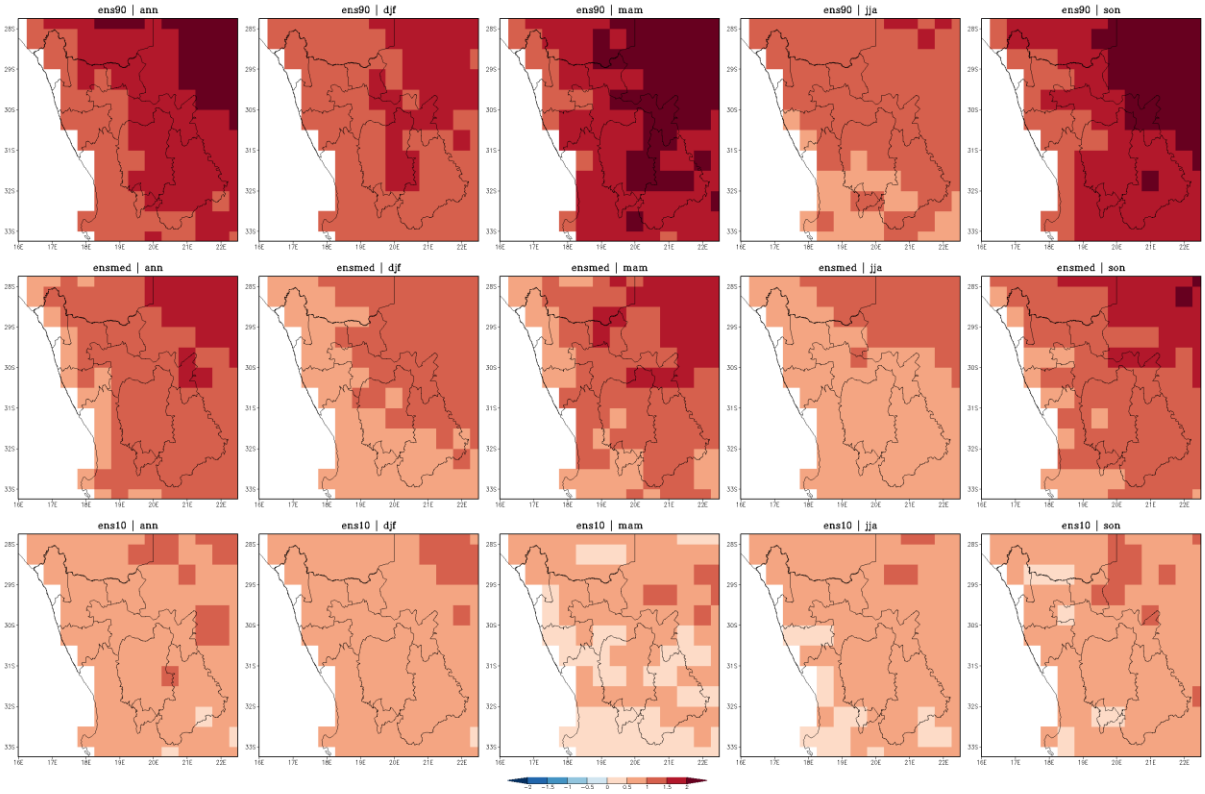

Figure B1.2.1.2a2: The **minimum temperature** anomaly with respect to the model historical period – Namakwa

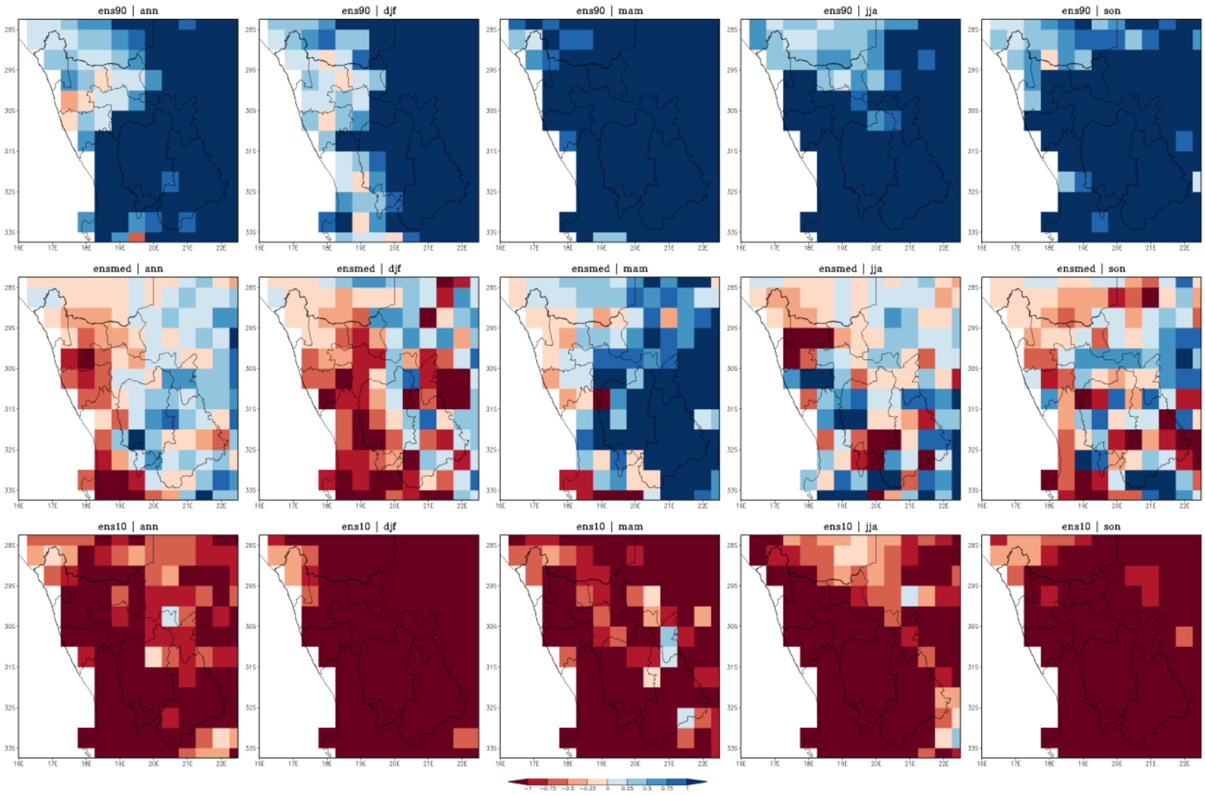

Figure B1.2.1.3a3: The **precipitation** anomaly with respect to the model historical period – Namakwa

B1.2.1.1b RCP8.5

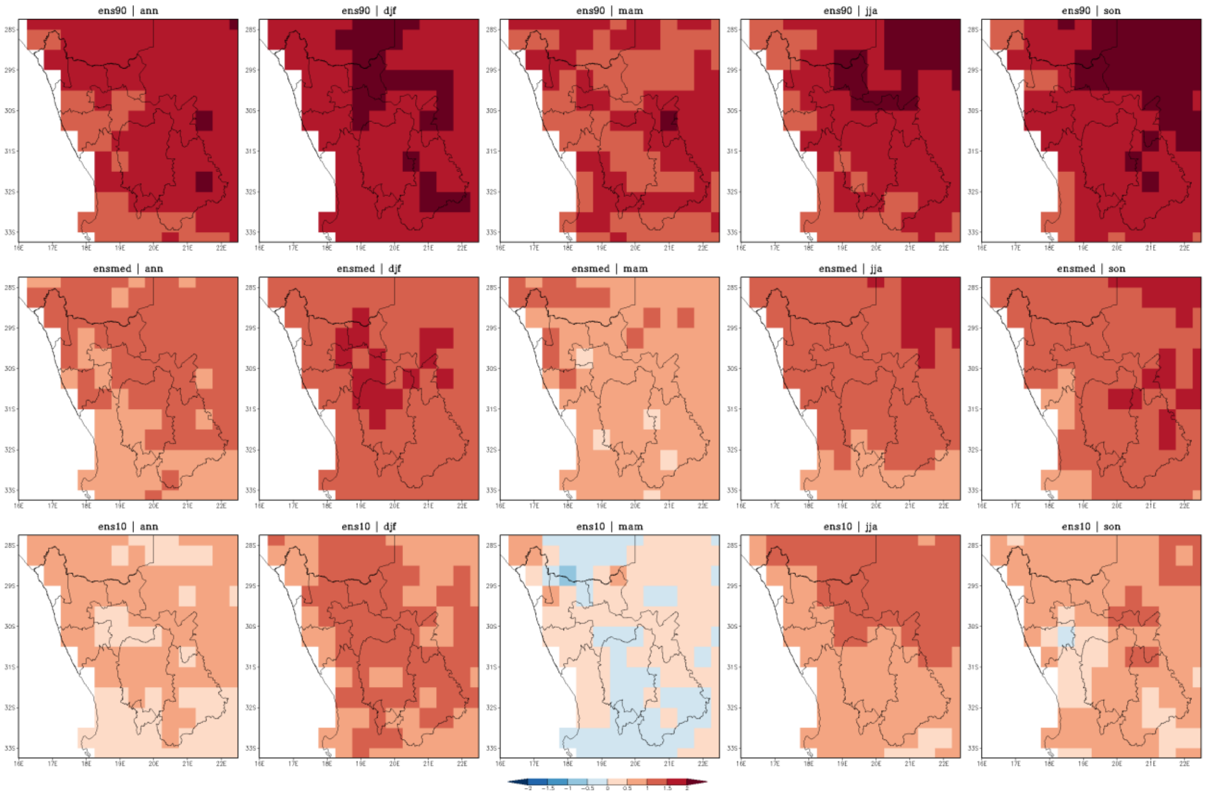

Figure B1.2.1.1b1: The **maximum temperature** anomaly with respect to the model historical period – Namakwa

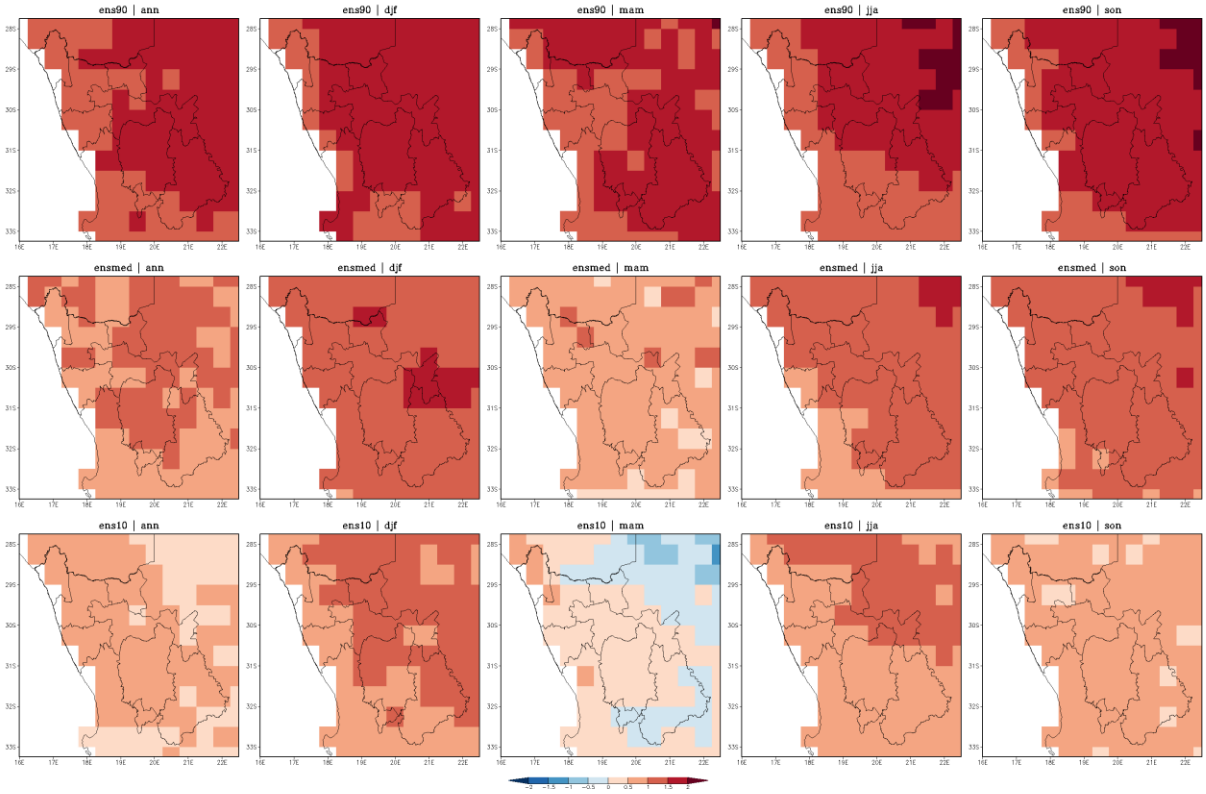

Figure B1.2.1.2b2: The **minimum temperature** anomaly with respect to the model historical period – Namakwa

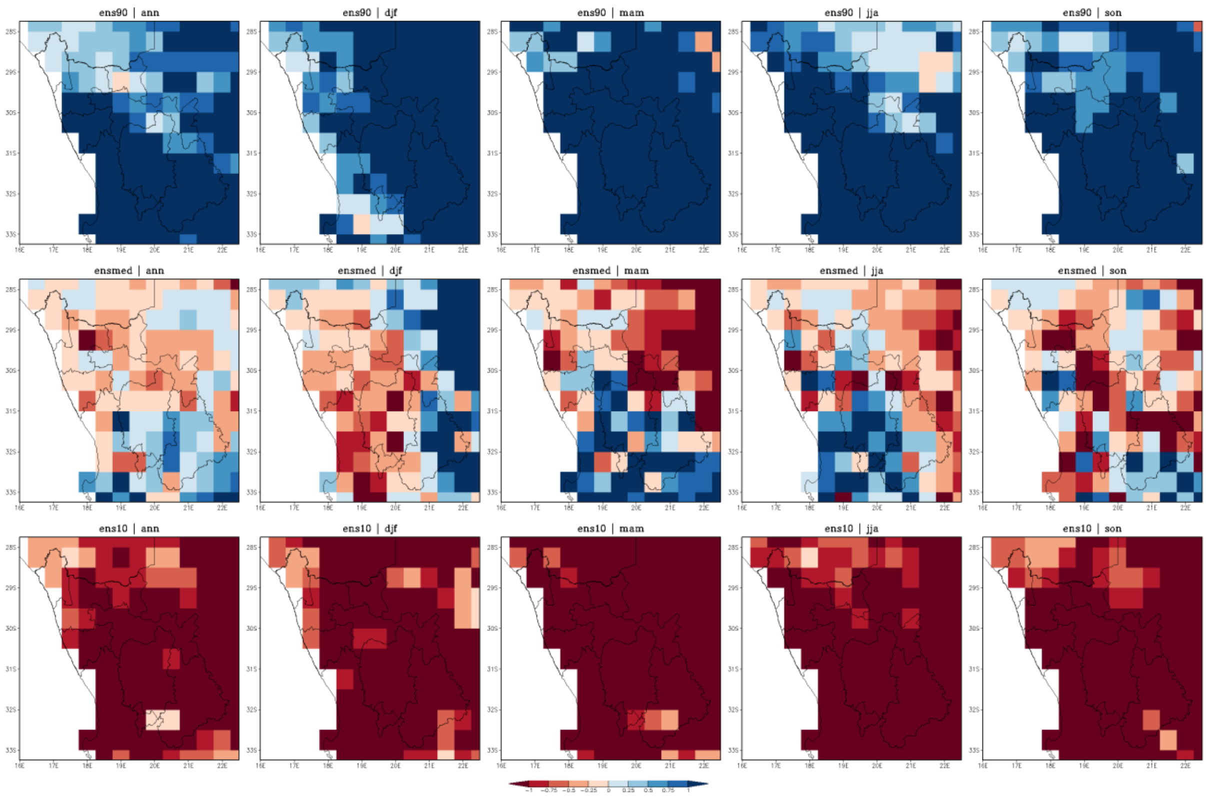

Figure B1.2.1.3b3: The **precipitation** anomaly with respect to the model historical period – Namakwa

B1.2.1.2 2050s

B1.2.1.1a RCP4.5

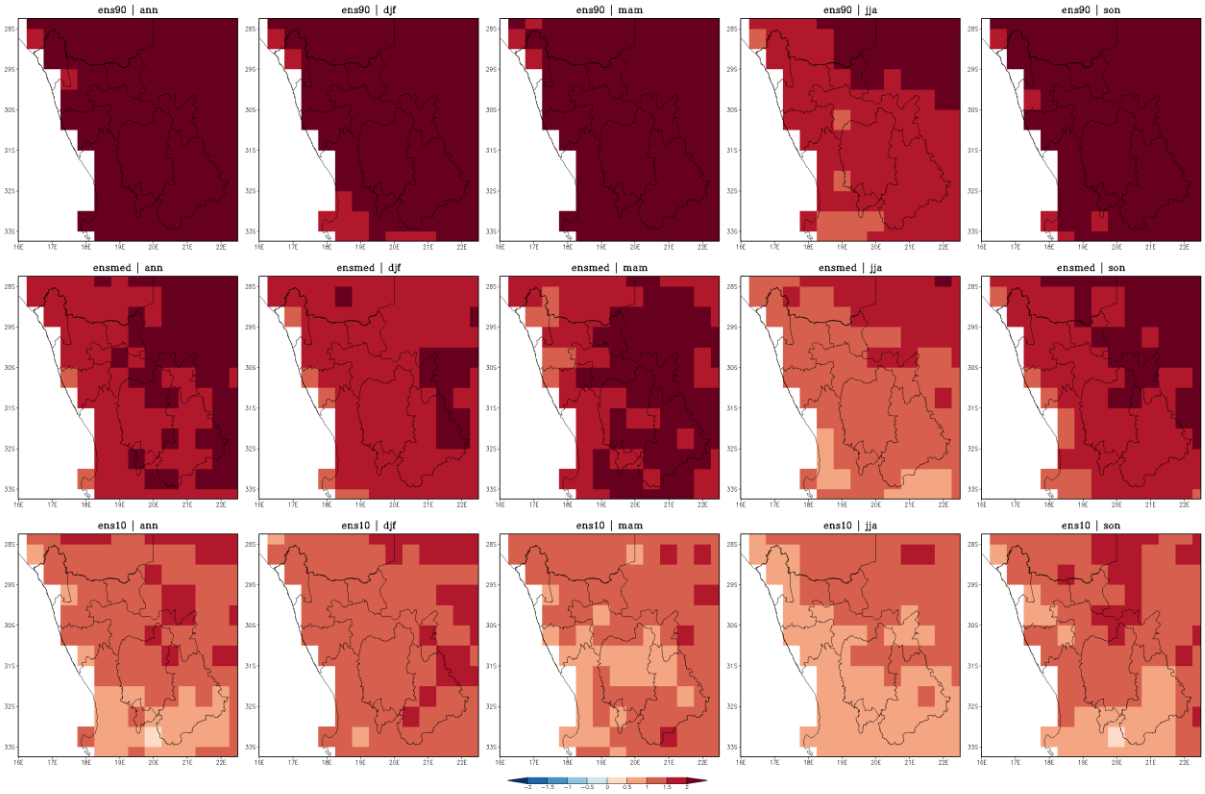

Figure B1.2.1.1a1: The **maximum temperature** anomaly with respect to the model historical period – Namakwa

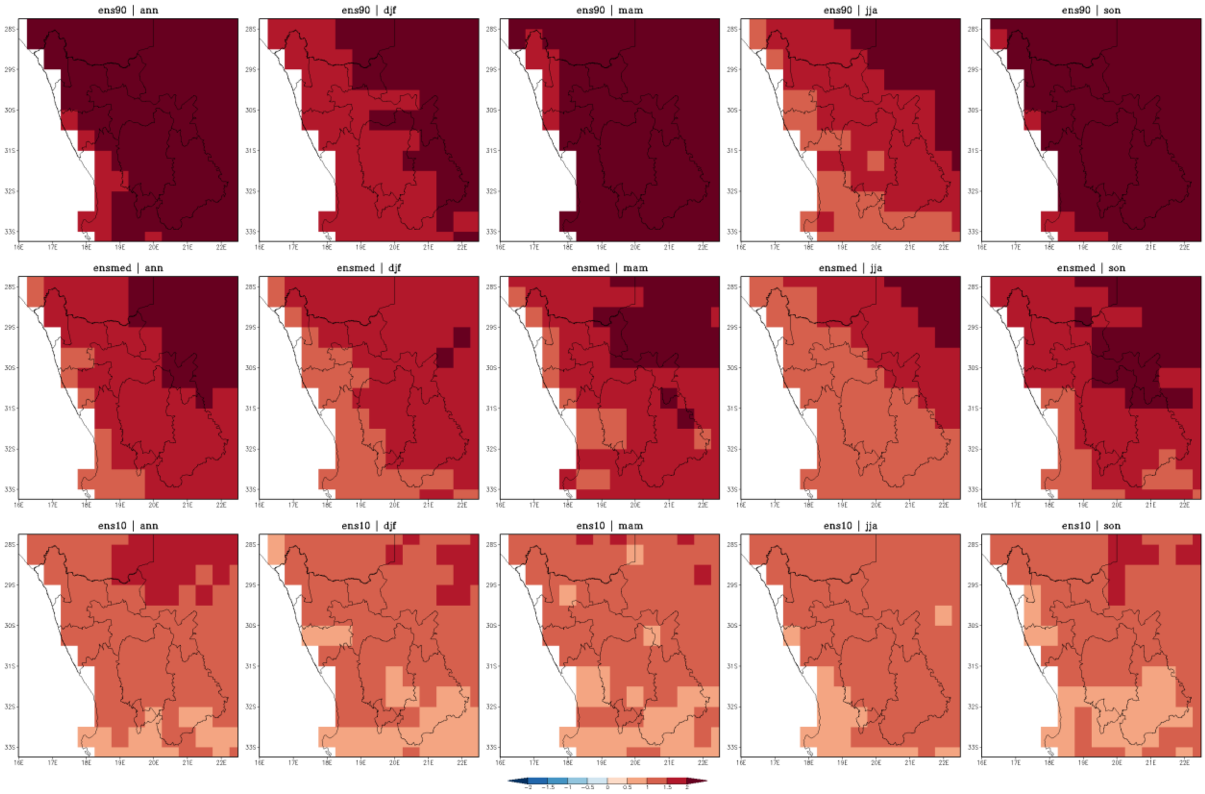

Figure B1.2.1.2a2: The **minimum temperature** anomaly with respect to the model historical period – Namakwa

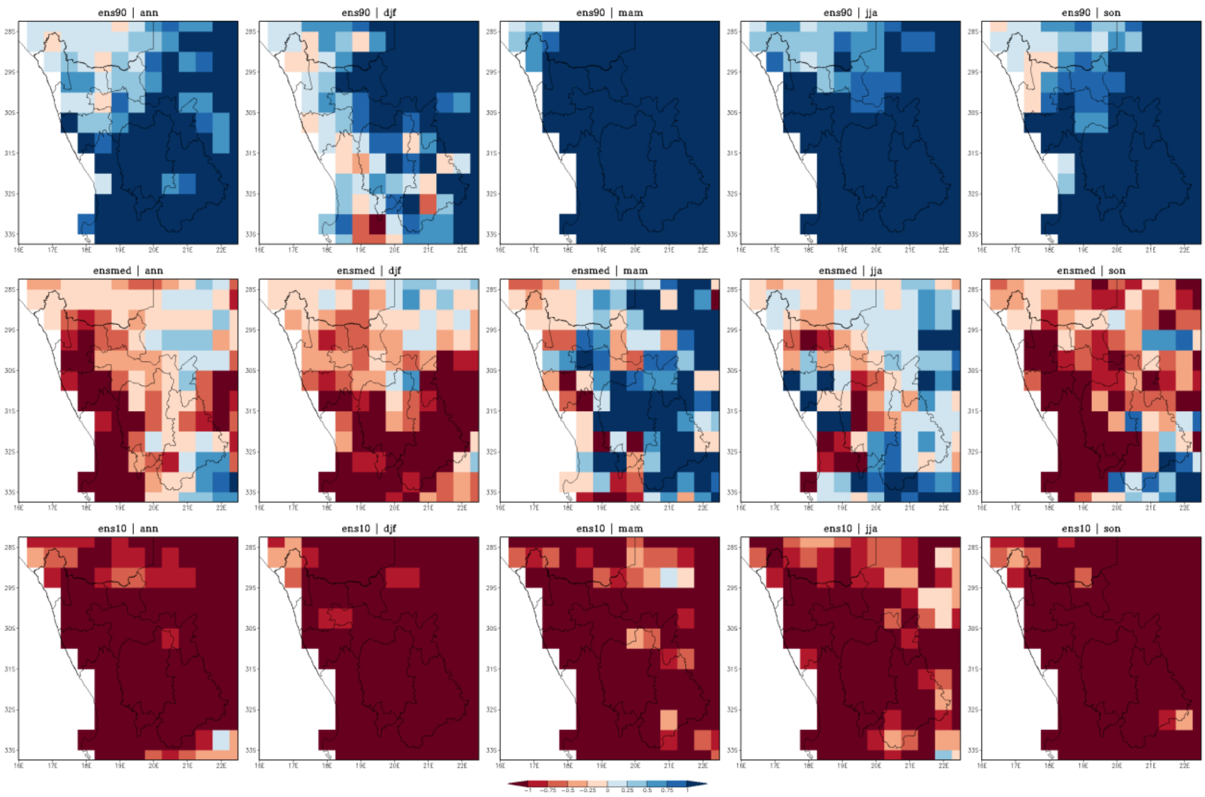

Figure B1.2.1.3a3: The **precipitation** anomaly with respect to the model historical period – Namakwa

B1.2.1.1b RCP8.5

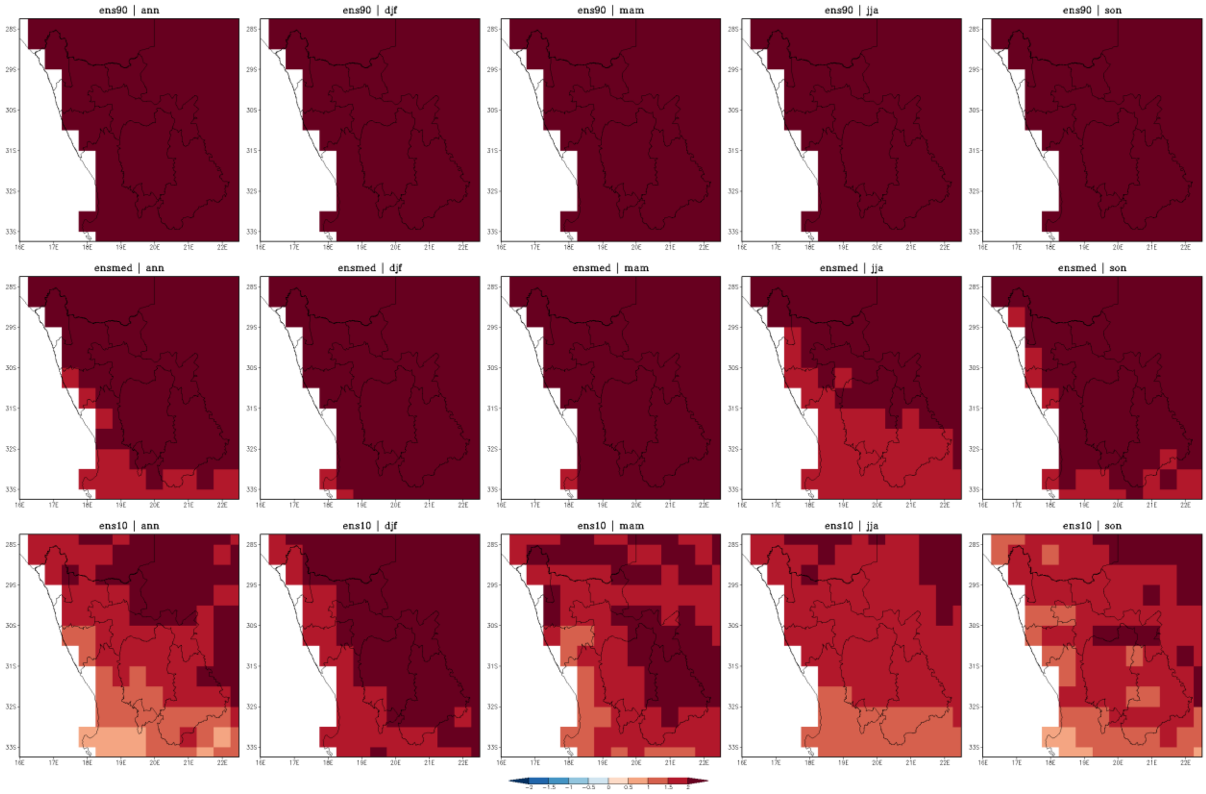

Figure B1.2.1.1b1: The **maximum temperature** anomaly with respect to the model historical period – Namakwa

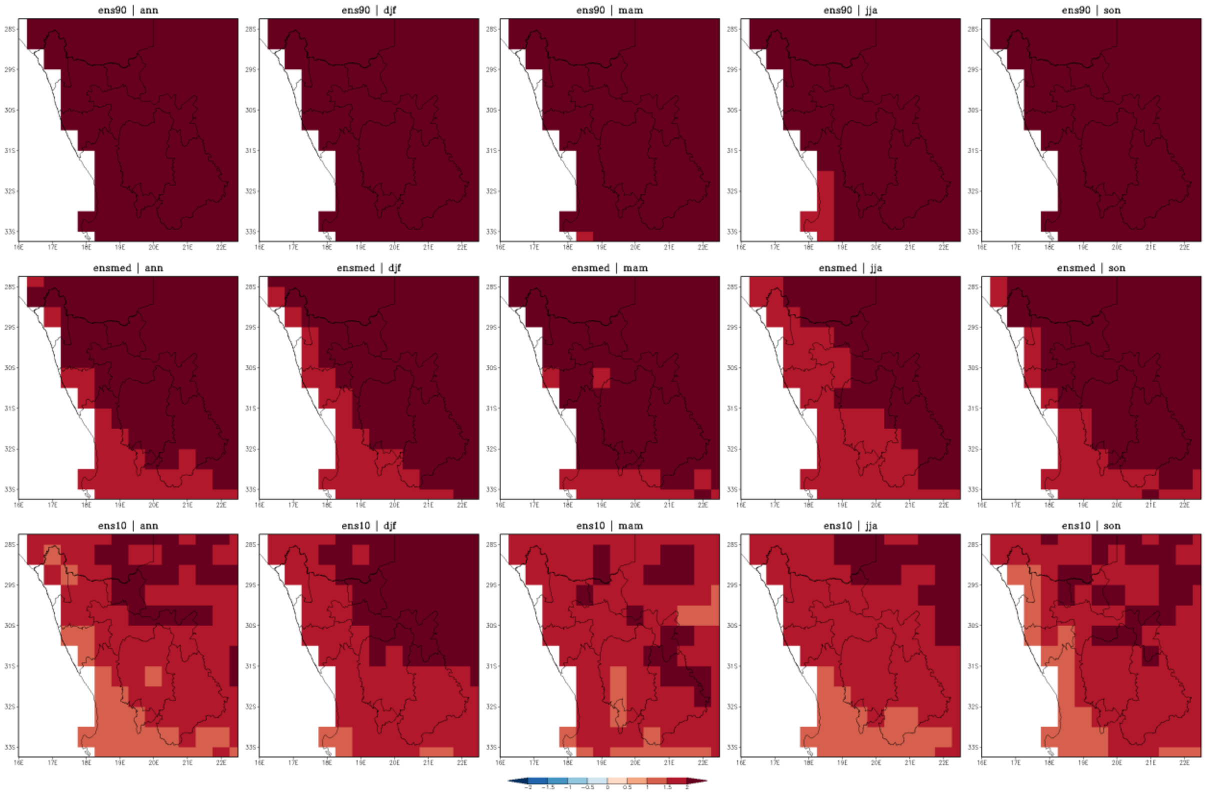

Figure B1.2.1.2b2: The **minimum temperature** anomaly with respect to the model historical period – Namakwa

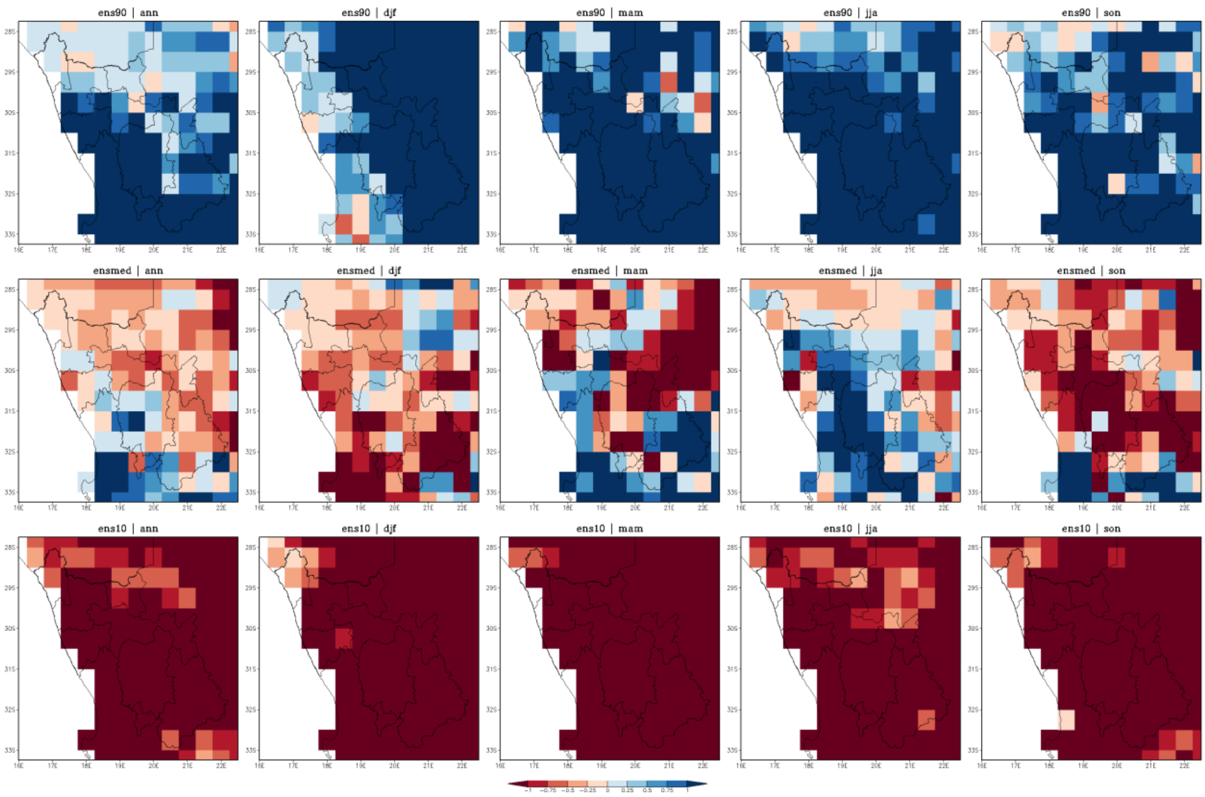

Figure B1.2.1.3b3: The **precipitation** anomaly with respect to the model historical period – Namakwa

B1.2.1.3 2080s

B1.2.1.1a RCP4.5

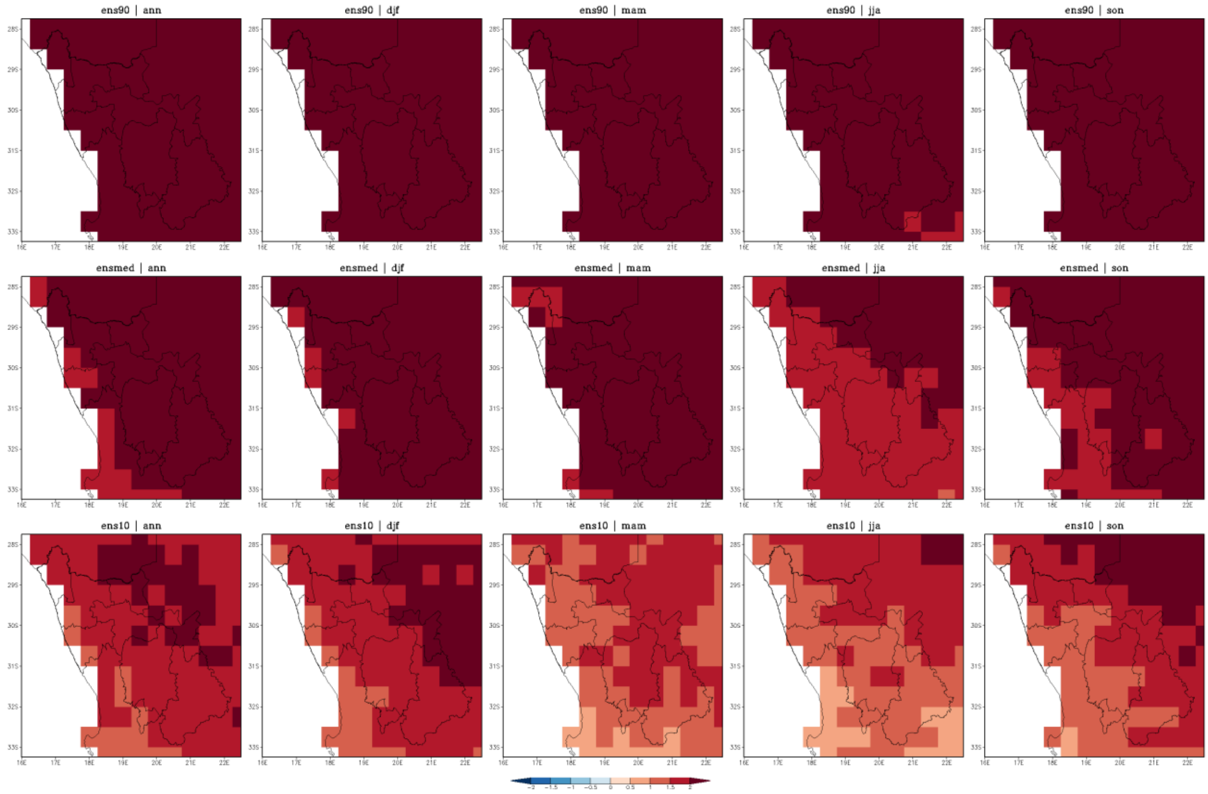

Figure B1.2.1.1a1: The **maximum temperature** anomaly with respect to the model historical period – Namakwa

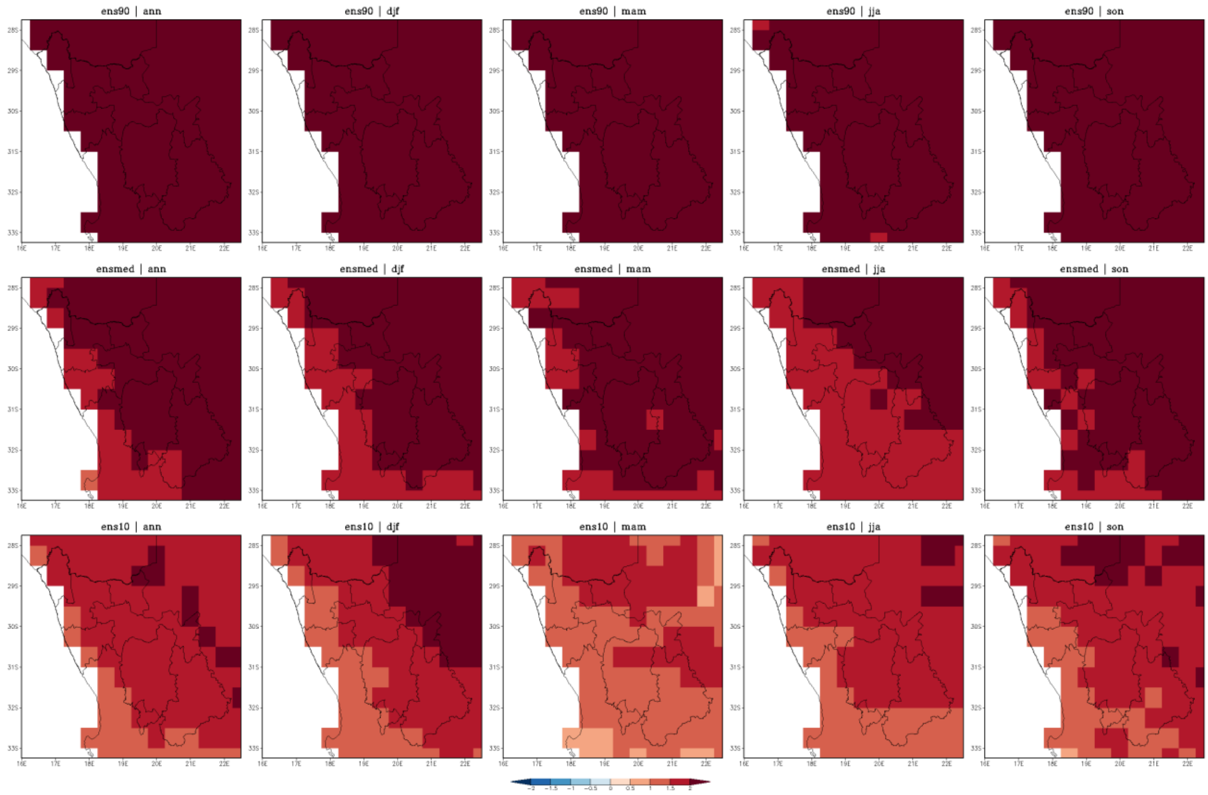

Figure B1.2.1.2a2: The **minimum temperature** anomaly with respect to the model historical period – Namakwa

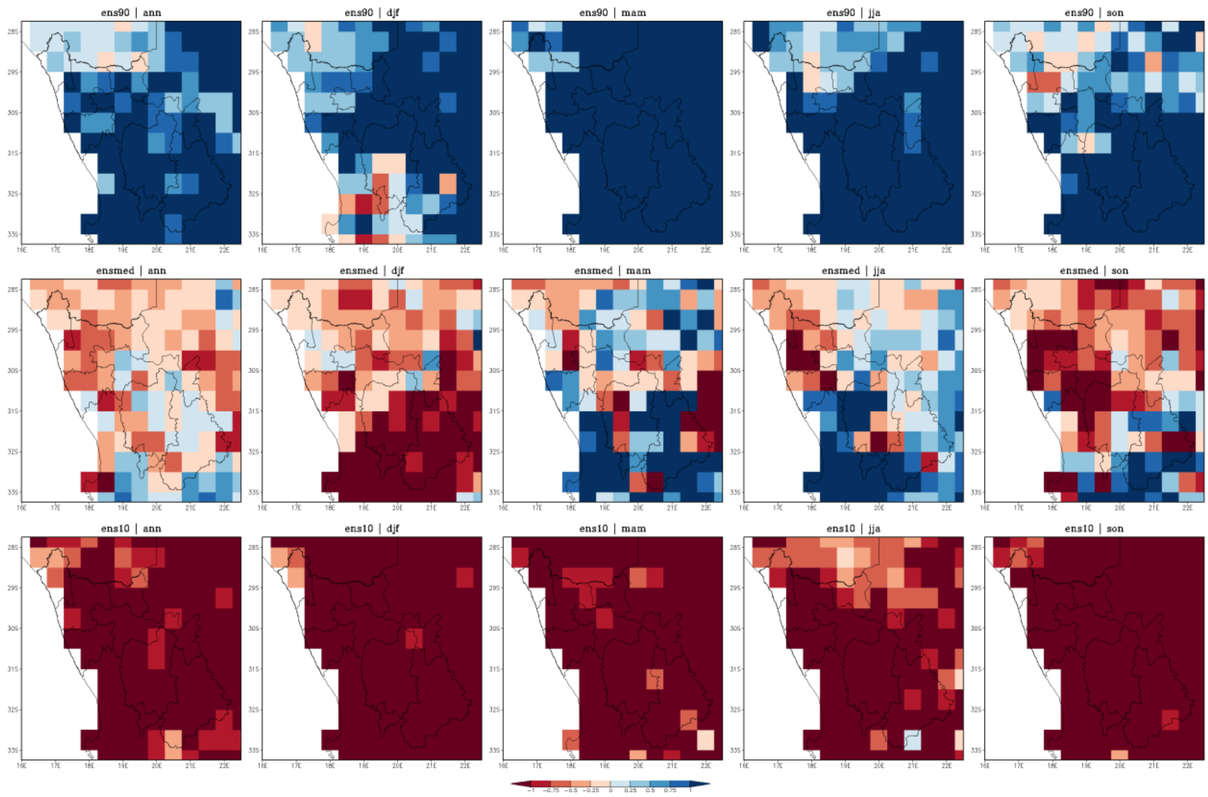

Figure B1.2.1.3a3: The **precipitation** anomaly with respect to the model historical period – Namakwa

B1.2.1.1b RCP8.5

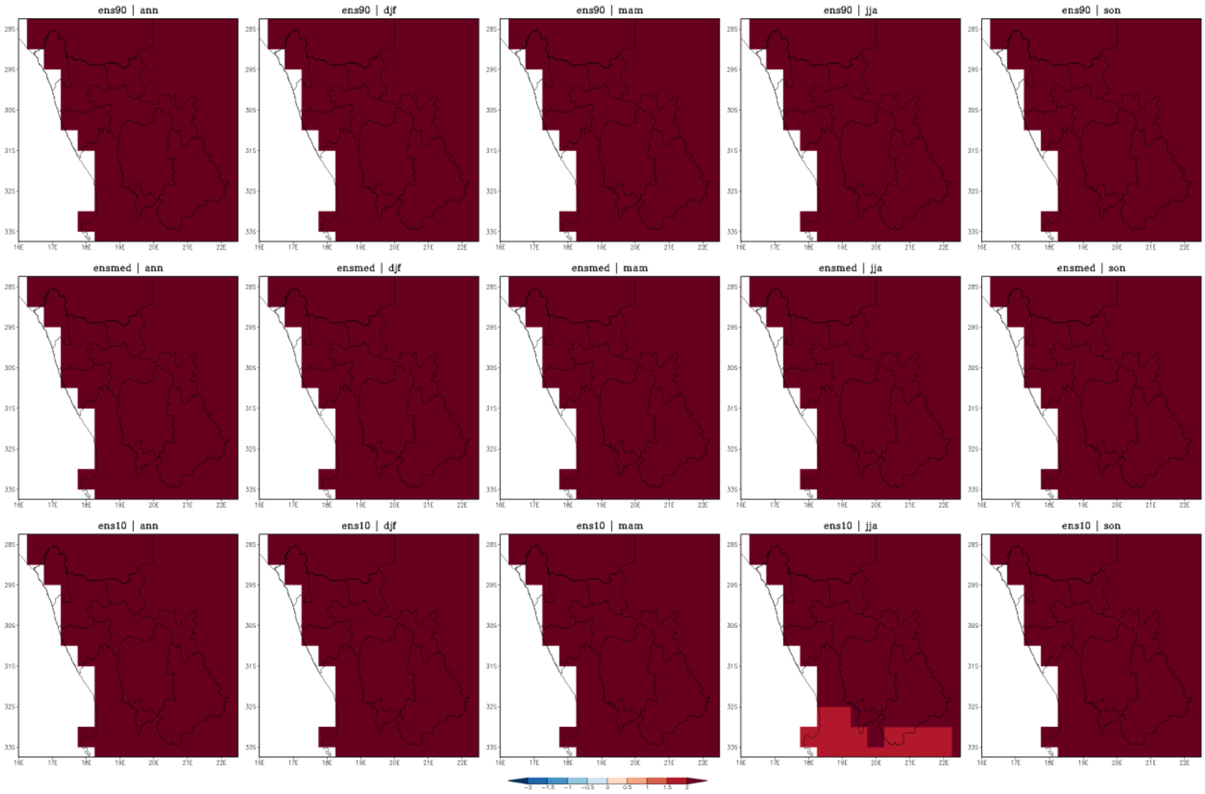

Figure B1.2.1.1b1: The **maximum temperature** anomaly with respect to the model historical period – Namakwa

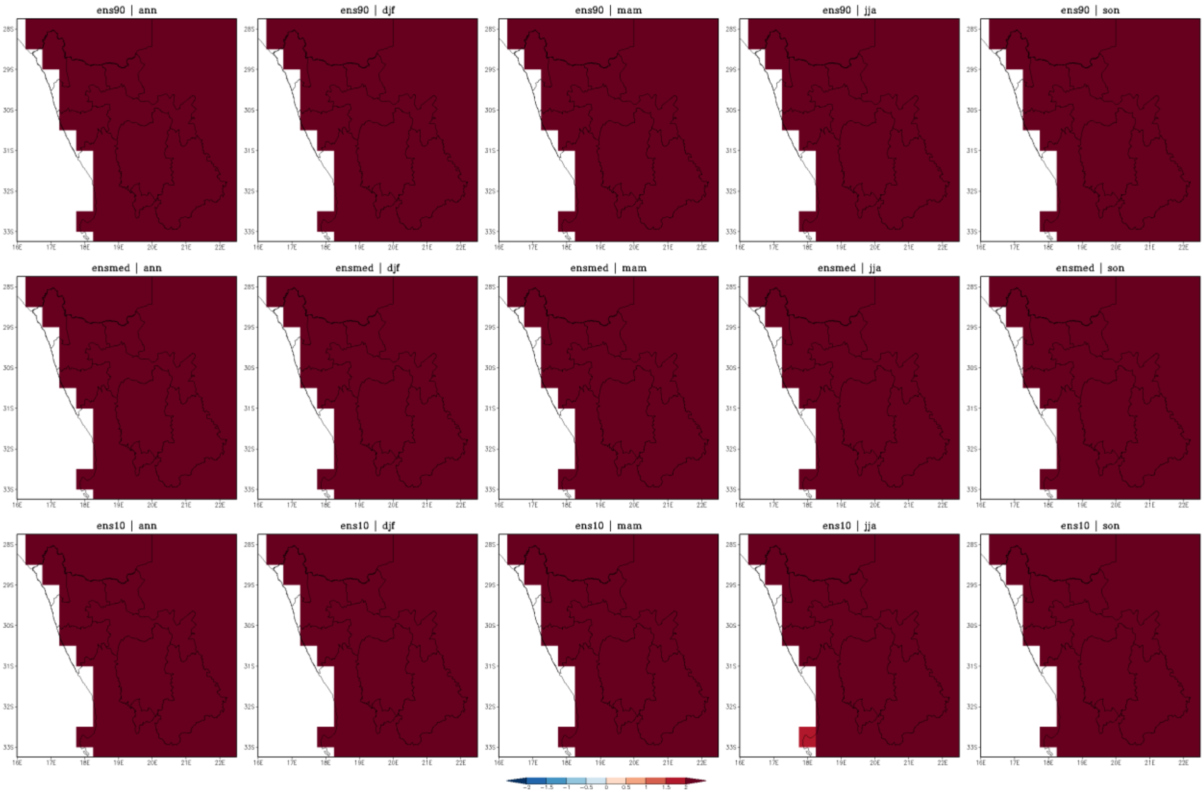

Figure B1.2.1.2b2: The **minimum temperature** anomaly with respect to the model historical period – Namakwa

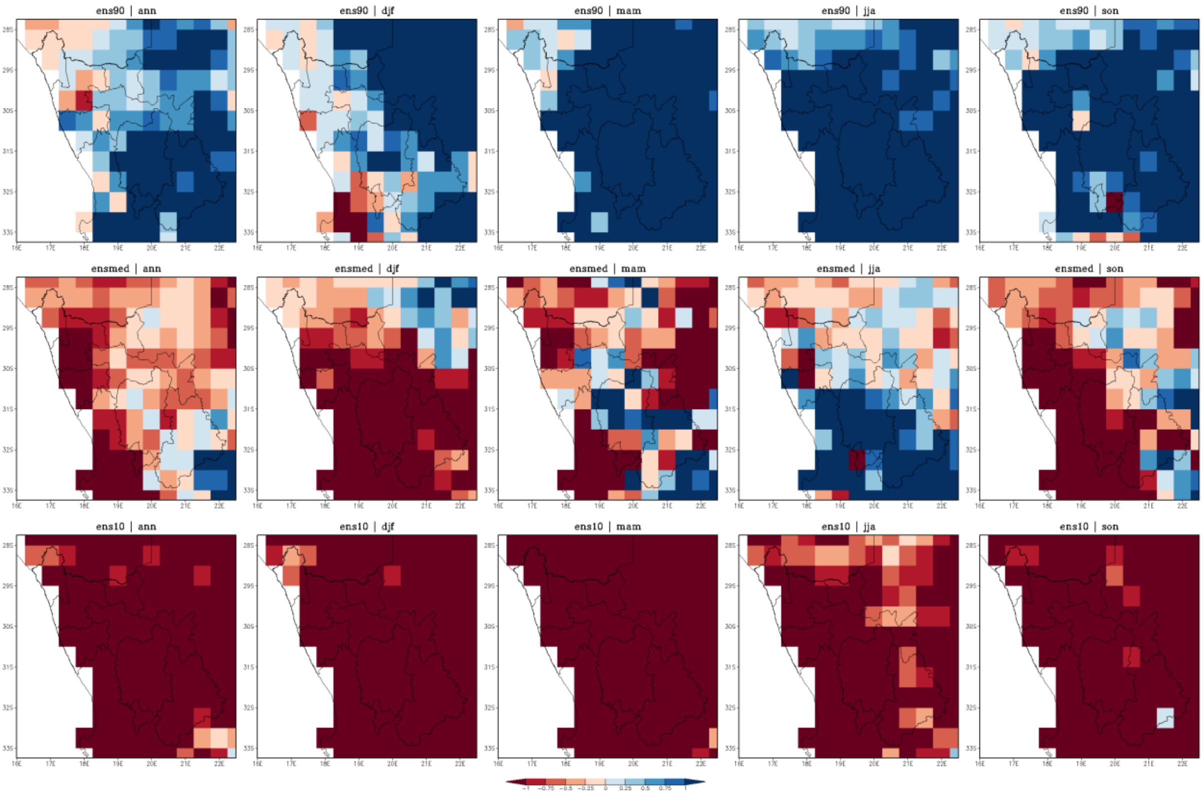

Figure B1.2.1.3b3: The **precipitation** anomaly with respect to the model historical period – Namakwa

B1.2.2 CCAM

B1.2.2.1 2020s

B1.2.2.1a RCP4.5

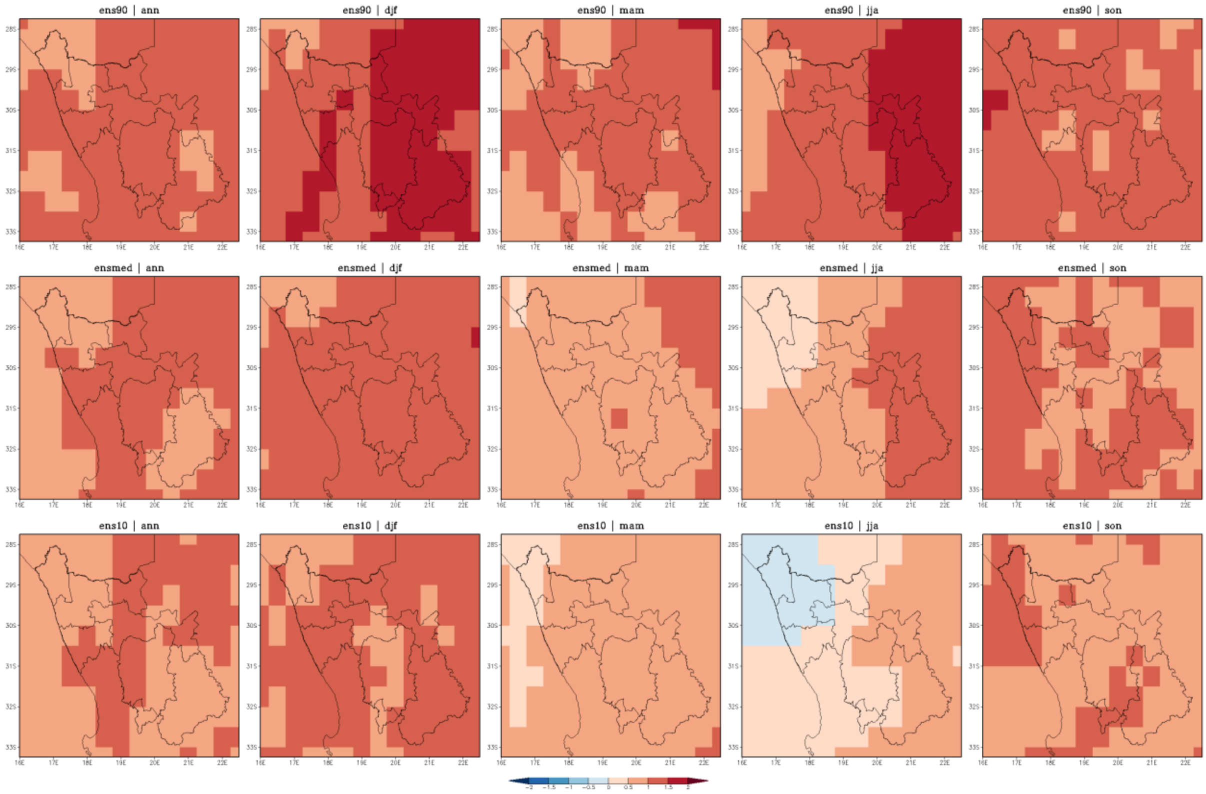

Figure B1.2.2.1a1: The **maximum temperature** anomaly with respect to the model historical period – Namakwa

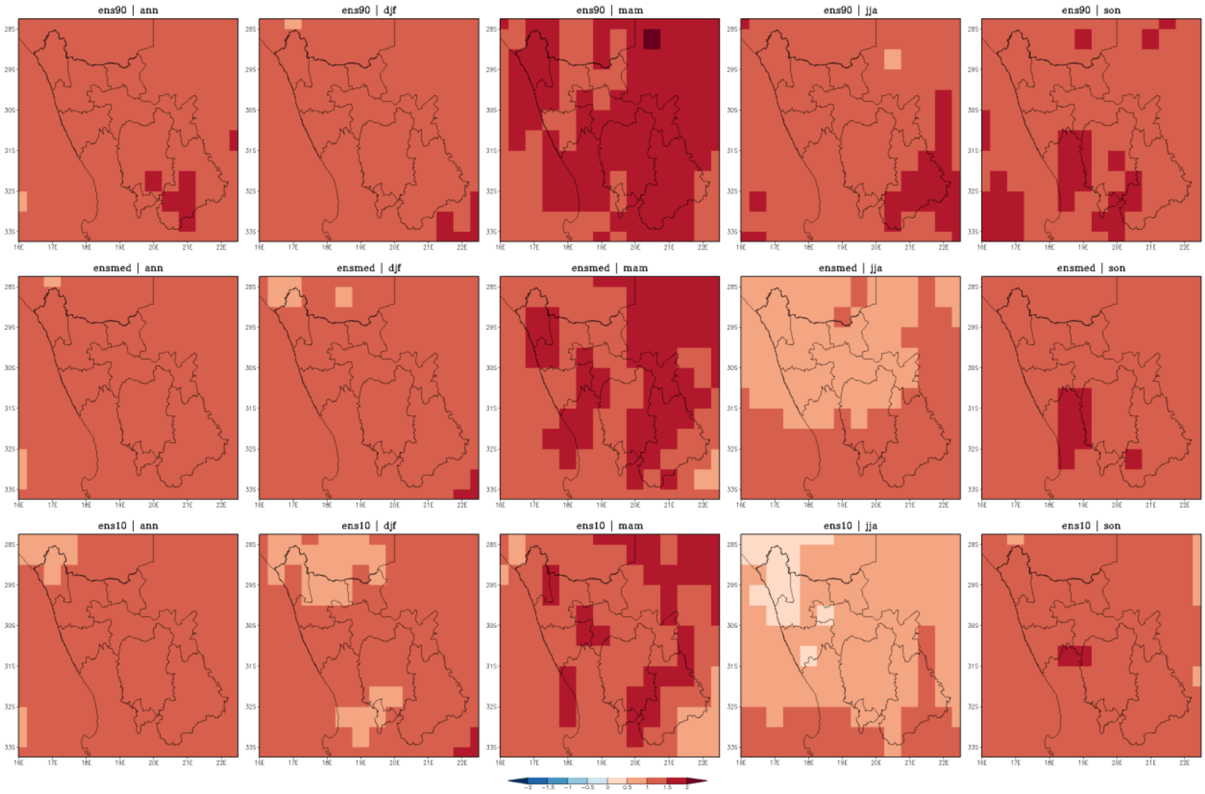

Figure B1.2.2.2a2: The **minimum temperature** anomaly with respect to the model historical period – Namakwa

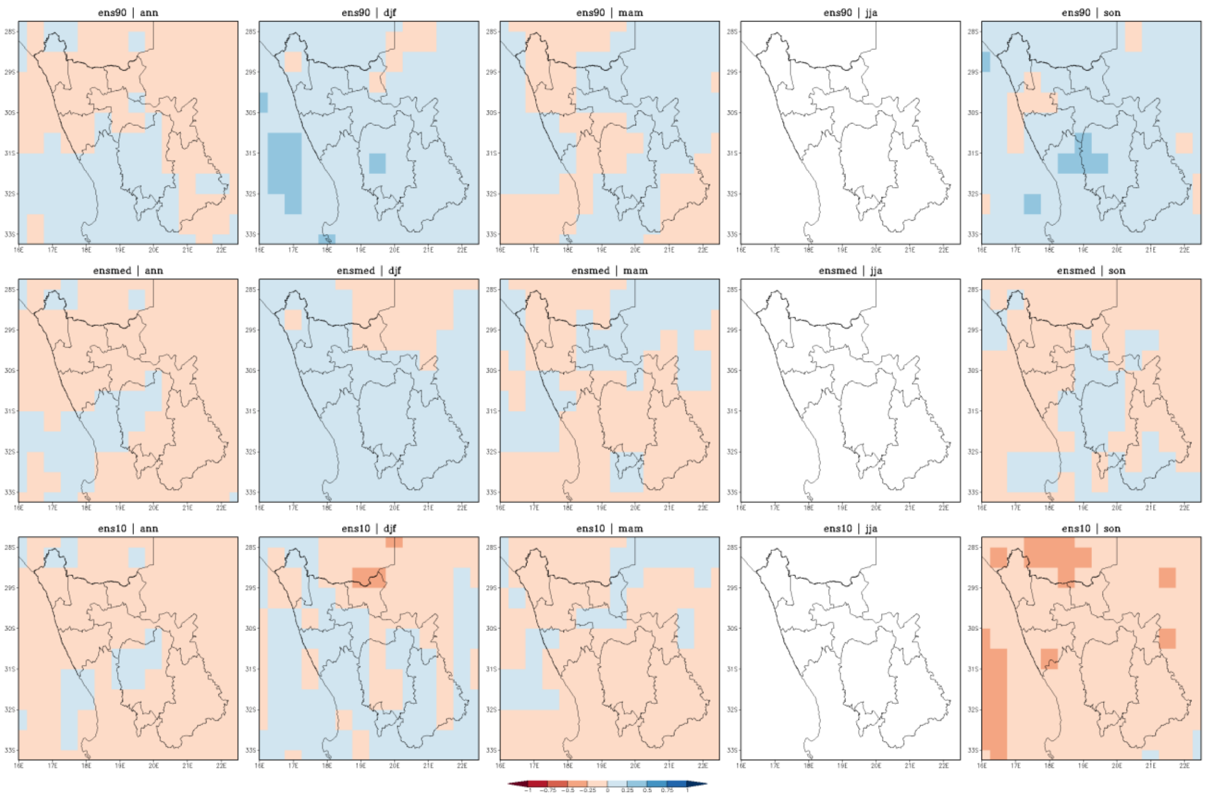

Figure B1.2.2.3a3: The **precipitation** anomaly with respect to the model historical period – Namakwa

B1.2.2.1b RCP8.5

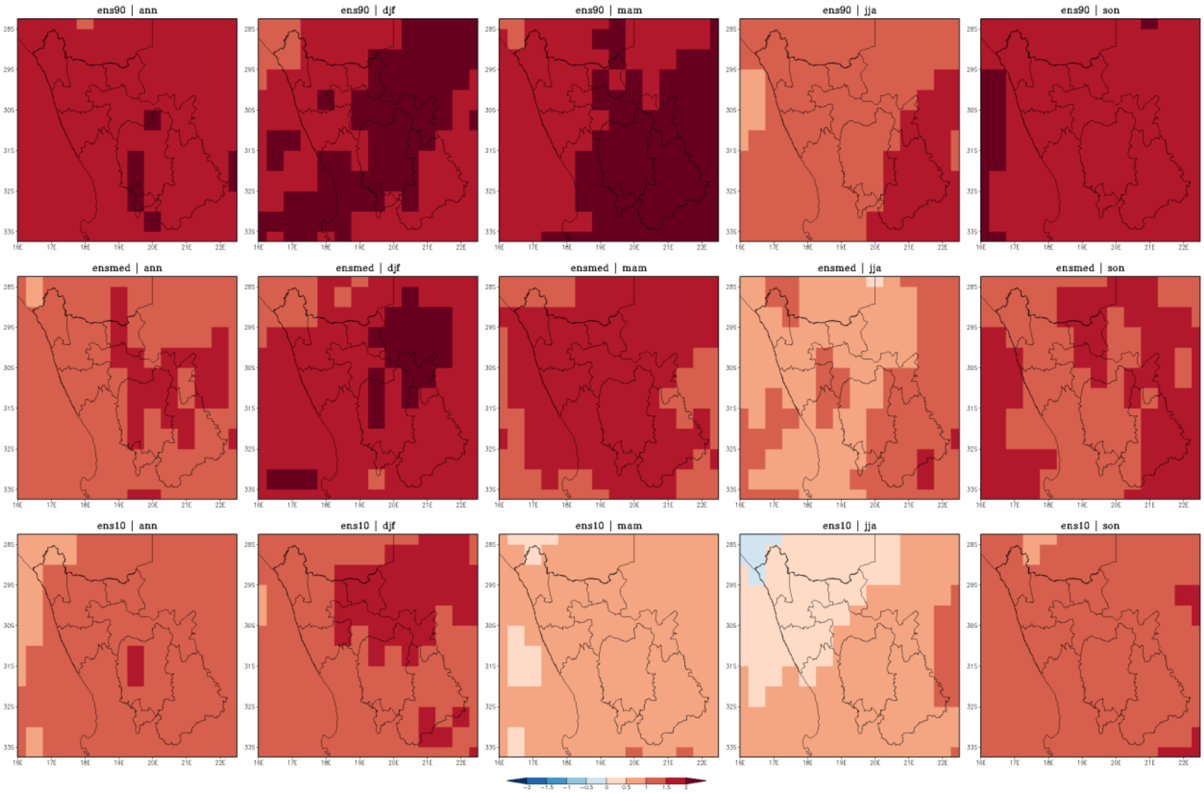

Figure B1.2.2.1b1: The **maximum temperature** anomaly with respect to the model historical period – Namakwa

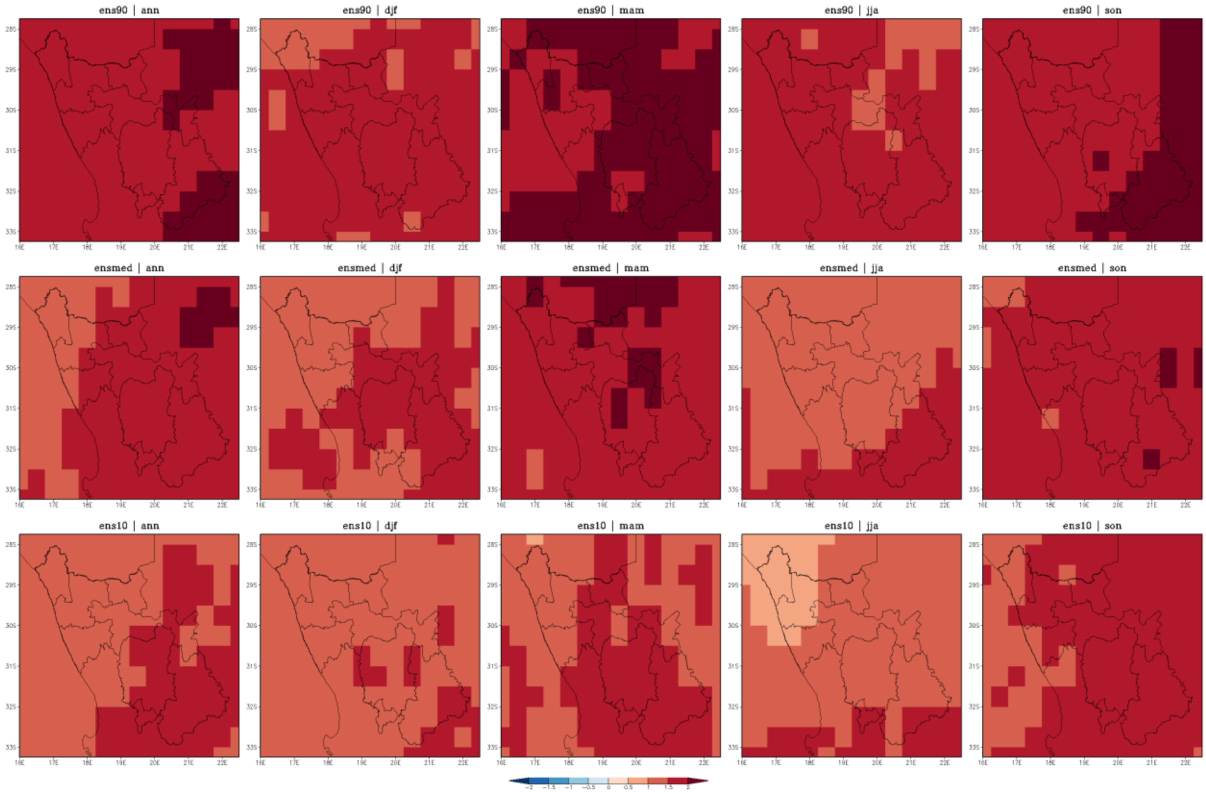

Figure B1.2.2.2b2: The **minimum temperature** anomaly with respect to the model historical period – Namakwa

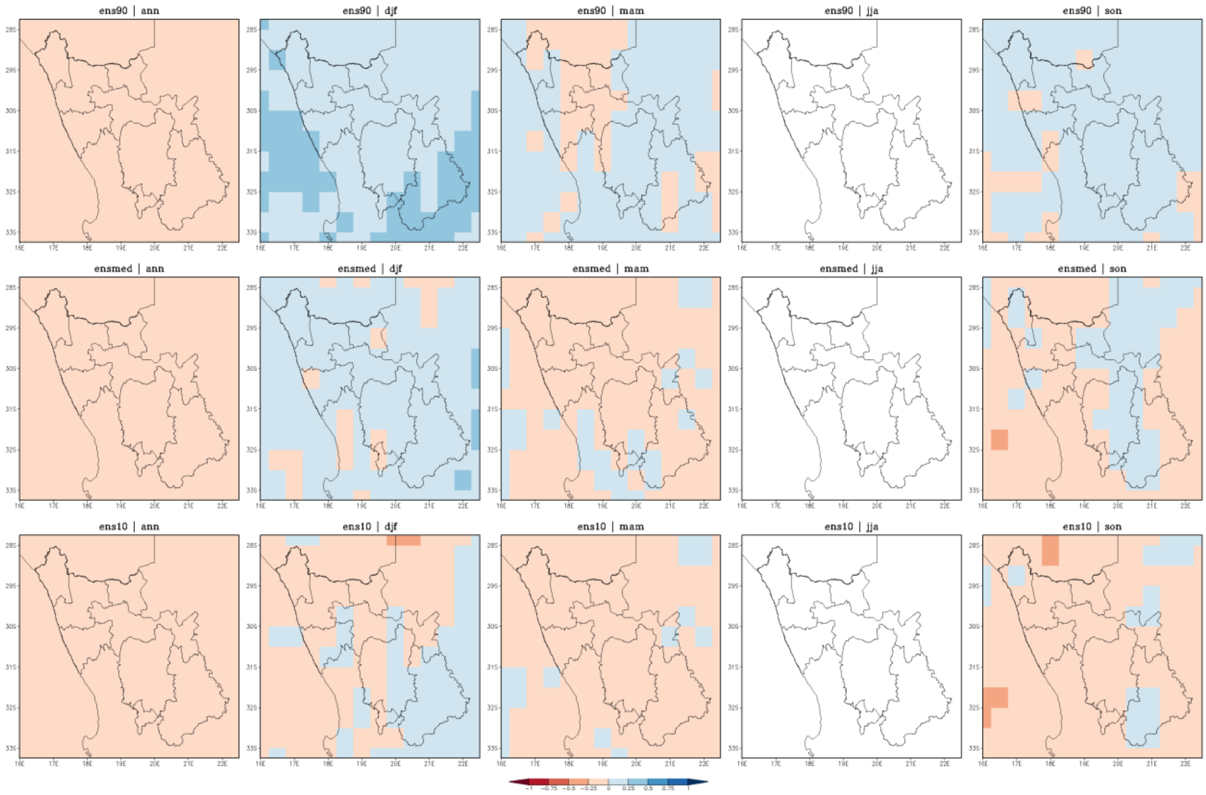

Figure B1.2.2.3b3: The **precipitation** anomaly with respect to the model historical period – Namakwa

B1.2.2.2 2050s

B1.2.2.2a RCP4.5

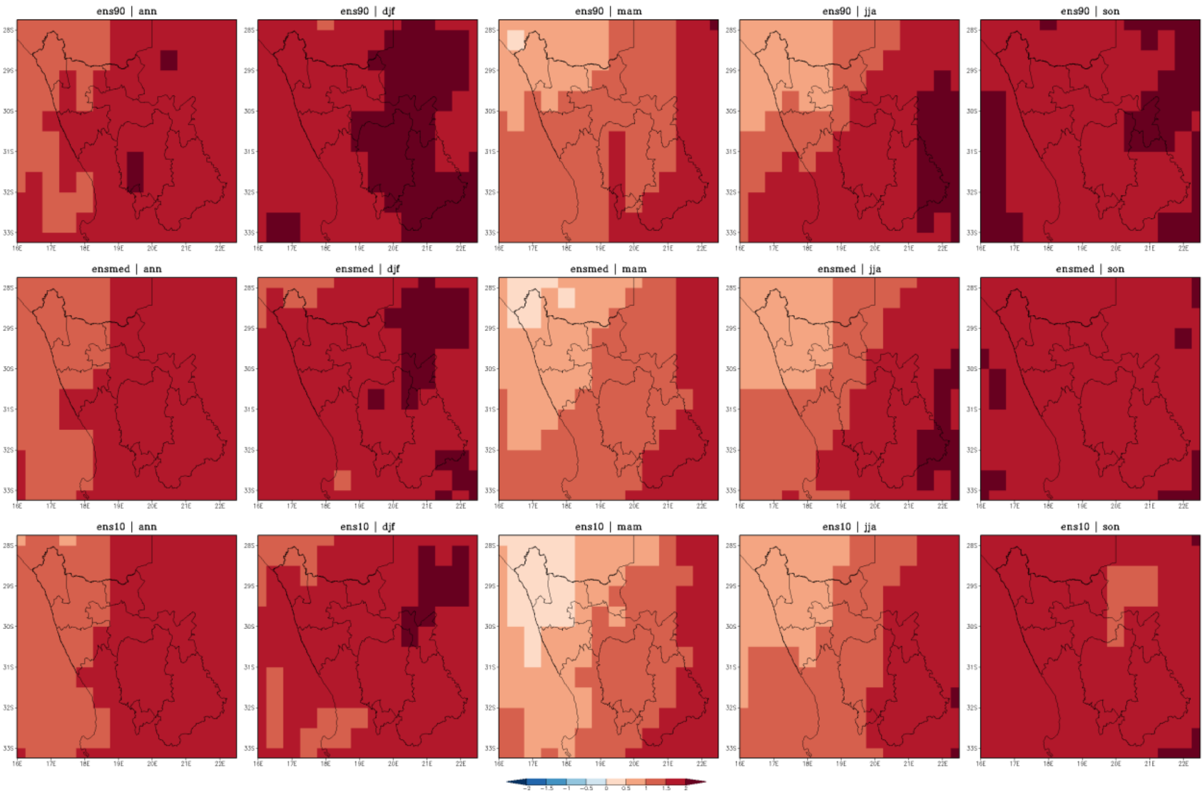

Figure B1.2.2.1a1: The **maximum temperature** anomaly with respect to the model historical period – Namakwa

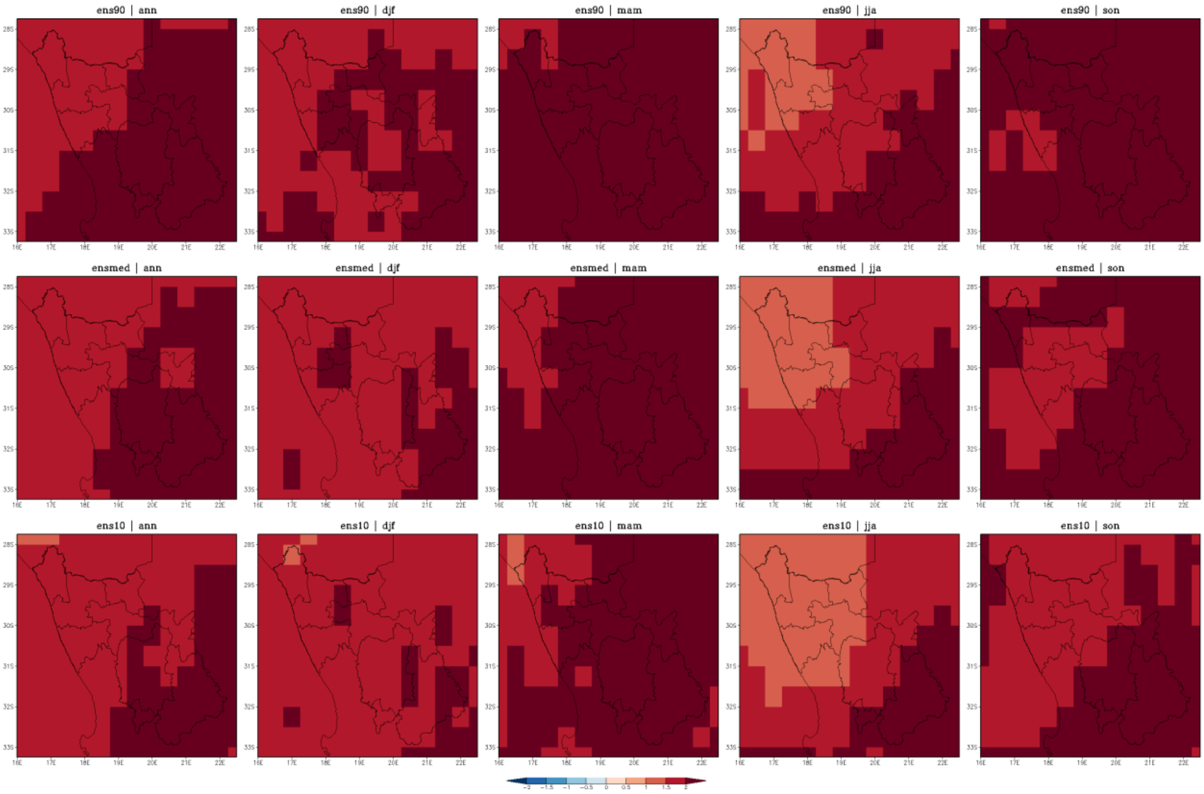

Figure B1.2.2.2a2: The **minimum temperature** anomaly with respect to the model historical period – Namakwa

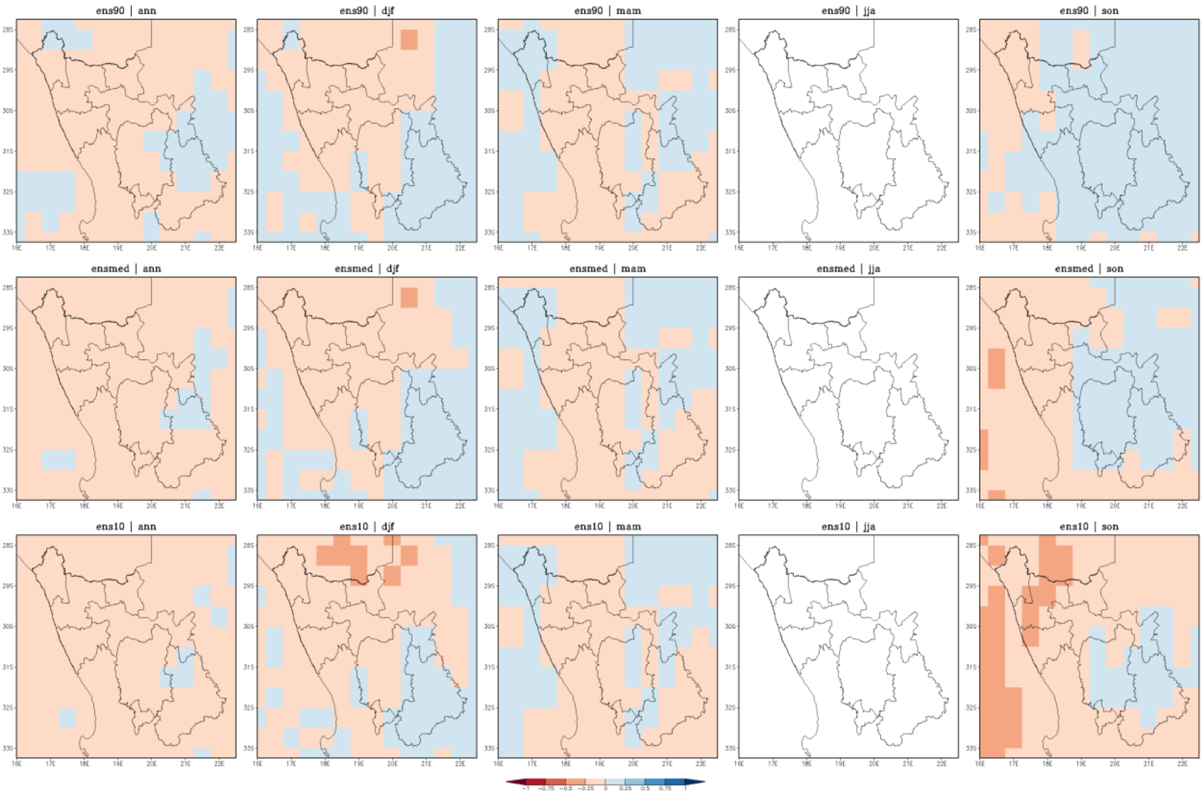

Figure B1.2.2.315a3: The **precipitation** anomaly with respect to the model historical period – Namakwa

B1.2.2.2b RCP8.5

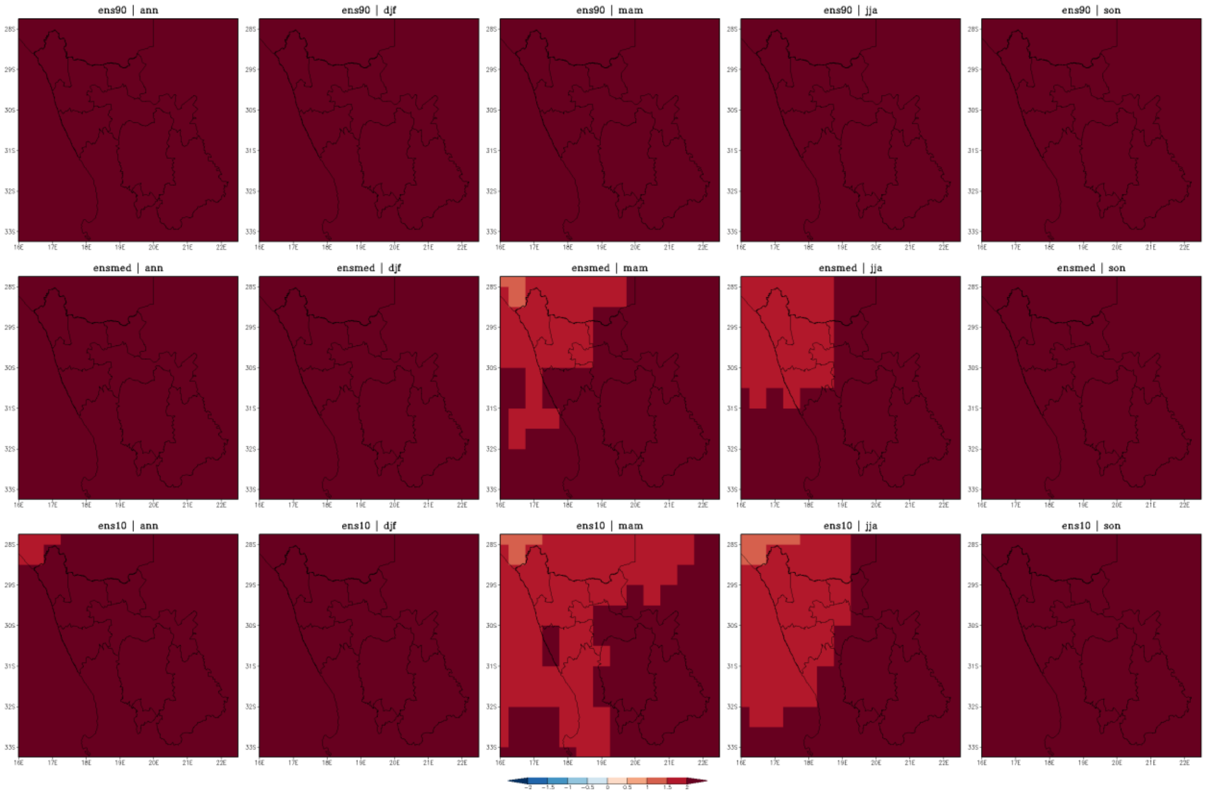

Figure B1.2.2.1b1: The **maximum temperature** anomaly with respect to the model historical period – Namakwa

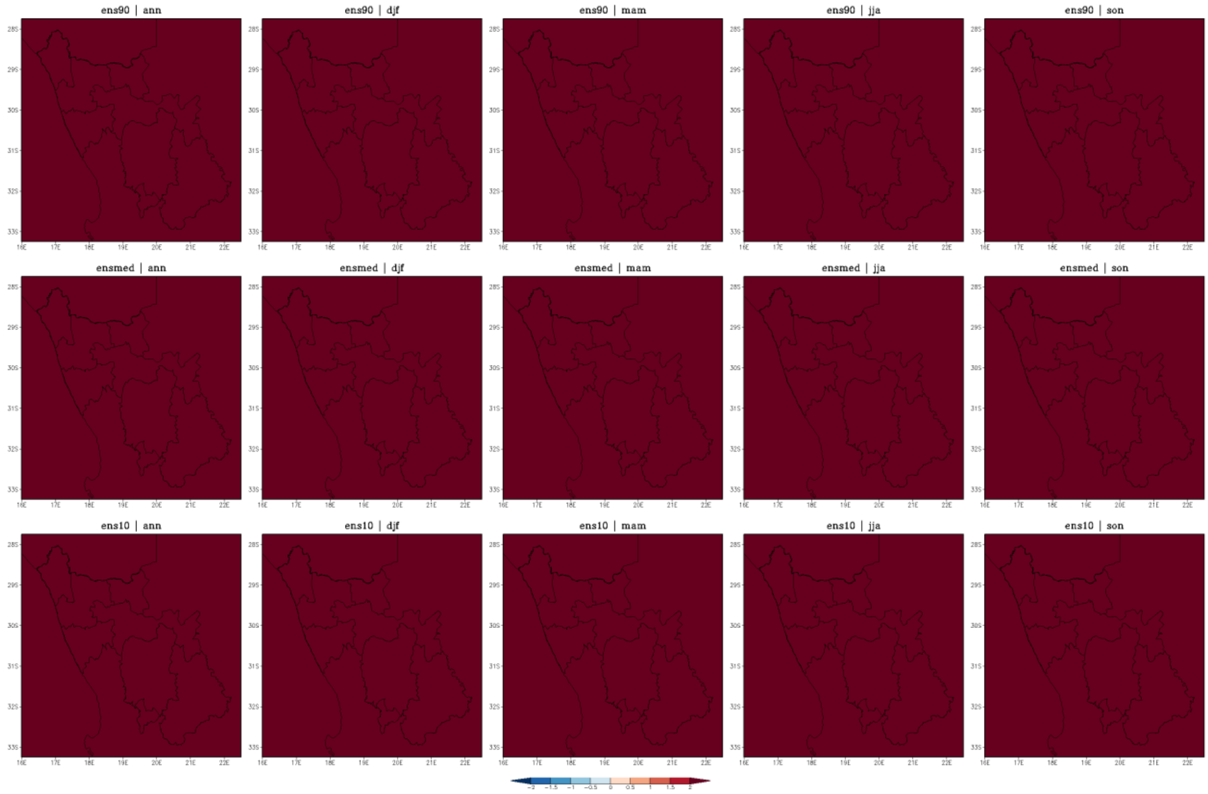

Figure B1.2.2.2b2: The **minimum temperature** anomaly with respect to the model historical period – Namakwa

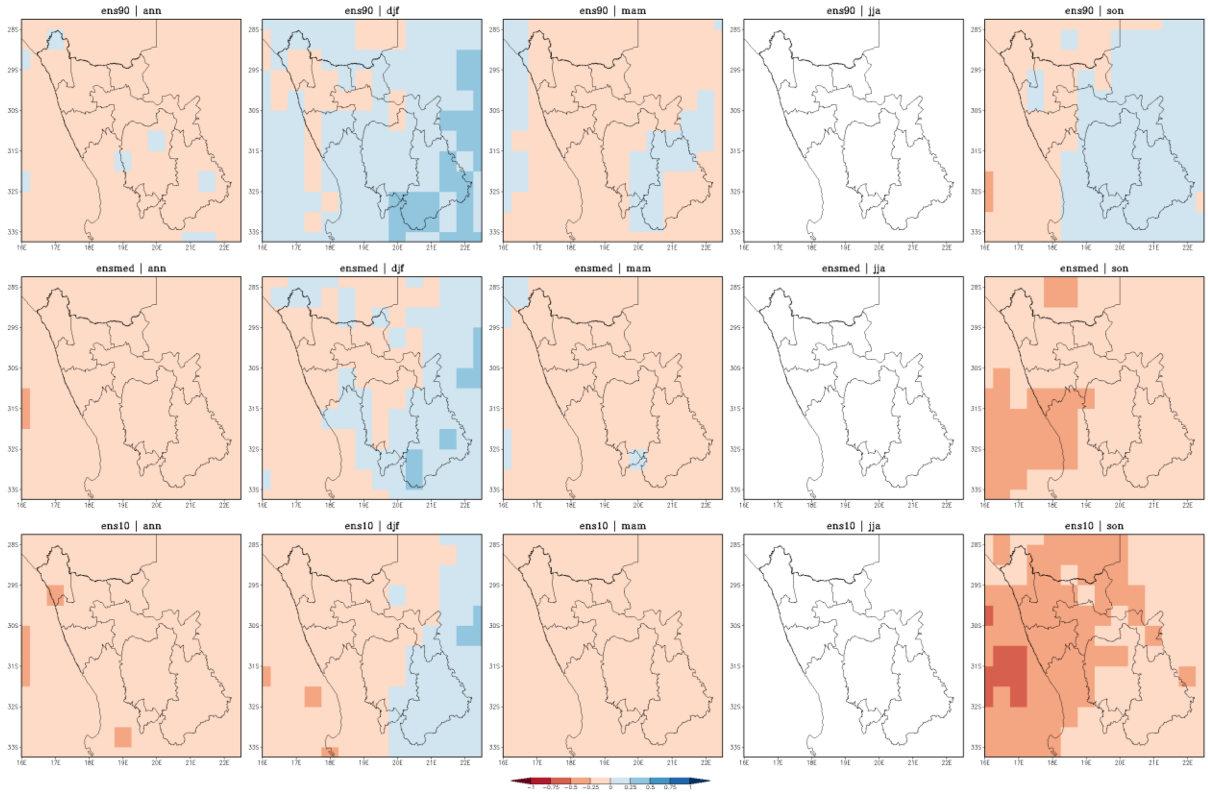

Figure B1.2.2.316b3: The **precipitation** anomaly with respect to the model historical period – Namakwa

B1.2.2.3 2080s

B1.2.2.3a RCP4.5

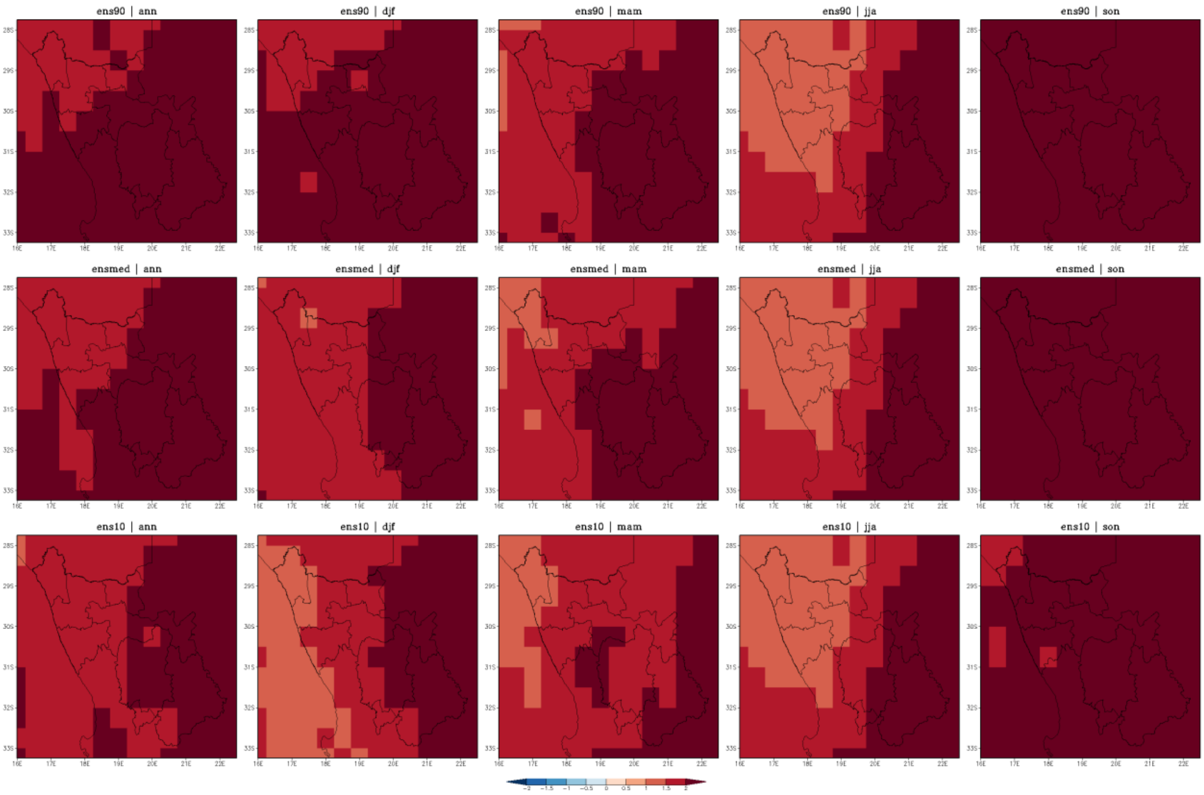

Figure B1.2.2.1a1: The **maximum temperature** anomaly with respect to the model historical period – Namakwa

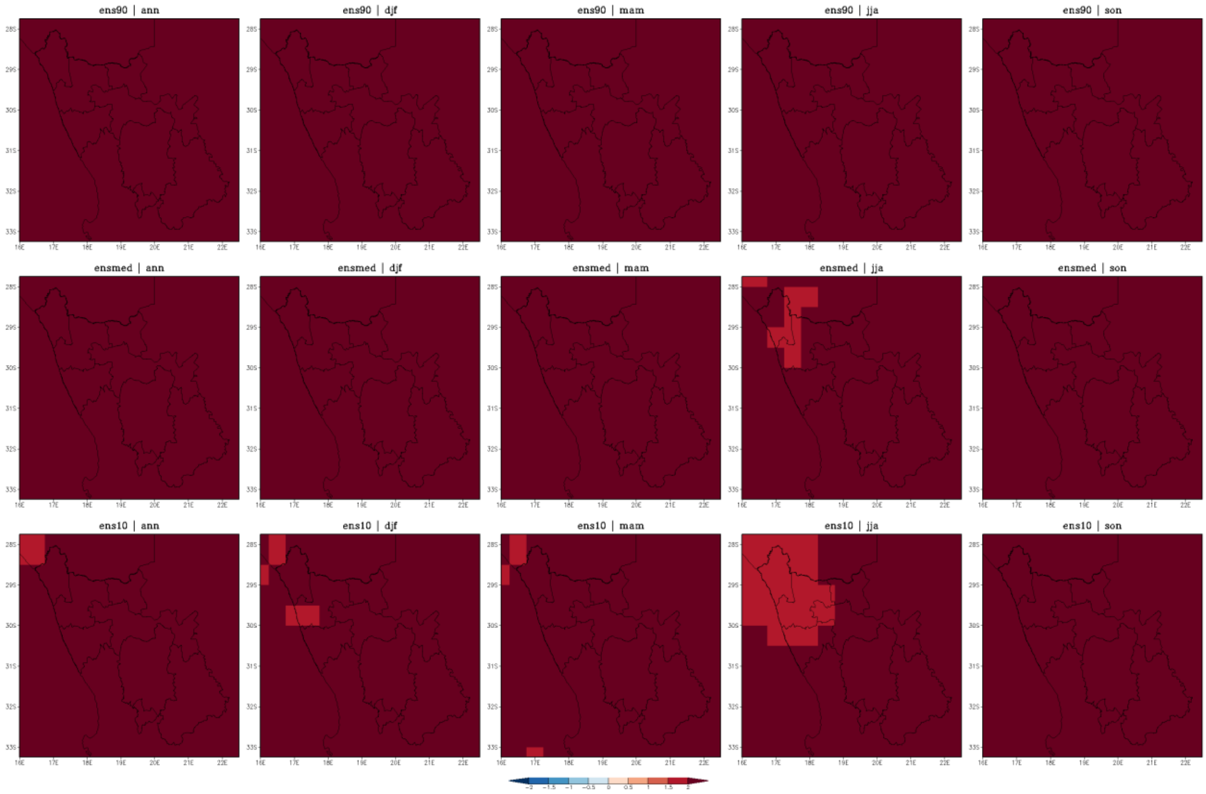

Figure B1.2.2.2a2: The **minimum temperature** anomaly with respect to the model historical period – Namakwa

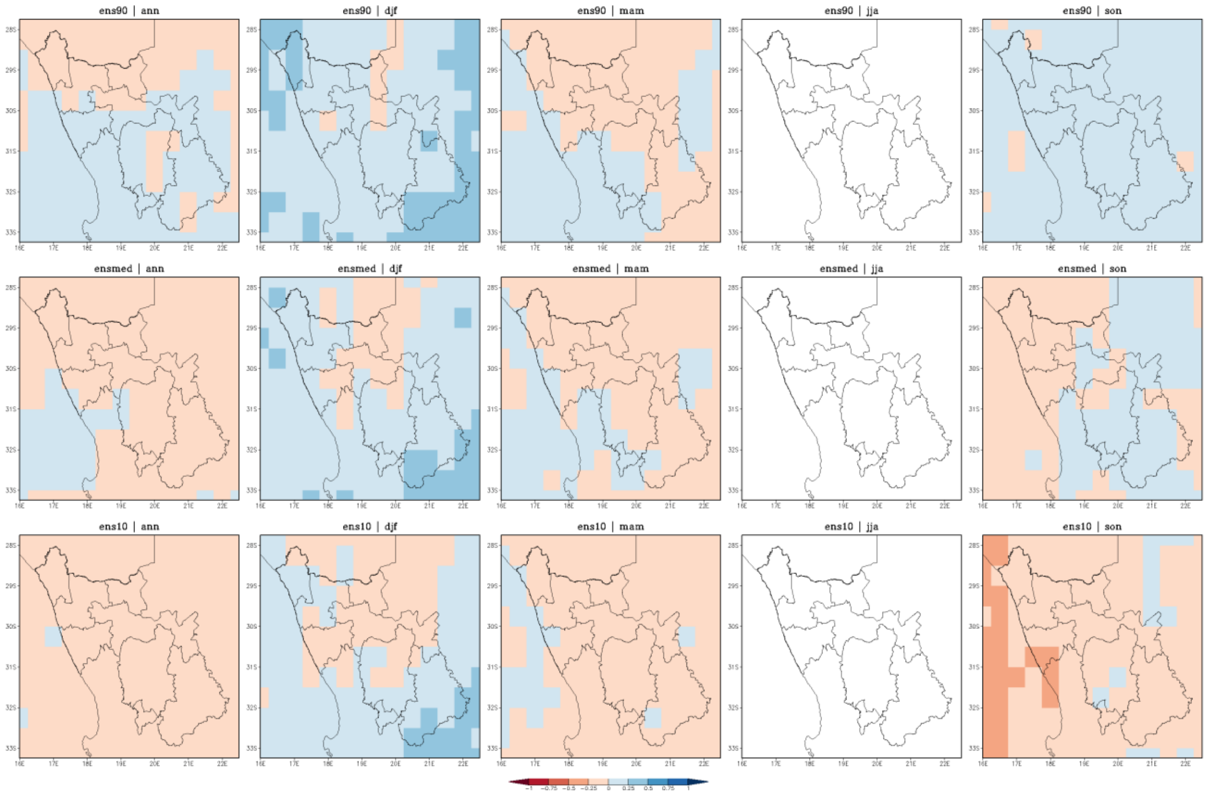

Figure B1.2.2.3a3: The **precipitation** anomaly with respect to the model historical period – Namakwa

B1.2.2.3b RCP8.5

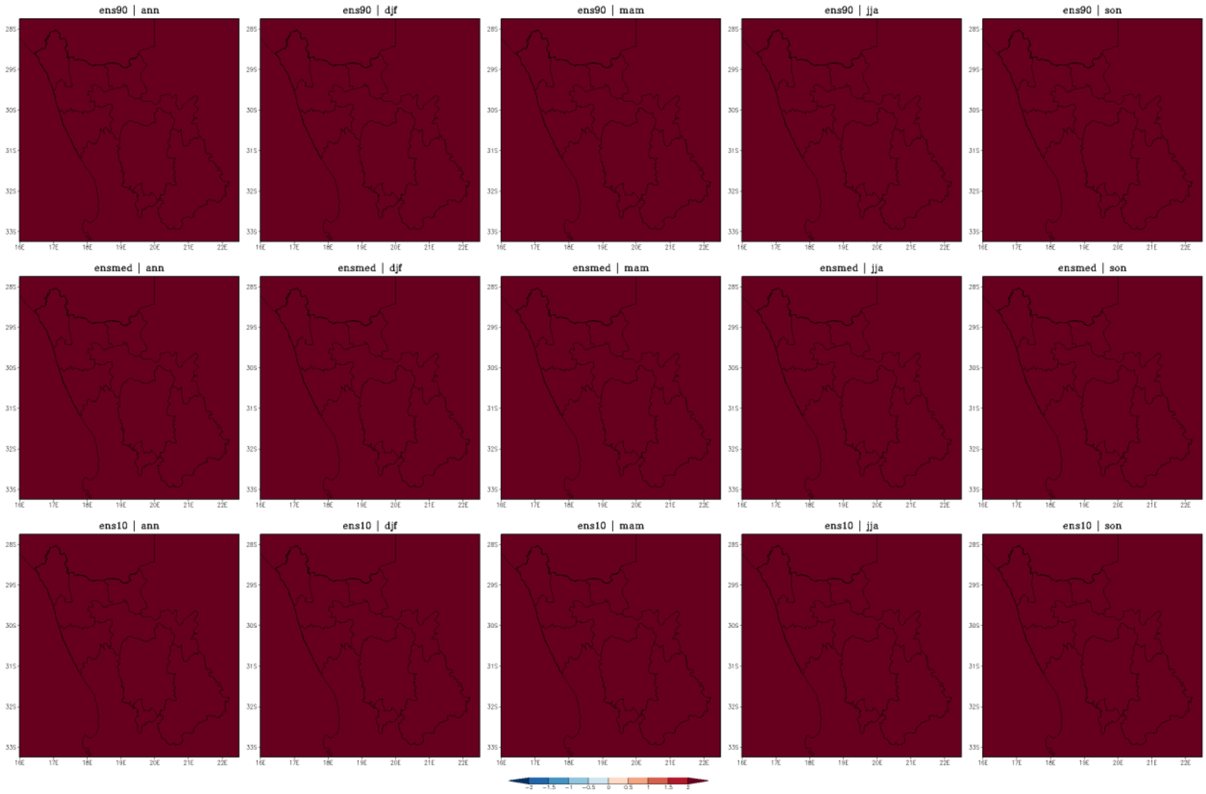

Figure B1.2.2.1b1: The **maximum temperature** anomaly with respect to the model historical period – Namakwa

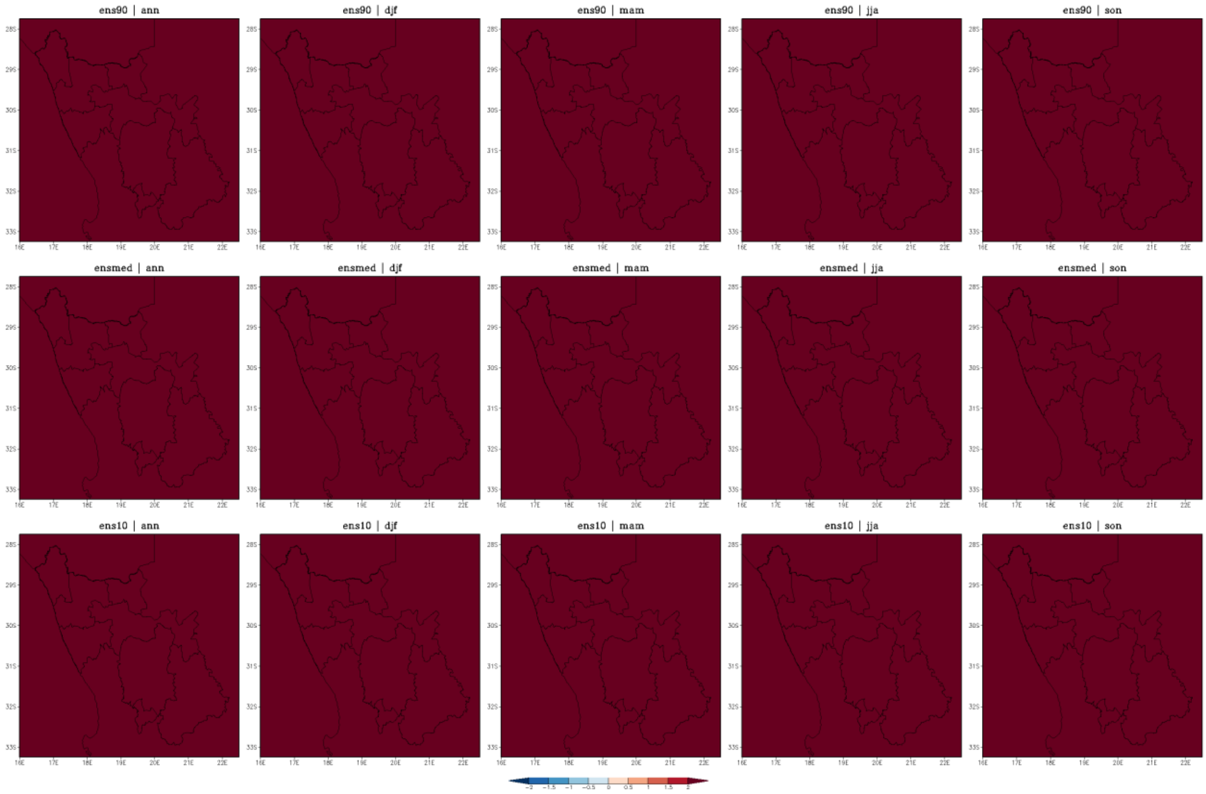

Figure B1.2.2.2b2: The **minimum temperature** anomaly with respect to the model historical period – Namakwa

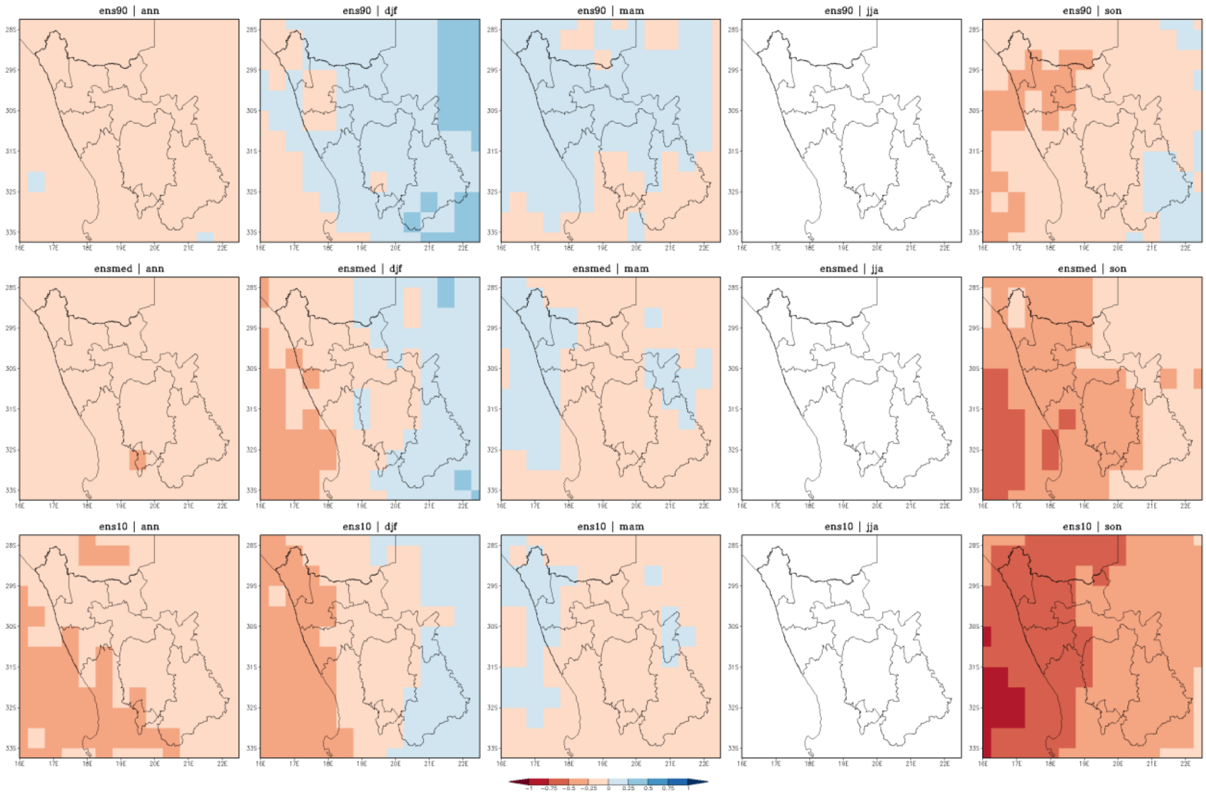

Figure B1.2.2.3b3: The **precipitation** anomaly with respect to the model historical period – Namakwa